Hippo tumour suppressor and Hedgehog pathway crosstalk at the primary cilia

Elysia Traynor

Wolfson College, University of Oxford

Submitted for the degree of Master of Science by Research, MSc(Res), in Oncology

Trinity Term 2017

Table of Contents

Word Count: 18,746

Hippo tumour suppressor and Hedgehog pathway crosstalk at the primary cilia

Elysia Traynor
Wolfson College, University of Oxford
Submitted for the degree of Master of Science by Research, MSc(Res), in Oncology
Trinity Term 2017

Inappropriate activation of the Hedgehog signalling pathway is implicated in broad range of cancers, particularly basal cell carcinoma and medulloblastoma. Recent attempts to target Hedgehog signalling clinically have yielded mixed patient responses, highlighting the need for further study into Hedgehog pathway regulation. Vertebrate Hedgehog signalling occurs within, and is dependent on, the primary cilia. The function of a critical negative regulator of Hedgehog signalling, Suppressor of Fused (Sufu), is regulated by post-translational modification within its intrinsically disordered region, spanning amino acids 279-360. Sufu has previously been shown to be stabilised by phosphorylation at Ser342/Ser346 and Ser352, where S342 phosphorylated Sufu appears to localise to the cilium tip. Here, S342 of Sufu was identified as a potential substrate of the Large Tumour Suppressor (LATS) kinases, LATS1 and LATS2, of the Hippo pathway. This project aimed to determine whether Sufu is regulated by LATS1/2 phosphorylation. LATS1/2 were found to interact with and phosphorylate Sufu at S342. This phosphorylation did not appear to affect the levels of Sufu or of its S352 phosphorylated form, indicating that LATS1/2 does not regulate Sufu stability. Immunofluorescent staining of endogenous Sufu confirmed that Sufu localises to the primary cilium and accumulates at the cilium tip. Reduction of LATS1/2 lead to removal of Sufu from primary cilia, suggesting that S342 phosphorylation of Sufu promotes the ciliary localisation of Sufu. Additionally, S352 phosphorylated Sufu localises to the basal body of primary cilia, confirming that Nek2A phosphorylation of Sufu inhibits its entry into the cilium. Comparison of the mRNA expression of two well-known Hedgehog target genes, *GLI1* and *PTCH1,* between wild type and *LATS1/2*$^{-/-}$ MEFs revealed that loss of LATS1/2 phosphorylation diminishes the repressive activity of Sufu on Hedgehog target gene transcription in response to Hedgehog pathway activation. Thus, LATS1/2 phosphorylation of Sufu at S342 appears to maintain its ability to repress Hedgehog target gene transcription. This adds to the growing body of literature showing that the Hippo and Hedgehog signalling pathways interact and coordinate to regulate cell proliferation. The data presented here unveils a novel role for LATS1/2 in restricting Hedgehog signalling via Sufu, and highlights the importance of LATS1/2 as tumour suppressors. This may identify LATS1/2 as potential targets in the treatment of Hedgehog signalling-dependent tumorigenesis.

Chapter 1: Introduction

1.1 Introduction

Tight regulation of the signalling pathways governing cell growth and function is critical to the maintenance of health and prevention of disease. The misregulation of a broad spectrum of signalling pathways can result in cancer – one of the most common chronic diseases of our aging population. Two of these pathways are the Hedgehog signalling pathway and the Hippo pathway.

Hedgehog signalling has a fundamental and wide-ranging role in tissue patterning during vertebrate embryonic development by governing cell fate determination, proliferation and survival (Ingham and McMahon, 2001). Inappropriate activation of the mitogenic Hedgehog signalling pathway can lead to a wide range of tumours, but principally basal cell carcinoma (Dahmane *et al*., 1997) and medulloblastoma (Zurawel *et al*., 2000). The earliest link between the Hedgehog signalling pathway and cancer was found in patients with an inherited loss-of-function mutation in the Hedgehog membrane receptor, Patched (Ptch1), causing an autosomal dominant condition known as Gorlin Syndrome or Nevoid Basal Cell Carcinoma (Hahn *et al.*, 1996; Johnson *et al.*, 1996). A key characteristic of this disease is the development of multiple basal cell carcinomas, and up to 5% of those with the condition develop medulloblastoma in childhood (Evans *et al*, 1991). There are also increasing links between Hedgehog signalling and the aetiology of other human cancers, such as glioblastoma, rhabdomyosarcoma, rhabdomyoma, breast, pancreatic, prostate (Karhadkar *et al.,* 2004) and haematological cancers (Teglund and Toftgard, 2010).

The primary function of the Hippo pathway is to restrict tissue overgrowth and control organ size by regulating cell proliferation and apoptosis (Tapon *et al.*, 2002). The core Hippo kinase unit achieves this by phosphorylating and inactivating the oncogenic transcriptional regulators Yes-associated protein (YAP) and transcriptional co-activator with PDZ-binding motif

(TAZ) (Huang *et al.* 2005; Zhao *et al*., 2007). Interruption of this tumour suppressive event can lead to many different cancers in humans, including hepatocellular carcinoma (Guo, Wang & Liang, 2015), prostate cancer (Zhao *et al.,* 2007), colorectal, lung and ovarian cancer (Steinhardt *et al.*, 2008).

1.2 Mammalian Hedgehog signalling in development and cancer

The Hedgehog (Hh) signalling pathway is critical for embryonic development in that it serves major morphogenic and mitogenic roles. In mammalian cells, Hh signal transduction is initiated by one of three spatially and temporally organised ligands: Sonic Hedgehog (Shh), Desert Hedgehog (Dhh) and Indian Hedgehog (Ihh), identified by Echelard *et al.* (1993). Shh is expressed in most mammalian tissues, whereas Dhh and Ihh expression is more tissue specific. However, there is some redundancy in function (Ingham and McMahon, 2001). Hedgehog ligand synthesis is unusual in that, after proteolytic cleavage, ligand proteins are modified by the covalent attachment of cholesterol (Porter, Young, and Beachy, 1996) and palmitate (Pepinsky *et al*., 1998) in the highly conserved amino terminal fragment before they are secreted. These lipid modifications are important in regulating the localisation, movement and function of Hh ligands (Farzan *et al*., 2008).

Sonic Hedgehog (Shh) is one of the best described morphogens, which generally have a spatially defined concentration gradient. Hedgehog (Hh) ligand is synthesised and secreted from cells within a specified region of vertebrate tissues (e.g. the zone of polarising activity (ZPA) in the developing limb), and travels away from this site across the tissue to recipient cells, setting up a morphogen gradient. Secretion of cholesterol-modified Hh ligand is mediated by Dispatched, a transmembrane protein that shares structural homology to the Hh receptor Patched (Burke *et al*, 1999). Cholesterol is key in the restriction of Hh movement and the establishment of this concentration gradient (Li *et al.*, 2006; Guerrero and Chiang, 2007). The interpretation of the

concentration, and length of time exposed to Shh ligand, by stem cells determines their gene expression profile, differentiation programme and, ultimately, cell fate (Ingham and McMahon, 2001).

The function of Hedgehog signalling is not limited to embryonic development - it also has an essential role in the maintenance of adult stem cell populations by regulating stem cell renewal. There is strong evidence to suggest that dysregulation of Hh-mediated stem cell renewal can lead to cancer development by the formation of cancer stem cells (Beachy, Karhadkar and Berman, 2004). This is exemplified by Hh-driven medulloblastoma, the most common malignant childhood brain tumour. During normal embryonic stem cell neurogenesis, Hh ligands act as mitogens and cell survival factors, driving proliferation of granule neural precursors in the developing cerebellum (Dahmane and Ruiz, 1999; Cai, Thorne and Grabel, 2008). However, adult neural stem cells are responsive to Shh (Ahn and Joyner, 2005). Genetic mutations in Hh pathway components, particularly Ptch1, Sufu and Smo, lead to increased neural stem cell proliferation, and are implicated in the development of up to 25% of sporadic human medulloblastoma (Raffel *et al*., 1997; Manoranjan *et al*., 2012).

1.3 The primary cilia

Vertebrate Hedgehog signal transduction occurs within and is dependent on primary cilia (Huangfu *et al*., 2003). The primary cilium, identified by Sorokin (1962), is a specialised non-motile sensory organelle projecting from the plasma membrane of many types of epithelial and non-epithelial mammalian cells. It is made up of nine doublet microtubules, forming the 9+0 ciliary axoneme, which extends from the mother centriole-derived basal body (Figure 1.1). The axoneme is surrounded by a ciliary membrane, which is continuous with the plasma membrane but differs slightly in its molecular composition. Cilia specific receptors and ion channel proteins, such as polycystin 1 and 2, are embedded in the ciliary membrane, which are critical in the initiation of

signal transduction in response to different mechanical or chemical stimuli, most notably, Sonic Hedgehog (Satir and Christensen, 2007). Given the importance of specificity in the proteins located in the ciliary membrane, a selectively permeable barrier, known as the transition zone, forms closely distal to the mother centriole. This is made up of transition fibres, Y links, and the ciliary necklace (Garcia-Gonzalo and Reiter, 2012).

The assembly and growth of primary cilia, termed ciliogenesis, occurs when cells exit the cell cycle. Ciliogenesis can be divided into distinct stages. Firstly, small cytoplasmic vesicles dock onto distal appendages of the mother centriole, and fuse to form the ciliary vesicle. The distal end of the mother centriole is remodelled to form the basal body. Microtubules then extend from the basal body, into a double layered sheath of membrane derived from the ciliary vesicle, as it migrates to the cell surface. This structure then merges with the plasma membrane and the microtubules extend further forming the ciliary axoneme, surrounded by a ciliary membrane (Sorokin, 1962). Growth and maintenance of the ciliary axoneme is dependent on intraflagellar transport (IFT), a process whereby two large protein complexes, IFT-A and IFT-B, transport proteins along the ciliary axoneme (Kozminski *et al*., 1993; Cole *et al*., 1998). Anterograde trafficking of cargo from the base to the tip of the cilium is dependent on the IFT-B complex and uses the microtubule plus end directed motor, kinesin-2. Retrograde trafficking of cargo from the distal tip back to the base is mediated by the microtubule minus end directed dynein motor, in association with the IFT-A complex (Rosenbaum and Witman, 2002). As protein synthesis does not occur in the primary cilium, delivery of axonemal proteins to the cilium tip for assembly relies on IFT function (Rosenbaum and Child, 1967). Dysfunction of ciliogenesis and ciliary function, caused by mutations in IFT and transition zone proteins, leads to a diverse range of pathologies with varying phenotypes and severity, known as ciliopathies (Basten and Giles, 2013).

Intraflagellar transport is critical to Hedgehog signal transduction. This was first demonstrated by Huangfu *et al*. (2003), who found that mutations in IFT proteins lead to defects

in Shh-dependent neural morphogenesis. They showed that mutations in genes encoding IFT-B complex proteins (IFT172 and IFT88), and kinesin-2 motor protein Kif3a, blocked Hh pathway activation in response to *Ptch1* gene knockout, indicating that these proteins act downstream of the Hh receptor Ptch, and upstream of the Hh effector Gli. Primary cilia are now known to be an integral aspect of Hedgehog signal transduction, as every important protein in the pathway localises and functions within the cilium (Goetz and Anderson, 2010). IFT is absolutely required for all events of the Hh signalling pathway downstream of Ptch and Smo (Huangfu and Anderson, 2005). The relationship between primary cilia and mammalian Hedgehog signalling is both intimate and complex, owing to the complexity of the Hedgehog signalling pathway.

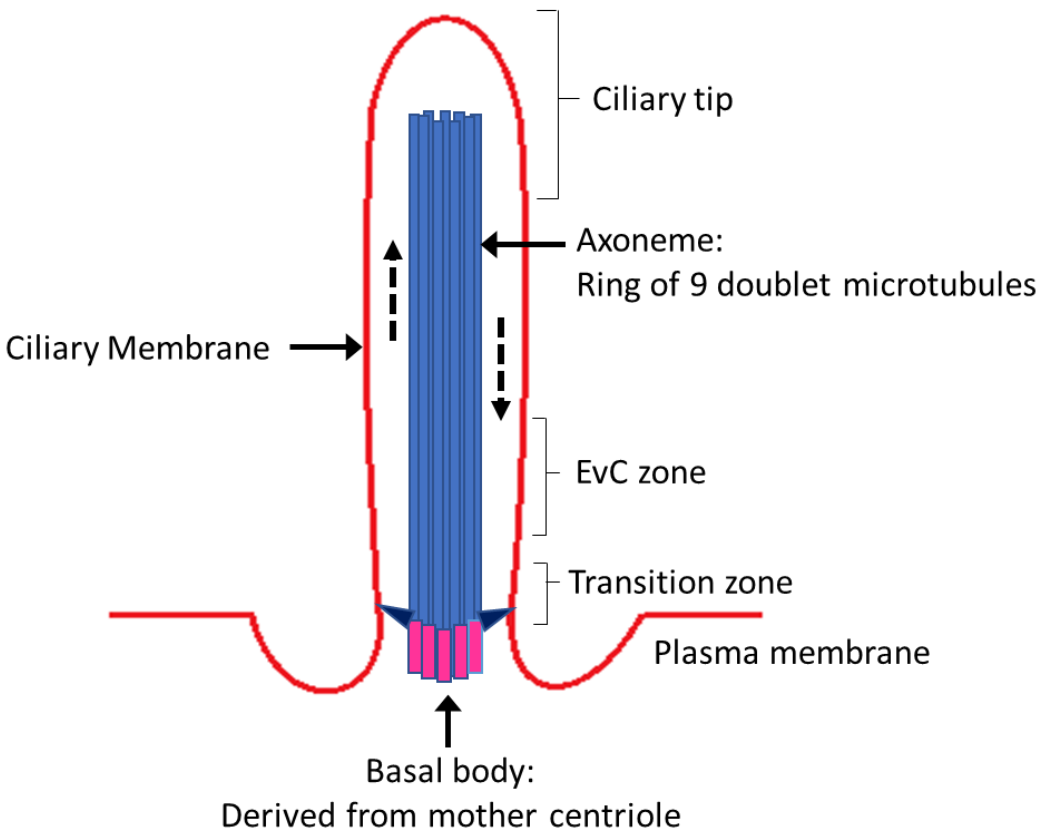

Figure 1.1 – The Primary Cilium
Schematic diagram of the key structures and regions within the primary cilium (described in the text).

1.4 Hedgehog signal transduction

The output of the Hedgehog signalling pathway is the transcription of Hedgehog target genes, including *GLI1, PTCH1* and *CCND2* (Dai *et al*., 1999; Yoon *et al*., 2002). This is mediated by three Glioma-associated oncogene family zinc finger transcription factors - Gli1, Gli2 and Gli3. Gli2 and Gli3, the dominant regulators of Hh target gene transcription, are able to act as both transcriptional activators and repressors due to the presence of both a C-terminal activator domain and N-terminal repressor domain. Activator or repressor activity is dictated by differential proteosomal processing, controlled by Hh signal transduction (Sasaki *et al.*, 1999). Gli2 is the principal transcriptional activator (Pan *et al.*, 2006), and Gli3 is the chief transcriptional repressor. Gli1, on the other hand, acts only as a transcriptional activator as it lacks the N-terminal repressor domain, but is dispensable in Hh target gene transcription (Park *et al*., 2000). Effectively, the transcriptional output of Hh signalling depends on the ratio of the activator to repressor forms of Gli2 and Gli3 (Hui and Angers, 2011).

The Hedgehog signalling pathway is initiated by binding of Hh ligand to its primary receptor, the 12-pass transmembrane receptor Patched (Ptch) (Marigo *et al*., 1996). In the absence of Hh ligand (Figure 1.2A), Ptch is present on the ciliary membrane and inhibits the activity of Smoothened (Smo), a 7-transmembrane spanning receptor, by preventing its translocation into the cilium (Rohatgi, Milenkovic, and Scott, 2007). G protein-coupled receptor 161 (Gpr161), bound to the stimulatory G protein Gαs, activates Protein Kinase A (PKA) at the base of the cilium by promoting Adenylyl Cyclase-mediated cAMP production (Mukhopadhyay *et al*., 2013). The core negative regulator, Suppressor of Fused (Sufu), binds to and sequesters full length Gli2 or Gli3 in the cytoplasm forming an inactive complex (Koger man *et al*., 1999; Dunaeva *et al*., 2003). Sufu binding stabilises full length Gli and promotes PKA phosphorylation of Gli2/3 at 6 conserved Serines within their C-terminal half (Wang, Fallon and Beachy, 2000; Niewiadomski *et al.*, 2014). This primes them for further phosphorylation by Casein Kinase 1 (CK1) and Glycogen

Synthase Kinase 3 β (GSK3β) (Humke *et al.*, 2010; Tempé *et al.*, 2006). Within the cilium, phosphorylated Gli2/3 are recognised and ubiquitylated by F-box E3 ubiquitin ligase beta-transducin repeat-containing protein (β-TRCP), which targets them for processing into their repressor form (GliR) by proteosomal cleavage of their C-terminal activation domain (Bhatia *et al.*, 2006; Wang and Li, 2006; Sasaki *et al.*, 1999). Localisation of Sufu-Gli2/3 to the cilium tip by IFT is required for processing of Gli2/3 into their repressor form (Haycraft *et al.*, 2005). GliR then translocates into the nucleus, binds to consensus sequence DNA of Hh target genes and represses their transcription.

Upon binding of Hh ligand to Ptch, Ptch and Gpr161 exit the cilium (Rohatgi, Milenkovic, and Scott, 2007; Mukhopadhyay *et al*., 2013), relieving Smo inhibition and reducing local PKA activity (Figure 1.2B). Hh-bound Ptch becomes internalised by endocytosis and is degraded (Incardona *et al*., 2000). Smo is phosphorylated at multiple sites by G protein-coupled receptor kinase 2 (GRK2) and CK1, which induces an activating conformational change and promotes its translocation into the cilium by IFT (Chen *et al*., 2011). Ellis-van Creveld syndrome proteins, EvC1 and EvC2, bind to hyper-phosphorylated Smo, anchoring Smo near the base of the cilium in a specialised region known as the EvC zone (Dorn, Hughes and Rohatgi 2012; Yang *et al.*, 2012). In response to Smo activation, Sufu/Gli complexes rapidly move into the cilium and accumulate at the cilium tip (Tukachinsky, Lopez and Salic, 2010). Localisation of Sufu/Gli complexes at the cilium tip is dependent on Kif7, which is critical in maintaining correct architecture of the cilium tip compartment (He *et al.*, 2014). Here, full length Gli2/3 are dephosphorylated at the 6 PKA-phosphorylated Serines and phosphorylated at a separate set of Serine/Threonine residues (Niewiadomski *et al.*, 2014). This promotes Kif3A-dependent dissociation of the Sufu-Gli complexes and processing of Gli into its activator form (GliA) by cleavage of the N-terminal repressor domain (Humke *et al*., 2010; Tukachinsky, Lopez and Salic, 2010, Sasaki *et al.*, 1999). GliA then exits the cilium and is able to activate Hh target gene transcription in the nucleus.

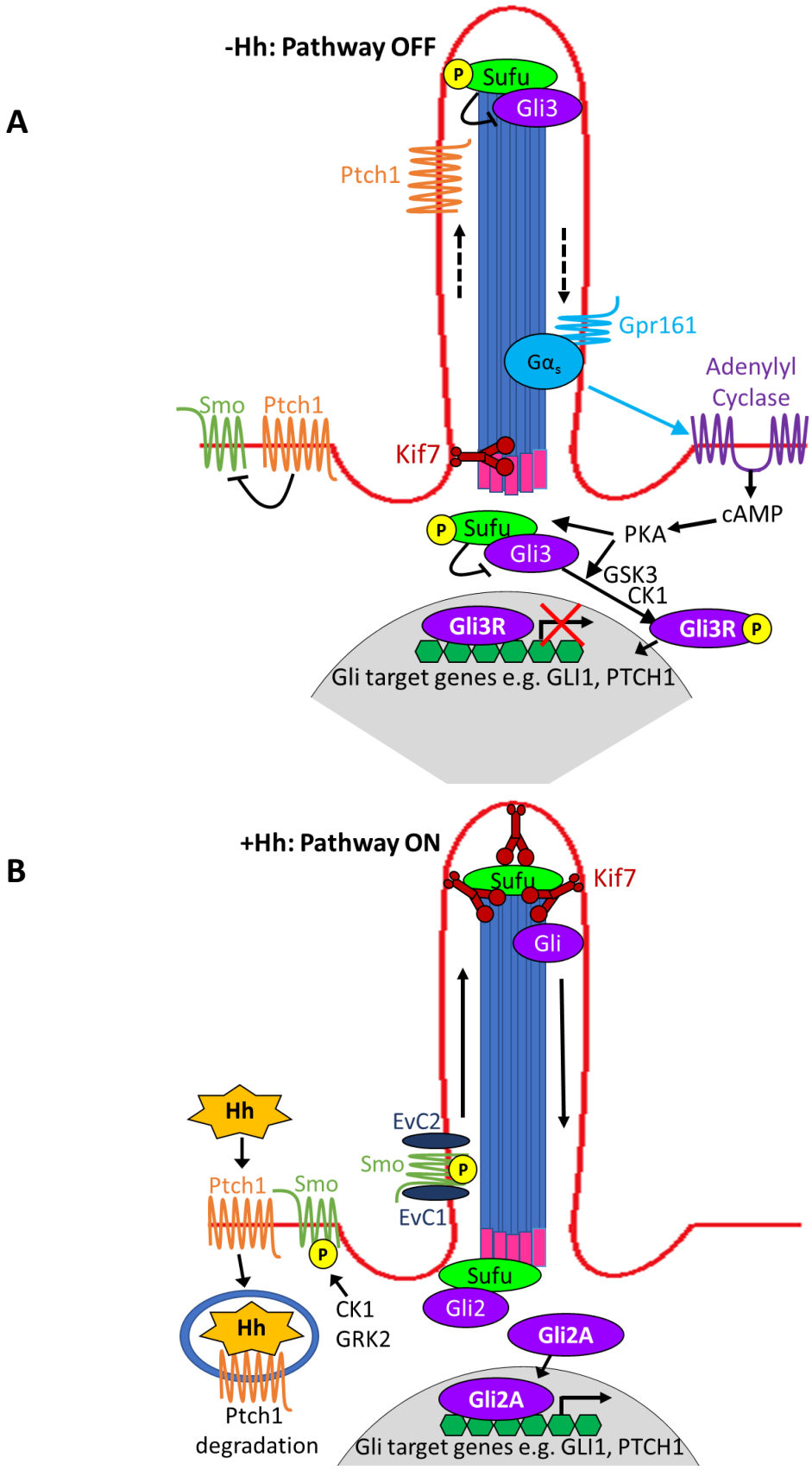

Figure 1.2 – Hedgehog signal transduction
Schematic diagram illustrating the key events of the Hedgehog signalling pathway in the absence (A) or presence (B) of Hedgehog (Hh) ligand (described in the text).

1.5 Suppressor of Fused

Suppressor of Fused (Sufu) (Figure 1.3) is a highly conserved negative regulator of Hedgehog signalling (Kogerman *et al*., 1999). It is absolutely essential for embryonic development as Sufu deletion leads to embryonic lethality (Cooper *et al.* 2005). Sufu directly interacts with all three Gli transcription factors, forming stable complexes which repress Gli transcriptional activity. Cherry *et al.* (2013) showed that hydrogen bonds between the histidine of a key N-terminal SYGHL motif in Gli and Tyr147 and Asp159 of Sufu were critical for binding. Subsequently, an additional interaction between a conserved C-terminal site of Gli and Sufu was found to be necessary for maximal inhibition of Gli activity (Han, Shi, and Jiang, 2015). This group found that interaction of Sufu with the N-terminal site of Gli represses Gli transcriptional activity by masking its nuclear localisation sequences (NLS), whereas its interaction with the C-terminal site of Gli inhibits its recruitment of transcriptional coactivator CBP in the nucleus. Thus, dual binding of Sufu to Gli transcription factors mediates both cytoplasmic retention of Gli, and inhibition of Gli transcriptional activity in the nucleus.

Aside from Gli, Sufu was found to interact with two transcriptional cofactors, p66b and Mycbp, in the nucleus. A model was proposed in which recruitment of p66b to Sufu-Gli represses Gli target gene transcription in the absence of Hh, which dissociates in response to pathway activation, allowing Mycbp to promote Gli transcriptional activity (Lin *et al.*, 2014). Sufu is also important in controlling cellular levels of full length Gli2/3, and consequently the production of their activator and repressor forms. Regulation of Gli protein levels by Sufu is achieved independently of cilia by antagonising the activity of Spop (speckle-type POZ protein), which targets full length Gli2 and Gli3 for ubiquitin-mediated proteosomal degradation (Chen *et al*., 2009). This suggests that Sufu is required for both activation and repression of Hh signalling. In support of this, it was recently discovered that Sufu stabilises Gli1 and, in response to Hh pathway activation, chaperones translocation of Gli1 into and Gli3R out of the nucleus (Zhang *et al.*, 2017).

Although originally viewed as a negative regulator of Hh signalling, it is now apparent that Sufu serves both positive and negative roles in its control of Gli-mediated gene transcription.

The subcellular localisation and function of Sufu is tightly regulated by binding interactions. Nucleocytoplasmic shuttling of Sufu is mediated by interactions with nuclear proteins, such as SAP18 and Galectin 3 (Paces-Fessy *et al.*, 2004). Ciliary localisation of Sufu is dependent on its interaction with Gli2 and Gli3 (Tukachinsky, Lopez and Salic, 2010). Although Sufu can inhibit Gli transcriptional activity in the absence of primary cilia (Jia *et al.*, 2009; Chen *et al.*, 2009), Smo-mediated inactivation of Sufu is dependent on cilia (Huangfu and Anderson, 2005). Therefore, localisation of Sufu-Gli complexes at the ciliary tip is necessary for ensuring appropriate pathway activation in response to ligand (He *et al.*, 2014).

Post-translational modifications are critical in the regulation of Sufu function and localisation. Structural analysis revealed the presence of an intrinsically disordered region (IDR) within Sufu, encompassing amino acids 279-360 (Cherry *et al.* 2013). Binding of Gli induces Sufu to switch from an open to closed conformation, and the IDR reorganises to stabilise the Sufu-Gli interaction. Hh pathway stimulation promotes Sufu to revert to its open conformation, releasing Gli (Zhang *et al.*, 2013). Removal of the IDR prevents Sufu inactivation in response to Smo activation, indicating that post-translational modification of residues within this region are responsible for inhibition of Sufu activity (Cherry *et al.* 2013). In agreement with this, phosphorylation of Sufu at Ser342, Ser346 and Ser352 have been characterised, which regulate Sufu stability, localisation and consequently, function.

Chen *et al*. (2011) reported that Sufu is phosphorylated at Serine 346 by PKA, which primes phosphorylation at Serine 342 by GSK3β. Substitution of these two residues for Alanine to block phosphorylation resulted in destabilisation of the protein and dampening of its repressor activity on Gli-mediated gene transcription, indicating that this dual phosphorylation serves to stabilise Sufu and retain its inhibitory function. They suggested that Hh pathway activation

promotes Sufu degradation by blocking of S342/S346 phosphorylation. They found that S342/S346 phosphorylated Sufu localises to the ciliary tip and, through mutational studies, deduced that S342/S346 phosphorylation promotes ciliary retention, proposing that dephosphorylation at the cilium tip allows Sufu to exit the cilium. They also demonstrated that S342/S346 phosphorylation of Sufu increased Smo-induced localisation of Sufu-Gli3 at the cilium tip, reinforcing the idea that Sufu and Gli translocate into the cilium in a complex. The stabilising effect of S342/S346 phosphorylation was confirmed by Raducu *et al* (2016), who demonstrated that E3 ubiquitin ligase F-box and leucine-rich repeat protein 17 (Fbxl17) binds to and polyubiquitylates Sufu, targeting it for proteosomal degradation. They observed that Alanine substitution of S342 and S346 increased Fbxl17 binding, whereas replacement of these residues with aspartate to mimic phosphorylation caused loss of Fbxl17 binding. This suggests that S342/S346 phosphorylation stabilises Sufu by blocking Fbxl17-mediated proteosomal degradation.

Raducu *et al.* (2016) discovered that phosphorylation of Sufu at S352, which occurs *in vivo*, inhibits Fbxl17 binding. Wang *et al.* (2016) found that the kinase responsible for S352 phosphorylation is NIMA-related expressed kinase 2A (Nek2A), and confirmed that S352 phosphorylation stabilises Sufu, supporting its role in blocking Fbxl17-mediated proteosomal degradation. In addition, this group showed that S352 phosphorylation by Nek2A may regulate translocation of Sufu into the primary cilia in response to Hh pathway activation. Recently, the significance of Nek2A in repressing Gli transcriptional activity was confirmed to be via Sufu phosphorylation, and Nek2A itself was identified as a Gli-transcriptional target (Zhou *et al.*, 2017). This unveils the presence of a negative feedback loop in which Hh-signalling attenuates further Gli-transcriptional activity via upregulation of Nek2A.

Given the mitogenic role of the Hedgehog signalling, Sufu is implicated as a tumour suppressor. Mice genetically engineered with a heterozygous loss-of-function mutation in *SUFU*,

in combination with loss of p53, are prone to the development of medulloblastoma and rhabdomyosarcomas, tumours associated with aberrant Shh signalling (Taylor *et al*., 2002). *SUFU* loss of heterozygosity was found to be key feature of those tumours (Lee *et al.,* 2007). Germline mutations in *SUFU* have been implicated in cases of Gorlin Syndrome (also known as nevoid basal cell carcinoma (BCC) syndrome) that are not attributed to *PTCH1* mutations, which confer a markedly (approximately 20X) higher risk of medulloblastoma development than in *PTCH1* mutation driven Gorlin Syndrome (Smith *et al.*, 2014). *SUFU* mutations have also been shown to drive basal cell carcinoma formation, all of which disrupt binding of Sufu to Gli, resulting in constitutive pathway activation (Urman *et al*., 2016).

A missense mutation in which S352 is replaced with Phenylalanine (S352F) was identified in medulloblastoma cases of Gorlin Syndrome patients (Smith *et al*. 2014). Raducu *et al.* (2016) showed that the S352F mutation favours Fbxl17 binding. In line with this, they demonstrated that Fbxl17 depletion by RNA interference (RNAi) impairs Hh signalling and reduced tumour progression in an orthotopic rat model of medulloblastoma. Analysis of gene expression profiles of each subtype of medulloblastoma revealed that in the Sonic Hedgehog (SHH) subtype, despite a substantial increase in *GLI1* mRNA, *SUFU* mRNA expression was comparable with other subtypes. This was explained by a significant increase in *Fbxl17* mRNA in SHH-subtype medulloblastoma, indicating that Fbxl17-mediated control of Sufu protein levels plays a key role in SHH-driven medulloblastoma.

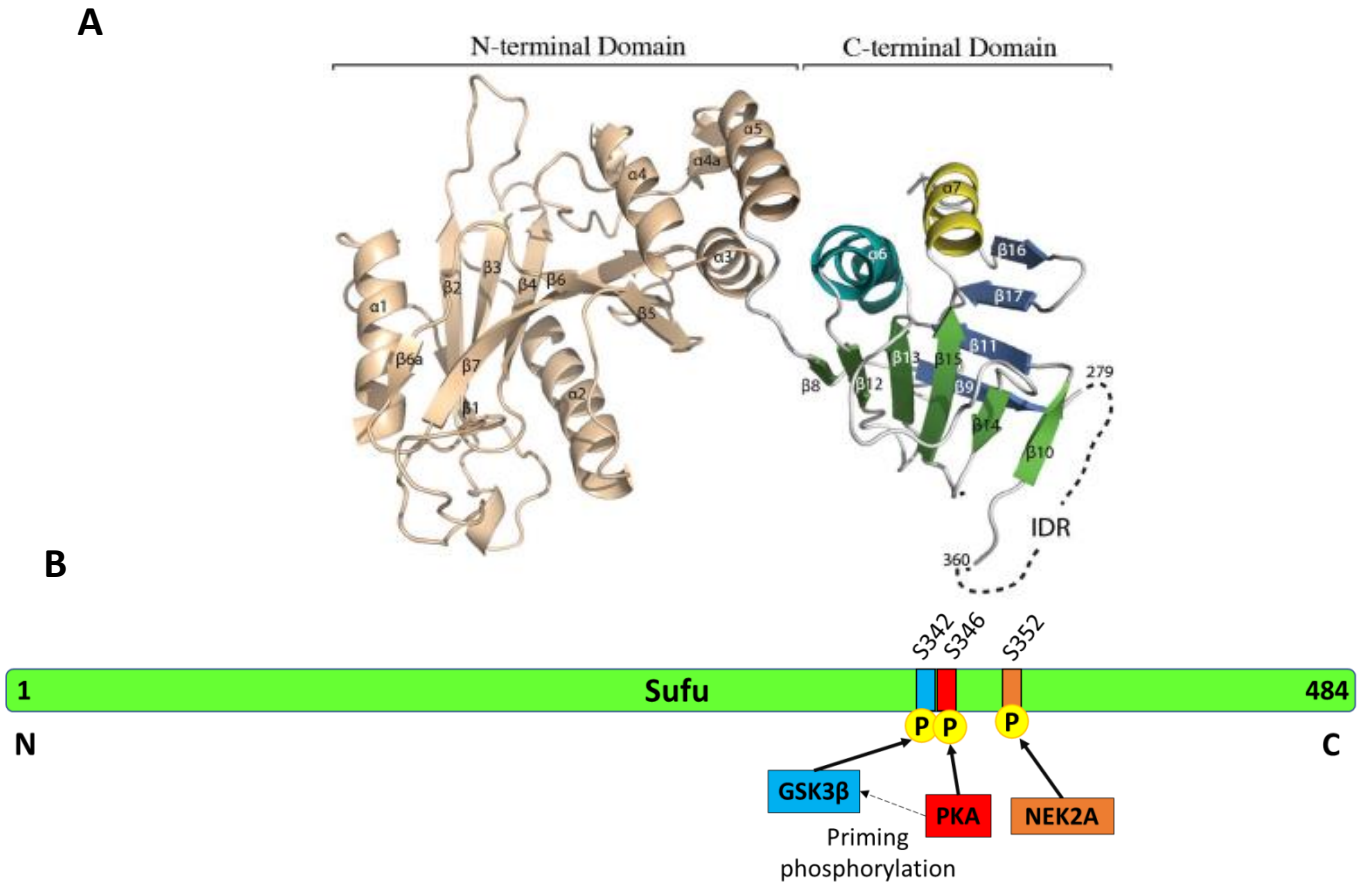

Figure 1.3 – Sufu structure and regulation

(A) Crystal structure of Sufu, showing its open 3D conformation and location of the highly mobile Intrinsically Disordered Region (IDR). *Image taken from Cherry et al. (2013).*

(B) Schematic diagram showing the three key phosphorylation sites within the IDR that regulate Sufu stability, localisation, and function. The protein kinase responsible for phosphorylation at each site is indicated.

1.6 The Hippo pathway

The Hippo Pathway is emerging as an important player in the control of tissue growth, having only been discovered two decades ago in genetic screens for tumour suppressor genes using *Drosophila melanogaster*. Loss-of-function mutations in the genes encoding the key proteins of the Hippo pathway result in hyperproliferation and tissue overgrowth phenotypes, demonstrating their importance in regulating the cell cycle and apoptosis (Justice *et al*., 1995; Xu *et al*., 1995; Tapon *et al*., 2002; Harvey *et al*., 2003; Lai *et al*., 2005). Once the first four pathway components had been identified, and links were made between them, a protein kinase cascade emerged. The first tumour suppressor gene to be identified encodes an NDR family protein kinase, Warts (Wts) - the central player of the Hippo pathway (Justice *et al*., 1995; Xu *et al*., 1995). Salvador (Sav) was then shown to function with and bind to Wts via direct interaction between the WW domain of Sav and the PPYX motif of Wts (Tapon *et al*., 2002). Shortly after, the Ste20 family protein kinase, Hippo (Hpo), was found to interact with both Sav and Wts, suggesting that they function as a complex (Harvey *et al*., 2003). The final tumour suppressor identified to function in the core Hippo kinase cascade was the Mob superfamily protein Mats (Mob as tumor suppressor), which interacts directly with Wts to form a protein complex which stimulates Wts kinase activity (Lai *et al*., 2005). Mammalian homologues for each of these tumour suppressor genes were identified, some many of which were found to be duplicated in mammals, indicating that the Hippo pathway is evolutionary conserved.

The functional output of the Hippo pathway is the phosphorylation and inactivation of transcriptional coactivators Yes-associated protein (YAP), and its paralogue, TAZ (Transcriptional co-activator with PDZ binding motif). Identification of the *Drosophila* homologue of YAP, Yorkie (Yki), revealed the mechanism by which the Hpo-Sav-Wts kinase cascade inhibits tissue overgrowth and promotes apoptosis. Overexpression of *Yki/YAP* yields the same phenotype as loss-of-function mutations in Hpo or Wts kinases, demonstrating that *Yki/YAP* functions as an

oncogene (Huang *et al*., 2005). Although YAP does not possess a PDZ binding motif, both YAP and TAZ contain WW domains that can bind to the PPYX motif of TEA domain (TEAD) family transcription factors, which mediate YAP/TAZ target gene transcription (Zhao *et al*. 2008). Phosphorylation of YAP/TAZ at a single Serine residue is required for 14-3-3 binding, and leads to their nuclear export, preventing transcriptional coactivation (Kanai *et al.*, 2000).

The Hippo pathway is now known to be an extensive protein network consisting of over 35 components (Harvey, Zhang, and Thomas, 2013), however, this review will focus on regulation and function of the core mammalian Hippo pathway components. The core kinase cascade of the mammalian Hippo pathway is activated in response to a diverse range of internal and external stimuli, including cell polarity, energy stress, cell contact, extracellular matrix stiffness, and growth factor receptor signalling (Meng, Moroishi and Guan, 2016). The mechanism by which each stimulus regulates Hippo pathway output is cell type and context specific (Oren and Aylon, 2013).

The core Hippo kinase cascade (Figure 1.4) is initiated during mitosis by phosphorylation of mammalian Ste20-like kinases 1/2 (MST1/2, homologues of *Drosophila* Hpo) within an activation loop, which activates MST1/2 via a change in 3D conformation (Praskova *et al.*, 2004). This can be performed by the Ste20-like TAO kinases (TAOK1/2/3) or via MST1/2 autophosphorylation, which is enhanced by dimerization (Boggiano, Vanderzalm, and Fehon, 2011; Poon *et al.* 2011; Praskova *et al.*, 2004; Glantschnig, Rodan and Reszka, 2002). Binding of RASSF polypeptides to MST1/2 via their SARAH domains are also important for MST1/2 activation, however, the precise role of RASSF in regulating MST1/2 remains unknown (Avruch *et al*., 2006). Subsequently, SAV1 (homologue of *Drosophila* Sav) and MOB1A/B (homologues of *Drosophila* Mats) are phosphorylated by active MST1/2. These two scaffolding proteins form an active complex with MST1/2 at the plasma membrane (not shown), which aid recruitment of Large Tumour Suppressor 1/2 (LATS1/2, homologues of *Drosophila* Wts) by binding of LATS1/2 to

membrane-associated MOB1A/B. MST1/2 phosphorylates LATS1/2 within their hydrophobic motifs (Chan *et al.* 2005; Hergovich, Schmitz and Hemmings, 2006). Additionally, Neurofibromin 2 (NF2, also known as Merlin) has an important role in the recruitment of LATS1/2 to the plasma membrane via direct binding, which promotes MST1/2-mediated LATS1/2 phosphorylation (Yin *et al.*, 2013). In fact, NF2 is the only Hippo pathway gene that fits the definition of a bona fide tumour suppressor, highlighting how important organisation of Hippo pathway components at the plasma membrane is for pathway function (Harvey, Zhang, and Thomas, 2013). MST1/2 phosphorylated LATS1/2 then undergo autophosphorylation, becoming fully active and able to phosphorylate YAP and TAZ (Chan *et al.* 2005; Huang *et al*., 2005). Recently, MAP4K family kinases (homologues of *Drosophila* Happyhour and Misshappen) were found to directly phosphorylate and activate LATS1/2, acting in parallel with MST1/2 (Meng *et al*., 2015). YAP/TAZ phosphorylation results in their cytoplasmic retention by binding to 14-3-3 or additional phosphorylation by Casein Kinase 1 δ/ε, leading to SCF (β-TRCP) E3 ubiquitin ligase mediated proteosomal degradation (Zhao *et al.*, 2007; Liu *et al*., 2010; Zhao *et al.*, 2010). Therefore, the pathway blocks the expression of YAP/TAZ target genes via TEAD transcription factors.

When the pathway is switched off, MST1/2 and LATS1/2 are unphosphorylated and inactive, allowing the YAP/TAZ to localise in the nucleus (Figure 1.4A). Nuclear YAP/TAZ bind to TEAD transcription factors, displacing transcriptional repressor VGLL4, and thereby induce the expression of genes involved in cell proliferation and survival (Koontz *et al*., 2013). Loss of LATS1/2-mediated phosphorylation of YAP/TAZ or overexpression of YAP/TAZ results in the inappropriate upregulation of YAP/TAZ target gene expression, leading to uncontrolled cell proliferation, neoplasia and inhibition of apoptosis. YAP/TAZ amplification is frequently observed in a range of human cancers (Steinhardt *et al.*, 2008). Therefore, the restriction of YAP and TAZ activity by the Hippo pathway is important in preventing cancer progression (Harvey, Zhang, and Thomas, 2013).

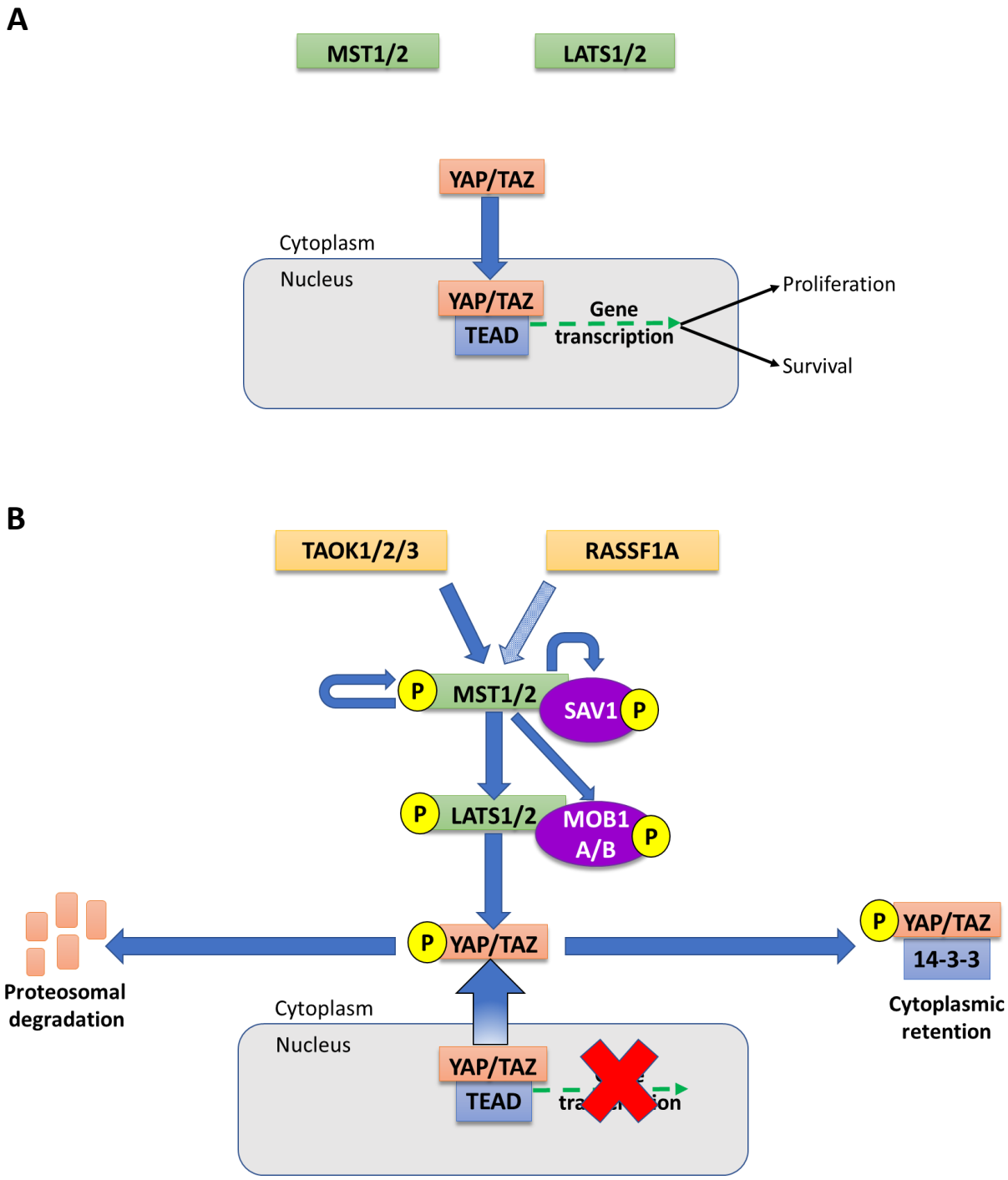

Figure 1.4 – The core mammalian Hippo pathway kinase cascade
(A) When the Hippo pathway is switched off, MST1/2 and LATS1/2 are unphosphorylated and inactive, allowing the YAP/TAZ to localise in the nucleus, bind to TEAD transcription factors, and induce the expression of genes involved in cell proliferation and survival.
(B) Activation of MST1/2 by phosphorylation (and via RASSF1A binding) initiates a kinase cascade that culminates in the phosphorylation of YAP/TAZ. This results in their nuclear export, 14-3-3 mediated cytoplasmic retention and proteosomal degradation.
Adapted from Meng, Moroishi and Guan (2016)

1.7 The LATS Kinases

The Large Tumour Suppressor (LATS) kinases, LATS1 and LATS2, are mammalian homologues of the *Drosophila* Warts Serine/Threonine kinase (Justice *et al*., 1995; Nishiyama *et al.*, 1999; Yabuta *et al*., 2000), which belong to the Nuclear Dbf2-Related (NDR) kinase subgroup of the AGC kinase family (Hergovich, Schmitz and Hemmings, 2006). LATS1/2 have highly conserved Serine/Threonine kinase domains at their C-terminal half, but there is low sequence similarity within the upstream non-kinase N-terminal half. Interaction between LATS1/2 and a myriad of other proteins, including Hippo pathway components, occurs at regions within the N-terminal half, which contains proline-rich repeats. In LATS1, one of these proline-rich repeats matches an SH3-binding consensus sequence (PXXPXR). Lack of this sequence in LATS2 is indicative of a divergence in function between LATS1 and LATS2 (Justice *et al*., 1995; Yabuta *et al*., 2000). In fact, the interactomes of LATS1 and LATS2 differ considerably, showing that although these two paralogues share many common functions, the mechanisms by which they execute their tumour suppressive role are surprisingly independent. LATS2 appears to have a much broader spectrum of binding partners, and consequently, a wider range of functions (Furth and Aylon, 2017). Consistent with their divergence in function, LATS1 and LATS2 are differentially regulated at the transcriptional, post-transcriptional and post-translational level. For example, a recent report showed that YAP directly up-regulates expression of *LATS2*, but not *LATS1*, in a negative feedback loop (Park *et al*., 2016).

LATS1/2 kinases are activated by direct MST1/2 phosphorylation within the hydrophobic motif site of their C-terminal catalytic domain (T1079 in LATS1), aided by binding of LATS1/2 to membrane-bound MOB1A/B, followed by LATS1/2 autophosphorylation within their activation loop site (S909 in LATS1) (Chan *et al.* 2005; Praskova *et al.*, 2008; Hergovich, Schmitz and Hemmings, 2006). Active LATS1/2 recognise and phosphorylate Serine residues within the NDR kinase consensus phosphorylation sequence HX(R/H/K)XX(S/T), with a preference for Serine

phosphorylation. LATS1/2 phosphorylate YAP at five Serine residues within HXRXXS consensus motif. Unlike other members of the ACG kinase family, the Histidine residue of this motif is critical for LATS phosphorylation (Hao *et al*., 2008).

LATS1/2 have many tumour-suppressive functions beyond YAP/TAZ phosphorylation, many of which are LATS1 or LATS2 specific. LATS1 localises to the centrosome during interphase, and is recruited to the mitotic apparatus during mitosis, where it binds to and is phosphorylated by CDK1 (Nishiyama *et al.,* 1999). Complex formation between Cyclin B/CDK1 and LATS1 inhibits CDK1 kinase activity, thereby supressing cell cycle progression at the G2/M transition, or promoting apoptosis (Tao *et al.*, 1999; Yang *et al.*, 2001). LATS2 is also recruited to the mitotic apparatus during mitosis, and regulates the cell cycle at the G1/S transition by inhibiting Cyclin E/CDK2 kinase activity (Li *et al*., 2003; Yabuta *et al.*, 2011). LATS2 was also found to localise to the centrosome throughout the cell cycle. During mitosis, LATS2 binds to and phosphorylates Ajuba, forming a complex that recruits γ-tubulin to the centrosome in order to regulate centrosome maturation and mitotic spindle arrangement (Abe *et al*., 2006). More recently, it was demonstrated that Aurora A phosphorylates LATS2 within its N-terminal region, resulting in translocation of LATS2 to chromosome-associated Aurora B during metaphase, and to the central spindle during anaphase. LATS1, in complex with LATS2, then phosphorylates Aurora B. This Aurora A-LATS1/2-Aurora B axis is proposed to prevent premature chromosome separation during mitosis (Yabuta *et al*., 2011).

Loss of *LATS1* or *LATS2*, but rarely both genes, results in tumour development. This was first shown in *LATS1* knockout mice, which develop ovarian stromal cell tumours and soft-tissue sarcomas and display hypersensitivity to carcinogenic agents (St John *et al.*, 1999). In accordance with their divergent functions, tumour types can be specific to loss of LATS1 or LATS2. For example, mutations and down-regulation of *LATS2* are specific to non-small cell lung cancer (Strazisar *et al.*, 2009; Yao *et al.*, 2015). In a tumorigenic *SAV1* knockout mouse model, tumour

progression was severely enhanced after deletion of *LATS2*, with only a mild effect seen after *LATS1* deletion (Park *et al*., 2016). *LATS1*/2 loss of heterozygosity and down-regulation have also been implicated in the tumorigenesis of other cancers including breast and cervical cancer (Fujii *et al.*, 1996; Deng *et al*. 2017).

1.8 Hippo and Hedgehog pathway crosstalk

The interaction between the Hippo pathway and Hedgehog signalling is largely unexplored, however recent work shows that these two signalling pathways do in fact interact. The first paper linking the Hippo pathway and Hedgehog signalling showed that YAP1 is amplified and up-regulated in SHH-subtype medulloblastoma. Accordingly, Shh up-regulates YAP1 expression and promotes its nuclear localisation in cerebellar granule neural precursors (CGNPs), leading to increased cell proliferation. This demonstrates that YAP1 can drive Shh-mediated medulloblastoma development (Fernandez-L *et al.*, 2008). This group also found that *Gli2* is a transcriptional target of YAP1-TEAD in CGNPs.

Both the Hedgehog and Hippo pathways are dependent on high cell density. For Hh signalling, this is due to the requirement of ciliogenesis for pathway function, which only occurs in quiescence, whereas the Hippo pathway is activated by high cell density due to its role in contact inhibition. This common dependence on cell contact prompted Tariki *et al.* (2014) to investigate the crosstalk between the two pathways. Interestingly, their data revealed that nuclear YAP1 binds to and represses Gli transcriptional activity in the absence of cell contact. Inversely, Hh signalling promotes YAP activity via post-transcriptional regulation to form a negative feedback loop (Tariki *et al.*,2014).

Hippo pathway components have been linked to primary cilia, which are essential for proper Hedgehog signal transduction. MST1/2-SAV1 localises to the basal body of primary cilia and promotes ciliogenesis by phosphorylating Aurora kinase A, causing dissociation of its cilia

disassembly complex with HDAX6, and by promoting ciliary localisation of IFT cargos in association with the NPHP transition-zone complex (Kim *et al.*, 2014). Both LATS1 and LATS2 localise to the centrosome and appear to have an indirect role in centrosome duplication (Hergovich, Cornils, and Hemmings, 2008). LATS2 is particularly important at the centrosome due to its role in recruiting γ-tubulin. Therefore, it is tempting to speculate that LATS1/2 function at primary cilia.

Research linking the Hippo pathway and Hedgehog signalling is on the rise. In the last year, at least two papers have reported that Hedgehog signalling positively regulates the Hippo pathway. In *Drosophila,* Hedgehog signalling was shown to act upstream of the Hippo pathway in regulating the maintenance of follicle stem cells by increasing the expression and nuclear localisation of YAP (Hsu *et al*., 2017). Most recently, Smo activation was found to increase YAP transcriptional activity in the epidermis, and YAP promotes epidermal GLI2 activation in basal keratinocytes through activation of β-catenin. This reciprocal positive regulation increases ROCK signalling, leading to dermal fibrosis and extracellular matrix remodelling in the development of basal cell carcinoma (Akladios *et al*., 2017).

1.9 Aims of the project

Considering the increasingly apparent crosstalk between the Hippo pathway and Hedgehog signalling, the overall aim of this project is to further characterise the interaction between these two cancer-linked signalling pathways. Within the conserved intrinsically disordered region of Sufu, already known to be critical in regulating its function, Serine 342 lies in a sequence that resembles the LATS kinase consensus phosphorylation site, HXRXXS (Figure 1.5). Therefore, this project tests the hypothesis that Sufu is regulated by LATS1/2 phosphorylation.

The initial aim of this project was to determine whether Sufu is phosphorylated by LATS1 or LATS2 at Serine 342 *in vivo*. Following confirmation that Sufu is a LATS kinase substrate, the

next aim was to investigate the effect of LATS1/2 phosphorylation on Sufu activity. Given that S342/S346 dual phosphorylation regulates the stability and ciliary localisation of Sufu, the effect of LATS1/2 phosphorylation on Sufu was determined by examining changes in Sufu protein levels and localisation within primary cilia. As Nek2A phosphorylation of S352 is known to stabilise Sufu, the project also aimed to determine whether LATS1/2 phosphorylation of Sufu affects the phosphorylation status at this closely distal site. Having established the regulatory role of LATS1/2 on Sufu activity, the final aim of this project was to investigate the effect of LATS1/2 phosphorylation on Sufu function by studying its ability to repress Gli-transcriptional activity.

SUFU_HUMAN

```
10         20         30         40         50
MAELRPSGAP GPTAPPAPGP TAPPAFASLF PPGLHAIYGE CRRLYPDQPN
        60         70         80         90        100
PLQVTAIVKY WLGGPDPLDY VSMYRNVGSP SANIPEHWHY ISFGLSDLYG
       110        120        130        140        150
DNRVHEFTGT DGPSGFGFEL TFRLKRETGE SAPPTWPAEL MQGLARYVFQ
       160        170        180        190        200
SENTFCSGDH VSWHSPLDNS ESRIQHMLLT EDPQMQPVQT PFGVVTFLQI
       210        220        230        240        250
VGVCTEELHS AQQWNGQGIL ELLRTVPIAG GPWLITDMRR GETIFEIDPH
       260        270        280        290        300
LQERVDKGIE TDGSNLSGVS AKCAWDDLSR PPEDDEDSRS ICIGTQPRRL
       310        320        330        340        350
SGKDTEQIRE TLRRGLEINS KPVLPPINPQ RQNGLAHDRA PSRKDSLESD
       360        370        380        390        400
SSTAIIPHEL IRTRQLESVH LKFNQESGAL IPLCLRGRLL HGRHFTYKSI
       410        420        430        440        450
TGDMAITFVS TGVEGAFATE EHPYAAHGPW LQILLTEEFV EKMLEDLEDL
       460        470        480
TSPEEFKLPK EYSWPEKKLK VSILPDVVFD SPLH
```

Figure 1.5 – The human Sufu protein sequence.
Serine 342 lies in a sequence that resembles the LATS kinase consensus phosphorylation site, HXRXXS (highlighted area with red star above S342). UniprotKB sequence for human Sufu (Isoform 1) accessed using: http://www.uniprot.org/uniprot/Q9UMX1#sequences

Chapter 2: Materials & Methods

2.1 Cell Lines and Reagents

HEK293T and ARPE-19 cell lines were purchased from ATCC (ATCC® CRL-3216™ and ATCC® CRL-2302™, respectively). Wild type (WT) and *Lats1/2*$^{-/-}$ mouse embryonic fibroblasts (MEFs) were a kind gift from Kun-Liang Guan (Mo *et al*., 2015). *Lats1/2*$^{-/-}$ MEFs were generated by infection of the Cre virus into *Lats1*$^{-/-}$ *Lats2*$^{fl/fl}$ MEFs, sourced from Dae-Sik Lim (Korea Advanced Institute of Science and Technology, Republic of Korea). WT and *Lats1/2*$^{-/-}$ MEFs were heavily infected with mycoplasma at the time they were obtained. These cells were treated using 25 µg/ml Plasmocin™ (#ant-mpt, InvivoGen) for two weeks, and tested negative using the PlasmoTest™ Mycoplasma Detection Kit (#rep-pt1, InvivoGen), prior to use in experiments. *Sufu*$^{-/-}$ MEFs were a kind gift from Dr. Stephan Teglund (Department of Biosciences and Nutrition, Karolinska Institutet, Sweden).

Small molecule Smoothened agonist (SAG) was purchased commercially (#4366, Tocris) in powder form and reconstituted in dimethyl sulfoxide (DMSO) (Sigma-Aldrich) to a stock solution of 200 µM. Small molecule Glycogen Synthase Kinase 3 (GSK3) inhibitor, SB216763, was obtained commercially (#120202, Abcam) in powder form and reconstituted in DMSO to a stock solution of 10 mM. Stock solutions in DMSO were aliquoted into Eppendorf tubes and stored at -20^{o}C.

Lambda Protein Phosphatase (LLP) was purchased commercially (#P0753S, New England Biolabs) in liquid form at 400,000 units/ml and stored at -80^{o}C prior to use. LLP was supplied with 10X NEBuffer for Protein MetalloPhosphatases and 10X $MnCl_2$, which were stored at -20^{o}C.

2.2 Cell Culture

HEK293T cells were grown in high glucose Dulbecco's Modified Eagle Medium (DMEM) (#D6429, Sigma-Aldrich) supplemented with 10% foetal bovine serum (FBS) (#F9665, Sigma-

Aldrich), 50 units/mL penicillin and 50 µg/mL streptomycin (#15070-063, Gibco). ARPE-19 cells were grown in DMEM/F-12 (1:1) containing L-Glutamine and 15 mM HEPES (#31330-038, Gibco) supplemented with 10% FBS (#10270-106, Gibco). MEFs were grown in DMEM containing 4.5 g/L D-Glucose and 0.11 g/L Sodium Pyruvate (#21969-035, Gibco), supplemented with 10% FBS. Sufu$^{-/-}$ MEF medium was supplemented with 20% FBS and 0.1 mM MEM Non-Essential Amino Acids (#11140-050, Gibco) to increase speed of cell growth. All cell lines were cultured in a humidified incubator at 37°C under 5% CO_2. During routine passage, cells were washed with sterilised PBS, incubated for 5 minutes in 0.25% Trypsin-EDTA (#25200-056, Gibco), and re-seeded into full medium as described. For storage, 1 - 1.5 million cells were resuspended in a mix of 90% FBS (#10270-106, Gibco) and 10% DMSO (Sigma-Aldrich), dispensed into 1.8 ml cryogenic tubes (Thermo Scientific™ Nunc™) and frozen at a rate of 1°C/minute to -80% in an isopropyl alcohol filled freezing container (Thermo Scientific™ Mr. Frosty™).

2.3 siRNA Knockdown

2.3.1 siRNA Sequences

LATS1 siRNA oligonucleotides, targeting human *LATS1* transcripts, were sourced from Eurofins Genomics. HPLC purified sihLATS1 was resuspended in RNase-free water into aliquots of 100 µM stock solution and stored at -20^{o}C.

Oligonucleotide sequences were:

Sense: 5’-GGUUCUGAGAGUAAAAUUAUU-3’ (RNA) 5’-TT-3’ (DNA)

Antisense: 5’-AAUAAUUUUACUCUCAGAACC-3’ (RNA) 5’-TT-3’ (DNA)

LATS2 siRNA oligonucleotides, targeting human *LATS2* transcripts, were initially sourced from Eurofins Genomics, ordered using a sequence found to effectively reduce LATS2 expression in Guo *et al*. (2015).

Oligonucleotide sequences, referred to as siRNA-1 (LATS2-homo-403) in this paper, were:

Sense: 5'-UACCAUAAAUACAAUCUUC-3'

Antisense: 5'-GAAGAUUGUAUUUAUGGA-3'

Desalted siRNA was resuspended in RNase-free water into aliquots of 100 µM stock solution, and stored at -20°C.

A siGENOME LATS2 siRNA SMARTpool (#M-003865-02-0005) was later obtained from Dharmacon, targeting five human accessions: NM_014572, XM_005266342, XM_017020542, XM_017020541 and XM_011535042. A dried pellet of 5 nmol siRNA was resuspended in RNase-free water into a 100 µM stock solution, and stored at -20°C. This SMARTpool was used for some knockdown experiments in ARPE-19 cells.

Ambion® Silencer® Select Pre-designed siRNA oligonucleotides, targeting human *SUFU* transcripts, were sourced from Life Technologies (supplied by Vincenzo D'Angiolella). siRNAs were resuspended in RNase-free water into aliquots of 10 µM stock solution and stored at -20°C.

Luciferase siRNA was used for control transfections. Dharmacon Luciferase Duplex (#P-002099-01-50) targets the oligonucleotide sequence: 5'-GCCAUUCUAUCCUCUAGAGGAUG-3'. The siRNA was resuspended in RNase-free water into aliquots of 100 µM stock solution and stored at -20°C.

2.3.2 siRNA Transfection

For forward siRNA transfections in ARPE-19 cells, 0.8-1 x 10^6 cells were seeded onto 6 cm plates (two per transfection condition) to achieve 60-80% confluence at the time of transfection. The following day, cells were transfected with 100 nM siRNA using Lipofectamine® 2000 (#11668-019, Invitrogen) in Opti-MEM® I Reduced Serum Medium (#11058-021, Gibco). In a sterile tube, a Lipofectamine® 2000 (Lipo 2000) master mix was made up by diluting Lipo 2000 in Opti-MEM®,

and incubated at room temperature for 5-10 minutes. Aliquots of stock siRNA were thawed from -20°C prior to transfection, and diluted in Opti-MEM® in separate sterile tubes. An equal volume of Lipo 2000 master mix was added to each diluted siRNA mix, pipetted up and down or vortexed to homogenise, and incubated at room temperature for 20 minutes. Media was aspirated away from each cell plate and replaced with 1.5 ml fresh penicillin/streptomycin-free media, then 500 µl of each siRNA and Lipo 2000 mix was added to two plates dropwise and swirled up and down to give an even coverage. This made the final volume of each plate up to 2 ml, containing approximately 2 µl siRNA stock and 5 µl Lipo 2000 per plate. Medium was replaced with fresh complete medium after 6-8 hours. Transfection was repeated the following day to improve knockdown. Cells were harvested 48-72 hours after the second transfection.

2.4 Plasmid DNA Transfection

2.4.1 Plasmids

Plasmids, kindly provided by Vincenzo D'Angiolella, were:

Empty Vector (GFP): pEGFP-C1 (Clontech) – Further details and plasmid map available at: https://www.addgene.org/vector-database/2487

HA-SUFU WT: Full-length human *SUFU* coding sequence (isoform 1, NCBI Reference Sequence: NM_016169.3), originally provided by Dr. Christian Siebold (Nuffield Department of Medicine, University of Oxford), was HA-tagged at the N-terminus and cloned into the pcDNA3.1 (+) vector.

HA-SUFU S342/6A and

HA-SUFU 351-353AAA: HA-tagged Sufu mutants were derived from the full-length construct, generated using the QuikChange site-directed mutagenesis kit (Stratagene).

2.4.2 Plasmid Transfection

HEK293T cells were seeded onto 10 cm plates to achieve 60-70% confluence at the time of transfection. Transfection of 5 µg plasmid DNA was performed using Polyethylenimine (PEI, #23966, Polysciences, Inc.). Volumes of plasmid, containing 5 µg DNA, were diluted in penicillin/streptomycin-free media up to a total volume of 400 µl in Eppendorf tubes, and mixed thoroughly by vortexing. PEI solution (2.5 mg/ml) was pre-warmed to 37^{o}C and mixed by vortexing, then 15 µl was added to the diluted DNA (3 µl PEI: 1 µg DNA). The DNA/PEI mix was then incubated for 15 minutes at room temperature. Cells were washed with PBS and 10 ml fresh complete medium was added to the plate prior to addition of DNA/PEI mixes in a dropwise manner. Plates were swirled thoroughly to evenly distribute the DNA/PEI mix before incubating the plates at 37^{o}C. Medium was changed after 12 hours and cells were harvested after a minimum of 30 hours. Green Fluorescent Protein (GFP) transfected cells were visualised using a ZOE™ Fluorescent Cell Imager (#145-0031, Bio-Rad) to determine the transfection efficiency. One plate of cells was left untransfected as an IgG control plate for Immunoprecipitation.

2.5 Protein Extraction

2.5.1 Protein Extraction from Monolayer Cultures

Cells growing on cell culture plates were harvested after the desired treatment or once confluent. Medium was removed from the cells, which were then washed twice in ice-cold PBS. Any coverslips on the plates were removed after the second wash. Cells were then scraped from the plate surface, collected in <1 ml ice-cold PBS, and transferred to clean Eppendorf tubes.

If cells were being taken for RNA extraction, cells were lifted from the culture dish using Trypsin. After removal of media and washing in PBS, they were incubated for 5 minutes in 0.25%

Trypsin-EDTA (#25200-056, Gibco). Once the cells had detached from the dish, the trypsin was neutralised with full medium (as described above) and cells were transferred to a clean 15 ml falcon tube. The cell suspension was homogenised by pipetting or inversion, cells were counted using a haemocytometer, and the volume of homogenised cell suspension containing approximately 50,000 cells was transferred to a clean Eppendorf tube. The remaining cell suspension was centrifuged at 250 x g for 5 minutes, resuspended in 1 ml ice-cold PBS, and transferred to a clean labelled Eppendorf tube for protein extraction.

Cell suspensions were centrifuged at 500 x g for 5 minutes at 4^{o}C. PBS supernatant was aspirated from the cell pellets, which were resuspended in ice-cold SDS lysis buffer (approximately 3 times the volume of the cell pellet). SDS lysis buffer contains 50 mM Tris-HCl, 2% w/v sodium dodecyl sulphate (SDS), cOmplete™ protease inhibitor cocktail (#04693116001, Roche) and PhosSTOP™ phosphatase inhibitor cocktail (#04906837001, Roche). Tubes of resuspended cells were inverted for a minimum of 30 minutes at 4^{o}C or sonicated at low power for a minimum of 10 pulses, then centrifuged at 20,000 x g for 20-30 minutes at 4^{o}C. Supernatants of cell lysate were collected and transferred to clean tubes, then stored at -20^{o}C.

2.5.2 Cell Lysate Protein Quantification

Cell lysates were boiled at 95^{o}C for 15 minutes to solubilise the lysis buffer prior to quantification of protein concentration using either the NanoDrop™ 1000 (ThermoFisher Scientific), Pierce™ Coomassie Plus (Bradford) Assay Kit (#23236, ThermoFisher Scientific), or DC™ protein assay (#5000111, Bio-Rad), according to the manufacturer's protocol. Lysates were then diluted in 4x NuPAGE™ LDS Sample Buffer (#NP0007, Invitrogen) containing 100 µM DL-Dithiothreitol (DDT, #43815, Sigma-Aldrich) and distilled water to make up SDS-PAGE loads with an equal amount of protein (typically 20-40 µg) in each sample.

2.6 Immunoprecipitation

Medium was removed from the cells, which were then washed in ice-cold PBS, scraped from the plate surface in 1 ml ice-cold PBS, collected and transferred to clean Eppendorf tubes. Tubes of cells were placed on ice, then centrifuged at 500 x g for 5 minutes at 4°C. PBS supernatant was aspirated away and cell pellets were placed on ice. Cells were resuspended in ice-cold PBS, centrifuged again, and PBS supernatant was removed. Cell pellets were placed on dry ice until lysis.

Immunoprecipitation (IP) Lysis buffer, containing 50 mM Tris (pH 7.5) in ultrapure water, 150 mM NaCl, 0.1% NP40 or Triton X-100, 10% Glycerol, 1 mM EDTA and 5 mM $MgCl_2$, was supplemented with addition of the following inhibitors immediately before use: 1mM DTT, 1 mM PMSF, 1:500 Protease Inhibitor Cocktail (#P8340, Sigma-Aldrich), 20 mM β-Glycerol Phosphate and 10 nM Okadaic Acid. Cell pellets were left to defrost slowly on ice, then resuspended in ice-cold IP lysis buffer (approximately 3 times the volume of the cell pellet). Tubes were then centrifuged at maximum speed for 10 minutes at 4°C. Supernatants of cell lysate were transferred to clean Eppendorf tubes and mixed by pipetting before transferring approximately 50 µl to clean tubes for protein quantification and loading of input samples. Immunoprecipitation of HA-tagged proteins (in the remaining volume of cell lysate) was performed using EZview™ Red Anti-HA Affinity Gel (#E6779, Sigma-Aldrich). The anti-HA monoclonal antibody bound agarose beads were washed in lysis buffer to remove ethanol, then resuspended in ice-cold lysis buffer and equal volumes were added to each tube of cell lysate. These tubes were then inverted at 4°C for between 1 and 3 hours. Following this, lysis buffer was aspirated away and the beads were washed three times in 800 µl ice-cold lysis buffer. NuPAGE™ LDS Sample Buffer with 1M DDT and distilled water were added to the cell lysate and immunoprecipitated protein tubes to make up SDS-PAGE loads.

2.7 Lambda Protein Phosphatase Assay

Lambda Protein Phosphatase (LLP) was used to test for antibody phospho-specificity. MEF cell lysates were homogenised by pipetting, then split into two equal volumes in Eppendorf tubes. To set up the reaction conditions, 10X NEBuffer for PMP (approximately 1 µl/ µg protein) and 10 mM $MnCl_2$ (1/10 of total volume for 1 mM final concentration) were added to each tube of cell lysate. Approximately 300 units of LLP were added one tube of each cell lysate and all tubes were incubated at 30°C for 1 hour. Cell lysates were then boiled at 95°C, before quantification of protein concentration using NanoDrop™ 1000, and adding of NuPAGE™ LDS Sample Buffer containing 100 µM DDT and distilled water to make up SDS-PAGE loads.

2.8 Sodium Dodecyl Sulphate Polyacrylamide Gel Electrophoresis (SDS-PAGE) and Electrotransfer

NuPAGE™ 4-12% Bis-Tris protein gradient gels were obtained commercially (#NP0321BOX/# NP0336BOX, Invitrogen) and stored at 4°C. Prior to loading, sample tubes were boiled at 95°C for 5-10 minutes. The pre-cast gels were warmed to room temperature, plastic combs were removed, and wells were washed out with distilled water before inserting into an XCell SureLock™ Mini-Cell tank (Life Technologies). The tank was then filled with 1X NuPAGE™ MOPS SDS Running Buffer (#NP000102, Invitrogen). Boiled samples were centrifuged at 2000 x g for 1 minute. When loading, 5 µl Precision Plus Protein™ Dual Color Standard (#1610374, Bio-Rad) or SeeBlue™ Plus2 Pre-stained Protein Standard (#LC5925, Invitrogen) was pipetted into the first lane of the each gel, followed by each sample (typically 20-40 µg). Any empty lanes were filled with 1X LDS Sample Buffer. The gel was connected to a power pack and run at 100V until the samples had passed through the stacking gel, then at 120V until samples had reached the bottom and the desired separation of standard bands had been reached.

Separated proteins in the gel were transferred to methanol activated Immobilon®-P PVDF Membrane (#IPVH00010, Millipore) by wet transfer using the Mini Trans-Blot® Electrophoretic Transfer Cell (#1703930, Bio-Rad), following the manufacturer's instructions. Transfer buffer, containing 25 mM Tris-HCL (pH 8.3), 190 mM glycine, and 20% v/v MeOH, was cooled to 4°C prior to use. The blot was run at 100V for 80 minutes, with an ice pack inside the tank to avoid overheating, and kept on a magnetic stirrer plate to maintain an even buffer temperature and ion distribution in the tank.

2.9 Western Blotting

After removal from the electrotransfer apparatus, membranes were washed in distilled water, then stained with Ponceau S Solution (#P7170-1L, Sigma-Aldrich) for up to 1 minute to visualise the protein bands, checking for equal sample loading. Membranes were then washed in distilled water to remove excess Ponceau S Solution and cut into sections so that each protein to be probed for is on a separate section of membrane. Membranes were washed in PBS/0.1% Tween-20 (PBST) to remove residual Ponceau S Solution before blocking in 5% w/v BSA (#A3059-100G, Sigma-Aldrich) or 5% w/v non-fat milk (Marvel) for 1 hour. Blocked membranes were then incubated in primary antibodies, diluted in blocking solution, overnight at 4°C. The following day, membranes were washed three times in PBST for 7-10 minutes, incubated in diluted horseradish peroxidase (HRP) conjugated secondary antibodies for 1 hour, and then washed in PBST another three times. Pierce™ ECL Western Blotting Substrate (#32106, Thermo Scientific) was used for signal detection, following the manufacturer's instructions. Blotted proteins were visualised by exposing the membranes to CL-XPosure™ Film (#34091, Thermo Scientific) in a dark room.

2.9.1 Antibodies

Target/ Name	Species	Clonality & Isotype	Company	Catalogue Number	Dilution
Primary Antibodies					
Actin	Goat	Polyclonal IgG	Santa Cruz	sc-1616	1:2000
GAPDH	Mouse	Monoclonal IgG1	Cell signalling	97166	1:2000
HA-tag	Mouse	Monoclonal IgG3	Millipore	05-904	1:2000
LATS1	Rabbit	Polyclonal IgG	Bethyl Laboratories	A300-477A	1:1000
LATS2	Rabbit	Polyclonal IgG	Novus Biologicals	NB200-199	1:1000
SUFU	Rabbit	Monoclonal IgG	Cell Signalling Technology	2522	1:1000
SUFU (P-S342)	Rabbit	Polyclonal IgG	Signalway Antibody	11552	1:1000
SUFU (P-S352, P-T353)	Rabbit	Polyclonal IgG	YenZym Antibodies, LLC.	Custom made*	1:1000
Secondary Antibodies					
Anti-Rabbit IgG, (HRP-linked)	Goat	Polyclonal IgG	Santa Cruz	sc-2030	1:5000
Recombinant Protein A/G, Peroxidase Conjugated	-	-	Thermo Scientific	32490	1:5000
Anti-Mouse IgG (HRP-linked)	Goat	Polyclonal IgG	Thermo Scientific	31430	1:5000

*For Raducu et al., (2016). Sufu (P-S352, P-S353) antibody was affinity-purified against the phosphorylated Human peptide #347~360: CLESDS-pS-pT-AIIPHEL, and absorbed against non-phosphorylated peptide CLESDSSTAIIPHEL, to ensure the specific recognition of phosphorylated Sufu.

2.9.2 Statistical Analysis

Quantitative analysis of western blot band intensity (measured as mean grey value) on scanned film was performed using Image J software. Relative band intensities were calculated using the following formulas:

$$\text{Net band intensity} = \frac{(255 - \text{band value})}{(255 - \text{background value})}$$

$$\text{Relative band intensity} = \frac{\text{Net band intensity of protein of interest}}{\text{Net band intensity of loading control}}$$

Relative band intensities were expressed relative to the band intensity of the appropriate control condition. Statistically significant differences were determined using an unpaired Student's t-test.

2.10 Immunofluorescence

Sterile glass coverslips were placed into 6 or 10 cm cell culture plates or 6-well plates when seeding cells (ARPE-19 and MEFs) for appropriate experiments. Cells were cultured until at high confluence and serum starved in 0-0.1% FBS DMEM for 24-48 hours prior to harvest. Coverslips were then transferred to a clean 12- or 24-well plate and washed in PBS. Some coverslips were washed in PHEM buffer (50 mM PIPES, 25 mM HEPES, 10 mM EGTA and 10 mM $MgSO_4$, pH adjusted to 7 with addition of NaOH or KOH). All coverslips were washed again in PBS, then fixed with 4% paraformaldehyde for 5 minutes at room temperature. Coverslips were washed three times with 0.3% Triton™ X-100 (#BP151-100, Fisher BioReagents™) in PBS for 1 minute on a rocking incubator, then cells were fixed in ice-cold 100% methanol for 5 minutes at -20^{o}C. Coverslips were washed three times with 0.3% Triton X-100 in PBS before permeabilisation with 0.5% Triton X-100 in PBS for 10 minutes. Coverslips were washed once more with 0.3% Triton X-100 in PBS prior to blocking for 2 hours at room temperature. Blocking solution consisted of 0.3% Triton X-100, 3% BSA and 5% goat serum in PBS. Blocked coverslips were washed three times with 0.3% Triton X-100 in PBS, then incubated with primary antibodies, diluted in blocking solution, overnight in darkness at 4^{o}C. The following day, coverslips were washed five times with 0.3% Triton X-100 in PBS, then incubated with secondary antibodies, diluted in blocking solution, for 2 hours in darkness at room temperature. Coverslips were washed twice with 0.3% Triton X-100 in PBS before mounting onto labelled microscope slides with ProLong™ Gold Antifade Mountant with DAPI (#P36935, Life Technologies).

2.10.1 Antibodies

Target (+ Conjugate)	Species	Clonality & Isotype	Company	Catalogue Number	Dilution
Primary Antibodies					
Acetylated-alpha-tubulin	Mouse	Monoclonal IgG2b	Sigma-Aldrich	T7451	1:2000
Gamma-tubulin	Mouse	Monoclonal IgG1	Sigma-Aldrich	T5326	1:1000
LATS1	Rabbit	Polyclonal IgG	Bethyl Laboratories	A300-477A	1:100
SUFU	Rabbit	Monoclonal IgG	Cell Signalling Technology	2522	1:100
SUFU (P-S342)	Rabbit	Polyclonal IgG	Signalway Antibody	11552	1:100
SUFU (P-S352, P-T353)	Rabbit	Polyclonal IgG	YenZym Antibodies, LLC.	Custom made*	1:100
Secondary Antibodies					
Anti-Rabbit IgG (Alexa Fluor® 488)	Goat	Polyclonal IgG	ThermoFisher Scientific	#A-11034	1:500
Anti-Mouse IgG1 (Alexa Fluor® 647)	Goat	Polyclonal IgG	ThermoFisher Scientific	#A-21240	1:500
Anti-Mouse IgG2b (Alexa Fluor® 568)	Goat	Polyclonal IgG	ThermoFisher Scientific	#A-21144	1:500

*For Raducu *et al*., (2016). Sufu (P-S352, P-S353) antibody was affinity-purified against the phosphorylated Human peptide #347~360: CLESDS-pS-pT-AIIPHEL, and absorbed against non-phosphorylated peptide CLESDSSTAIIPHEL, to ensure the specific recognition of phosphorylated Sufu.

2.10.2 Confocal Fluorescence Microscopy

Fluorescently labelled cells were imaged using Zeiss LSM 780 or 710 confocal laser scanning microscopes at 100x magnification. Appropriate fields of view were located using the Cyanine 3 (Cy3) laser. Z-stacks were taken through each sample, encompassing the entire thickness of each primary cilium in that field of view. Settings for the 488 nm laser were kept consistent when imaging each coverslip with the same primary antibodies. Maximum intensity projections of each Z-stack were created using ZEN black edition software.

2.10.3 Image analysis

Mean immunofluorescence intensity values were generated on Image J software by Dr Rhodri Wilson, using the following analysis pipeline:

Violet (633 nm) channel - “centrosomes”

Red (594 nm) channel - “primary cilia”

Green (488 nm) channel - “Sufu”

Blue (405 nm) channel - nucleus (Not used)

1. Open image
2. Split into colour components
3. Segment primary cilia and centrosomes using an Otsu global threshold.
4. Calculate distance transform between centrosomes and primary cilia; use minimum distances to associate centrosomes with primary cilia. Discard primary cilia without centrosomes and centrosomes without primary cilia.
5. Determine primary cilia regions - base, through and tip - using the distance transform within the segmented cilia.
6. Measure intensity of Sufu in each region of the primary cilia, calculate mean intensity for each region type.
7. Store values, close all images.

Statistical analysis of mean intensity values was performed by expressing intensity values as a percentage relative to the intensity of the appropriate control condition and pooling these values over four experiments. Statistically significant differences were determined using an unpaired Student’s t-test, comparing the mean intensity values of the experimental condition to the mean intensity values of the control condition.

2.11 RNA Extraction

Eppendorf tubes containing approximately 50,000 cells in full medium (as described above in section 2.5.1) were centrifuged at 500 x g for 5 minutes at 4°C. The supernatant of medium was aspirated from each cell pellet, which was then resuspended in 50 µl of ice-cold PBS. The tubes were centrifuged again (5 minutes at 500 x g, 4°C) and PBS supernatant was aspirated away. Cell lysis for RNA extraction was performed using the Power SYBR™ Green Cells-to-CT™ Kit (#4402953, Life Technologies). Cell pellets were thoroughly resuspended in 25 µl ice-cold Lysis Solution (containing 1:1000 diluted DNase I) and incubated for 5 minutes at room temperature. To inactivate the lysis reagents, 2.5 µl ice-cold Stop Solution was added and mixed in thoroughly by pipetting. Tubes were incubated at room temperature for 2 minutes before proceeding to reverse transcription, or storing the RNA lysates at -20°C.

2.12 Reverse Transcription

RNA lysates were reverse transcribed to synthesise complementary DNA (cDNA) using the Power SYBR™ Green Cells-to-CT™ Kit (#4402953, Life Technologies). For each 25 µl reaction, 2.5 µl RNA lysate was added to 22.5 µl of RT master mix (containing 12.5 µl 2X SYBR RT Buffer, 1.25 µl 20X RT Enzyme Mix and 8.75 µl nuclease-free water) in PCR tubes and mixed thoroughly. PCR tubes were centrifuged briefly before inserting into a MyCycler™ Thermal Cycler System (#1709703, Bio-Rad), programmed with the protocol: 37°C for 60 minutes, 95°C for 5 minutes, then 4°C once complete. Tubes of cDNA were then placed on ice to proceed with qRT-PCR or stored at -20°C.

2.13 Real Time quantitative Polymerase Chain Reaction (qRT-PCR)

2.13.1 Primer Sequences

Primer pair sequences were found using the PrimerBank public resource (found at https://pga.mgh.harvard.edu/primerbank/index.html) and used to design primer pairs, ordered from Sigma-Aldrich. Primer pairs, supplied in solution at 100 µM, were diluted 1/10 in nuclease-free water (10 µl forward primer, 10 µl reverse primer, 80 µl water) to give a 10 µM final concentration of each primer. Primer oligonucleotide sequences were:

LATS2 (Human)

Primer Pair 1:

Forward: 5'- ACTTTTCCTGCCACGACTTATTC -3'

Reverse: 5'- GATGGCTGTTTTAACCCCTCA -3'

Primer Pair 2:

Forward: 5'- ACCCCAAAGTTCGGACCTTAT -3'

Reverse: 5'- CATTTGCCGGTTCACTTCTGC -3'

GLI1 (Mouse)

Primer Pair 1:

Forward: 5'- CCAAGCCAACTTTATGTCAGGG -3'

Reverse: 5'- AGCCCGCTTCTTTGTTAATTTGA -3'

Primer Pair 2:

Forward: 5'- GACTTTCTGGTCTGCCCTTTT -3'

Reverse: 5'- AGCCCGCTTCTTTGTTAATTTGA -3'

PTCH1 (Mouse)

Primer Pair 1:

Forward: 5'- GCCTTCGCTGTGGGATTAAAG -3'

Reverse: 5'- CTTCTCCTATCTTCTGACGGGT -3'

Primer Pair 2

Forward: 5'- AAAGAACTGCGGCAAGTTTTTG -3'

Reverse: 5'- CTTCTCCTATCTTCTGACGGGT -3'

GAPDH

Mouse Primer Pair:

Forward: 5'- CTCCACTCACGGCAAATTCA -3'

Reverse: 5'- CGCTCCTGGAAGATGGTGAT -3'

Human Primer Pair:

Forward: 5'- AATCCCATCACCATCTTCCA -3'

Reverse: 5'- TGGACTCCACGACGTACTCA -3'

GAPDH was used as the housekeeping gene endogenous control, use to normalise quantitation of mRNA expression for differences in the amount of cDNA sample added to each reaction.

2.13.2 qRT-PCR Cycles for Relative Gene Expression

Prior to the PCR reaction, cDNA samples were diluted ¼ in nuclease-free water (25 µl cDNA in 75 µl water). For each 10 µl reaction in MicroAmp™ Optical 96-Well Reaction Plates (#4306737, Applied Biosystems™), 4 µl of diluted cDNA was added to 5 µl Power SYBR green PCR Master Mix (#4367659, Applied Biosystems™), 0.2 µl of the relevant 10 µM primer pair mix and

0.8 µl nuclease free water. Reaction plates were sealed with MicroAmp™ optical adhesive film and centrifuged at 1700 x g for 1 minute. PCR cycles were run on either a StepOnePlus™ Real-Time PCR System (#4376600, Applied Biosystems™) or a 7500 Fast Real-Time PCR System (#4351107, Applied Biosystems™) at standard speed. Cycle conditions were: 10-minute hold at 95 °C, followed by 40 cycles of 15 seconds at 95°C, 1 minute at 60 °C. Each reaction condition was performed in triplicate, plus a negative control without cDNA sample for each primer pair. Quantification of target mRNA expression, relative to *GAPDH*, was done using the $2^{-\Delta CT}$ method (Livak and Schmittgen, 2001):

$$\Delta C_T = C_T\,(\text{target}) - C_T\,(\textit{GAPDH})$$

where C_T = cycle threshold (number of cycles required for the fluorescent signal to cross the threshold)

Relative fold changes in mRNA expression were pooled over three experiments, and statistically significant fold change values were determined using an unpaired Student's t-test on GraphPad Prism 6 (GraphPad Software, Inc.).

Chapter 3: Results

3.1 Part I – Investigation of Sufu as a potential substrate of LATS1/2

3.1.1 Introduction

Large Tumour Suppressor (LATS) kinases, LATS1 and LATS2, are homologous Serine/Threonine kinases that belong to the Nuclear Dbf2-Related (NDR) kinase subgroup of the AGC kinase family. The LATS/NDR kinase family subgroup recognise and phosphorylate substrates with the consensus sequence HX(R/H/K)XX(S/T), with a preference for Serine phosphorylation. LATS1 and LATS2 interact with and phosphorylate YAP/TAZ at Serine residues in five different sites, all five of which are within a HXRXXS motif (Zhao *et* al., 2007; Hao *et al*., 2008). Within a conserved region of Suppressor of Fused (Sufu), Serine 342 (S342) lies within a sequence that bears strong resemblance to this HXRXXS motif. Given the recent links made between Hippo and Hedgehog signalling, it was hypothesised that LATS1/2 may regulate Sufu by phosphorylation at S342.

3.1.2 Knockdown of *LATS1* and *LATS2* in ARPE-19 cells

To determine whether Sufu is regulated by LATS1/2 phosphorylation, single and combined gene knockdown of *LATS1* and *LATS2* was achieved by siRNA transfection in a human retinal pigmented epithelium (RPE) cell line, ARPE-19 (Figure 3.1). The siRNA transfection procedure was performed twice to improve knockdown. Cells transfected with siRNA targeting Luciferase were used as a control. RPE cells were chosen for these experiments as they are widely used in the study of the primary cilia. They readily form cilia in response to serum starvation, with

full ciliation being achieved within 48 hours (Plotnikova *et al*., 2009). Therefore, these cells are useful for investigating changes in protein ciliary localisation.

Initially, LATS1/2 depletion was tested with or without addition of smoothened agonist (SAG), a potent activator of Hedgehog signalling, to the culture medium 24 hours prior to harvest. Here, treatment with SAG was primarily used for the study of Sufu ciliary localisation by immunofluorescence. However, lysates of cells treated with SAG were loaded on the same SDS-PAGE gel, alongside those without SAG treatment, to confirm knockdown of *LATS1* by western blot (Figure 3.1A). Densitometric analysis revealed a 60-80% reduction in LATS1 protein levels, compared to control cells, when treated with SAG. The western blot membrane was also probed for LATS2, but unfortunately the bands observed did not resolve well enough for analysis of protein levels. Therefore, knockdown of *LATS2* was confirmed by qRT-PCR analysis of mRNA expression (Figure 3.1B), which showed that *LATS2* mRNA expression was 65-80% lower in cells transfected with siRNA targeting *LATS2* transcripts, relative to control cells. Levels of Sufu and S342 or S352 phosphorylated Sufu were also detected and quantified (discussed in 3.1.3 and 3.1.6).

3.1.3 LATS2 phosphorylates Sufu at S342

Chen *et al.* (2011) showed that GSK3β phosphorylates Sufu at S342, after a priming phosphorylation at S346 by PKA, and that inhibition of GSK3β using SB216763 abolished phosphorylation of endogenous Sufu at S342. Therefore, single and combined siRNA-mediated gene knockdown of *LATS1* and *LATS2* was performed in ARPE-19 cells as before, and cells were subsequently treated for 24 hours with the same GSK3 inhibitor, SB216763 (Figure 3.2). To assess the phosphorylation status of Sufu at S342, Chen *et al.* (2011) generated an antibody that specifically recognises the S342 phosphorylated form of Sufu and is able to recognise endogenous Sufu. Using the same antibody, levels of S342 phosphorylated Sufu (P-S342 Sufu) were compared by western blot analysis, using treatment with SB216763 for 24 hours as the experimental control

(Figure 3.2A). This enabled the relative contribution of GSK3β and LATS1/2 on S342 phosphorylation to be examined empirically.

Analyses of S342 phosphorylated Sufu levels by western blot in three independent experiments were quantified (Figure 3.2B). In agreement with Chen et al. (2011), inhibition of GSK3 (GSK3i), drastically reduced phosphorylation of endogenous Sufu at S342 (approximately 60% reduction). This confirms that GSK3β is the dominant kinase acting at this site. Significant reductions in levels of S342 phosphorylated Sufu were observed after LATS2 knockdown (~50% reduction), indicating that LATS2 phosphorylates Sufu at S342. In contrast, only slight reductions in S342 phosphorylation were detected after LATS1 knockdown (~10% reduction), but combined LATS1/2 knockdown resulted in a more dramatic decrease than LATS2 knockdown alone (significant in presence of GSK3i). This suggests that there may be some redundancy in function between LATS1 and LATS2 at this site.

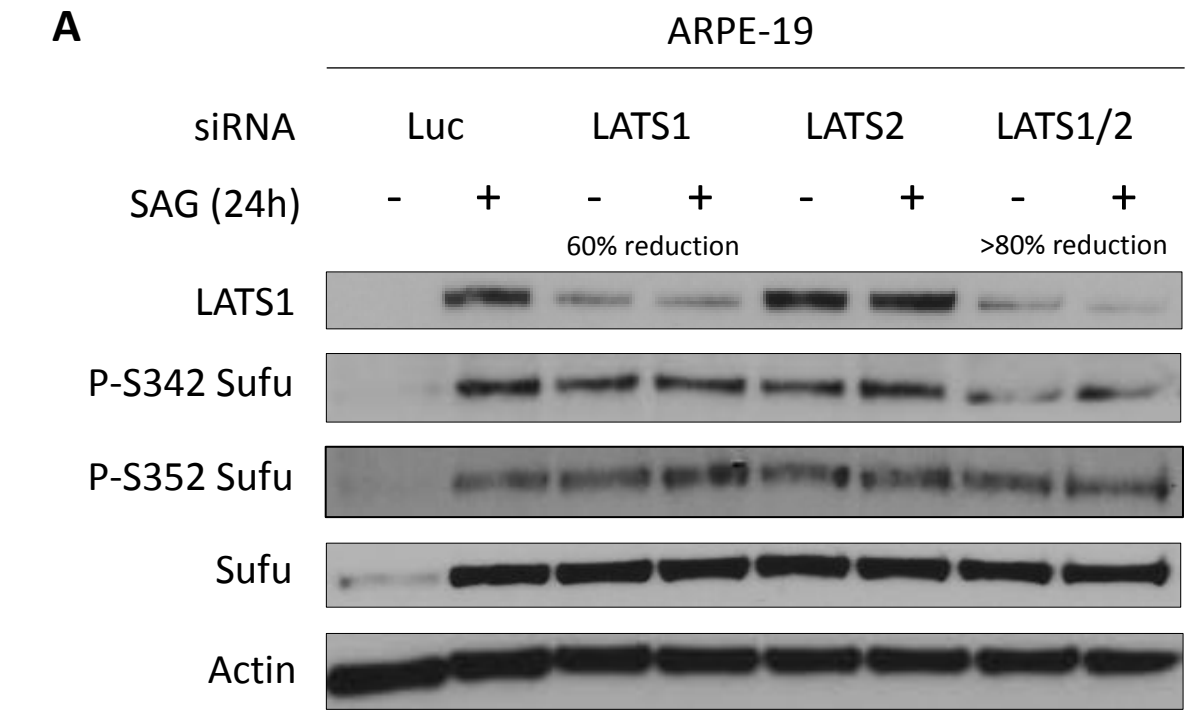

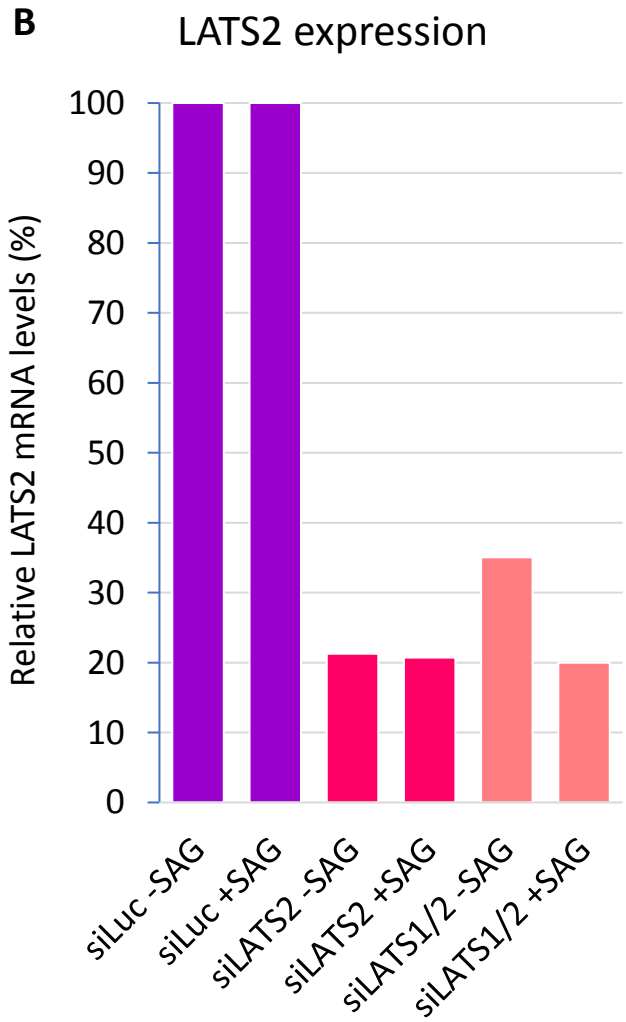

Figure 3.1 – Knockdown of LATS1/2 in ARPE-19 cells.

Single or combined siRNA-mediated gene knockdown of *LATS1* and *LATS2* in ARPE-19 cells, with or without the addition of 200 nM Smoothened agonist (SAG), a potent activator of Hedgehog signalling. Control cells were transfected with siRNA targeting Luciferase (Luc). Cells were serum starved in 0.1% FBS DMEM for 24-48 hrs and treated with SAG for 24 hrs prior to harvest.

(A) Analysis of LATS1, Sufu, S342 phosphorylated Sufu (P-S342 Sufu) and S352 phosphorylated Sufu (P-S352 Sufu) in cell lysates by western blot. Quantification of LATS1 bands, relative to Actin loading control, was performed on Image J, and the reduction in protein levels are labelled above the relevant pair of bands. Image is representative of three independent experiments.

(B) Quantification of LATS2 mRNA levels, relative to control cells (siLuc +/-SAG), confirming between 65-80% reduction in LATS2 mRNA expression.

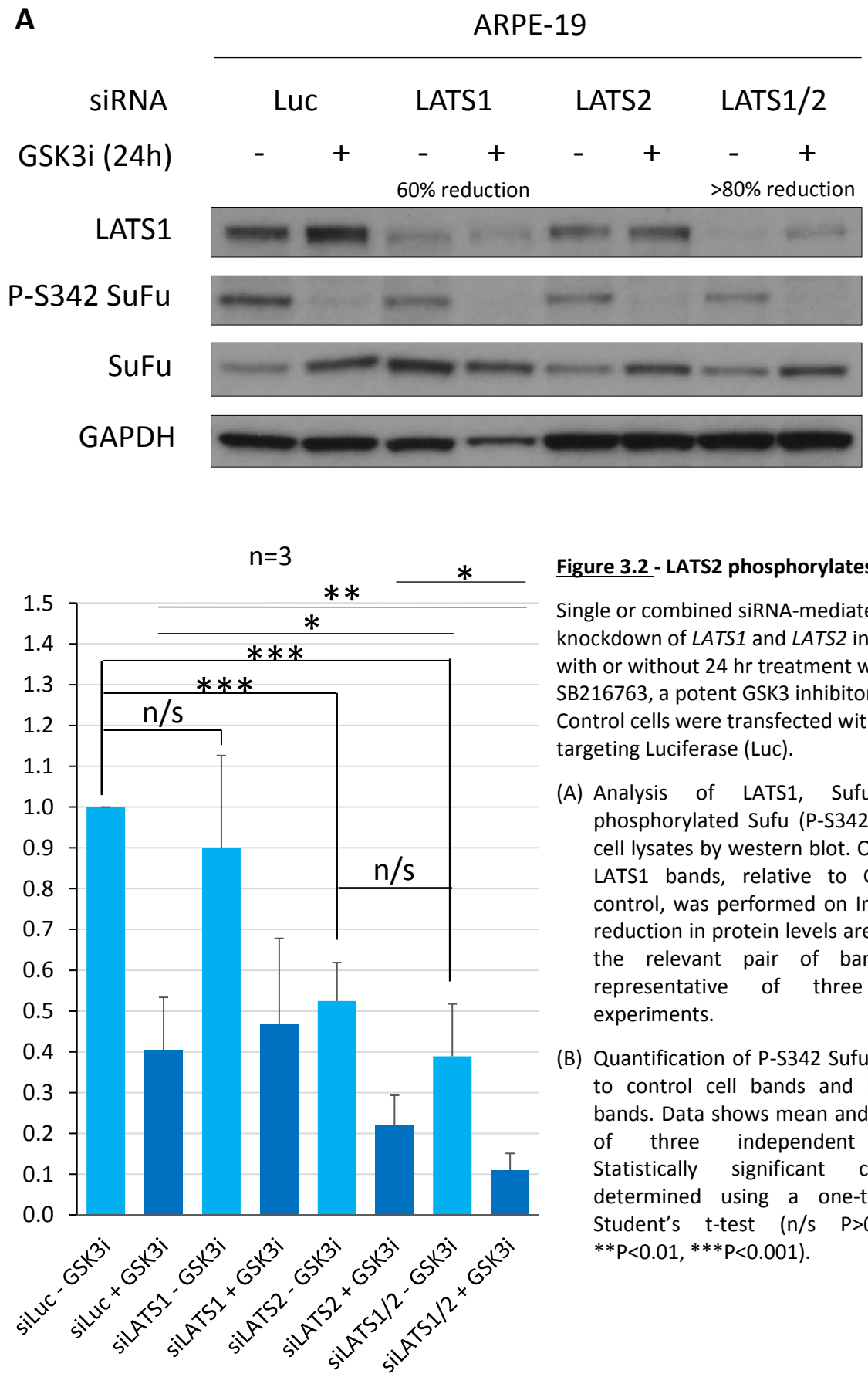

Figure 3.2 - LATS2 phosphorylates Sufu at S342

Single or combined siRNA-mediated gene knockdown of *LATS1* and *LATS2* in ARPE-19 cells, with or without 24 hr treatment with 10 µM SB216763, a potent GSK3 inhibitor (GSK3i). Control cells were transfected with siRNA targeting Luciferase (Luc).

(A) Analysis of LATS1, Sufu, and S342 phosphorylated Sufu (P-S342 Sufu) levels in cell lysates by western blot. Quantification of LATS1 bands, relative to GAPDH loading control, was performed on Image J, and the reduction in protein levels are labelled above the relevant pair of bands. Image is representative of three independent experiments.

(B) Quantification of P-S342 Sufu bands, relative to control cell bands and loading control bands. Data shows mean and SD (error bars) of three independent experiments. Statistically significant changes were determined using a one-tailed unpaired Student's t-test (n/s P>0.05, *P<0.05, **P<0.01, ***P<0.001).

3.1.4 LATS2 interacts with Sufu

To test for an interaction between LATS1/2 and Sufu, the presence of endogenous LATS1 or LATS2 in HA-tagged Sufu immunoprecipitates was determined by western blot analysis. HEK293T cells were transfected with plasmids containing HA-tagged full length Sufu. Untransfected cells were used as a negative control to detect non-specific rabbit immunoglobulin G (IgG), and cells transfected with empty vector (EV) plasmids containing a GFP tag were used to determine the transfection efficiency. Visualisation of these cells 48 hours post-transfection indicated that the transfection was successful and that the transfection efficiency was very high (Figure 3.3A). HA-tagged proteins were isolated by immunoprecipitation (IP). Western blot analysis showed that the IP was successful as the bands of HA-tag and Sufu protein are lost in the IgG and EV (GFP) controls, but very strong signal is detected in the HA-Sufu transfected cells (Figure 3.3B). Although the bands observed do not resolve well, endogenous LATS2 could be weakly detected in HA-tagged Sufu immunoprecipitates, whereas LATS1 could not be detected, suggesting that LATS2 interacts with Sufu. This corresponds with the finding that LATS2 is dominant over LATS1 in phosphorylation of Sufu at S342. The very low level of LATS2 detected, and lack of LATS1 detection, could be explained by the transient nature of kinase binding to substrate. If time allowed, optimisation of the IP methodology, and use of a higher concentration of LATS1 and LATS2 antibodies in western blotting may have improved detection.

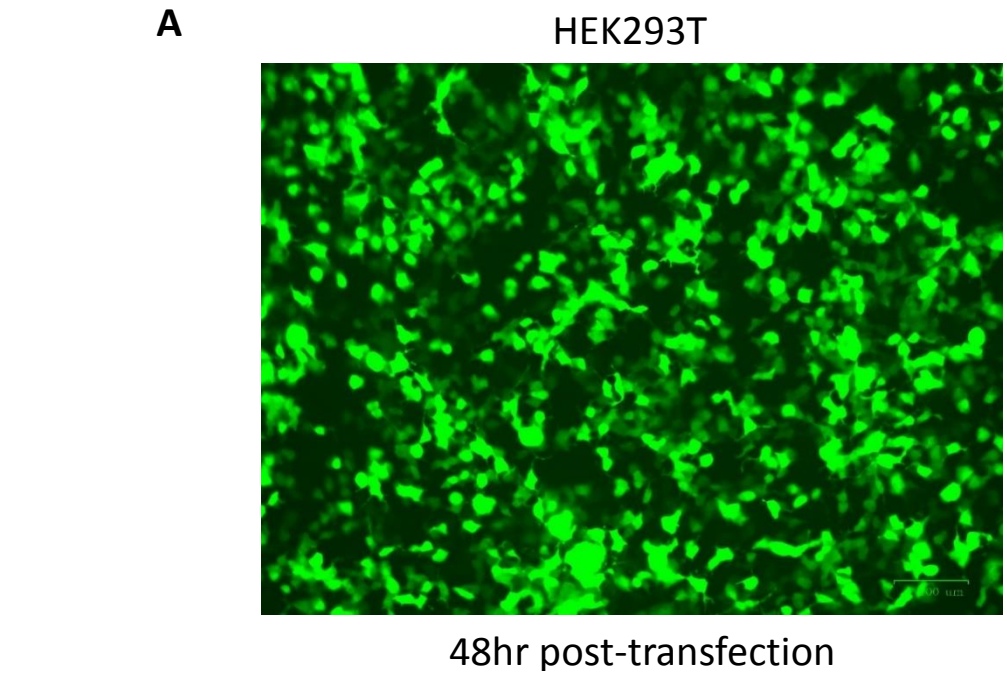

<u>Figure 3.3</u> – LATS2 interacts with Sufu

(A) Visualisation of HEK293T cells transfected with plasmids containing a Green Fluorescent Protein (GFP) tag to determine the transfection efficiency. Image taken 48 hours post-transfection.

(B) Detection of LATS2 in immunoprecipitates of HA-tagged Sufu in HEK293T cells by western blot. Cells were either untransfected, transfected with GFP-tagged empty vector (EV(GFP)) plasmids, or transfected with plasmids containing HA-tagged full length Sufu (HA-Sufu). Untransfected cells were used as a negative control to detect non-specific rabbit immunoglobulin G (IgG). A weak band for LATS2 in HA-tagged protein immunoprecipitates (IP: HA) of HA-Sufu transfected cells may indicate that LATS2 interacts with Sufu.

3.1.5 LATS1/2 phosphorylation does not regulate Sufu stability

Chen *et al.* (2011) reported that dual phosphorylation of Sufu at S342 and S346 by GSK3β and PKA, respectively, stabilises Sufu by blocking Shh signalling induced degradation. This was later confirmed by Raducu *et al.* (2016), who showed that the E3 ubiquitin ligase Fbxl17 (F-box and leucine-rich repeat protein 17) targets Sufu for proteosomal degradation, downstream of Ptch and Smo, and phosphorylation of both S342 and S346 inhibits Fbxl17 recognition and binding. Both groups demonstrated that S342 and S346 dual phosphorylation stabilises Sufu by using S342/6A or S342/6D mutants. Neither group, however, looked that the contribution of S342 phosphorylation, in isolation, to Sufu stabilisation. Therefore, neither group can conclude that S342 phosphorylation alone regulates Sufu stability. To determine whether S342 phosphorylation by LATS1/2 regulates Sufu stability, the effect of *LATS1/2* gene knockdown on levels of endogenous Sufu was examined by western blot (bands shown in Figure 3.1A, 3.2A and 3.4A). Quantification of Sufu protein bands from three independent experiments revealed that LATS1/2 knockdown had no significant effect on Sufu protein levels (Figure 3.4B). This suggests that S342 phosphorylation of Sufu by LATS1/2 does not regulate Sufu stability.

3.1.6 LATS1/2 phosphorylation does not affect phosphorylation of Sufu at S352

Raducu *et al.* (2016) found that phosphorylation of Sufu at S352 reduces binding of Fbxl17, thereby stabilising Sufu by blocking Fbxl17-mediated proteosomal degradation. Additionally, they generated an antibody that specifically recognises Sufu phosphorylated at both S352 and T353. This antibody can recognise endogenous Sufu, which they used to demonstrate that S352 and T353 are phosphorylated *in vivo*. To generate this antibody, six different polyclonal antibodies had been raised against a peptide of human Sufu, in which S352 and T353 are

phosphorylated. Given access to these antibodies, the ability of each antibody to specifically recognise S352 phosphorylated Sufu was tested. HEK293T cells were transfected with plasmids containing HA-tagged full-length human Sufu (WT) or a non-phosphorylatable mutant with alanine substitution at S352 (S352A). Western blot analysis of HA-tagged protein immunoprecipitates (Appendix Figure 1) revealed that only one antibody (top pair of bands) is phospho-specific as it was unable to recognise the S352A mutant. This antibody also gave a clear signal for the full-length protein sequence, and so this antibody was chosen to investigate the effect of LATS1/2 depletion on phosphorylation of Sufu at S352 (Figure 3.4B). Quantification of S352 phosphorylated Sufu (P-S352-Sufu) protein bands from three independent experiments indicated that LATS1/2 phosphorylation at S342 does not affect phosphorylation of Sufu at S352 (Figure 3.4B).

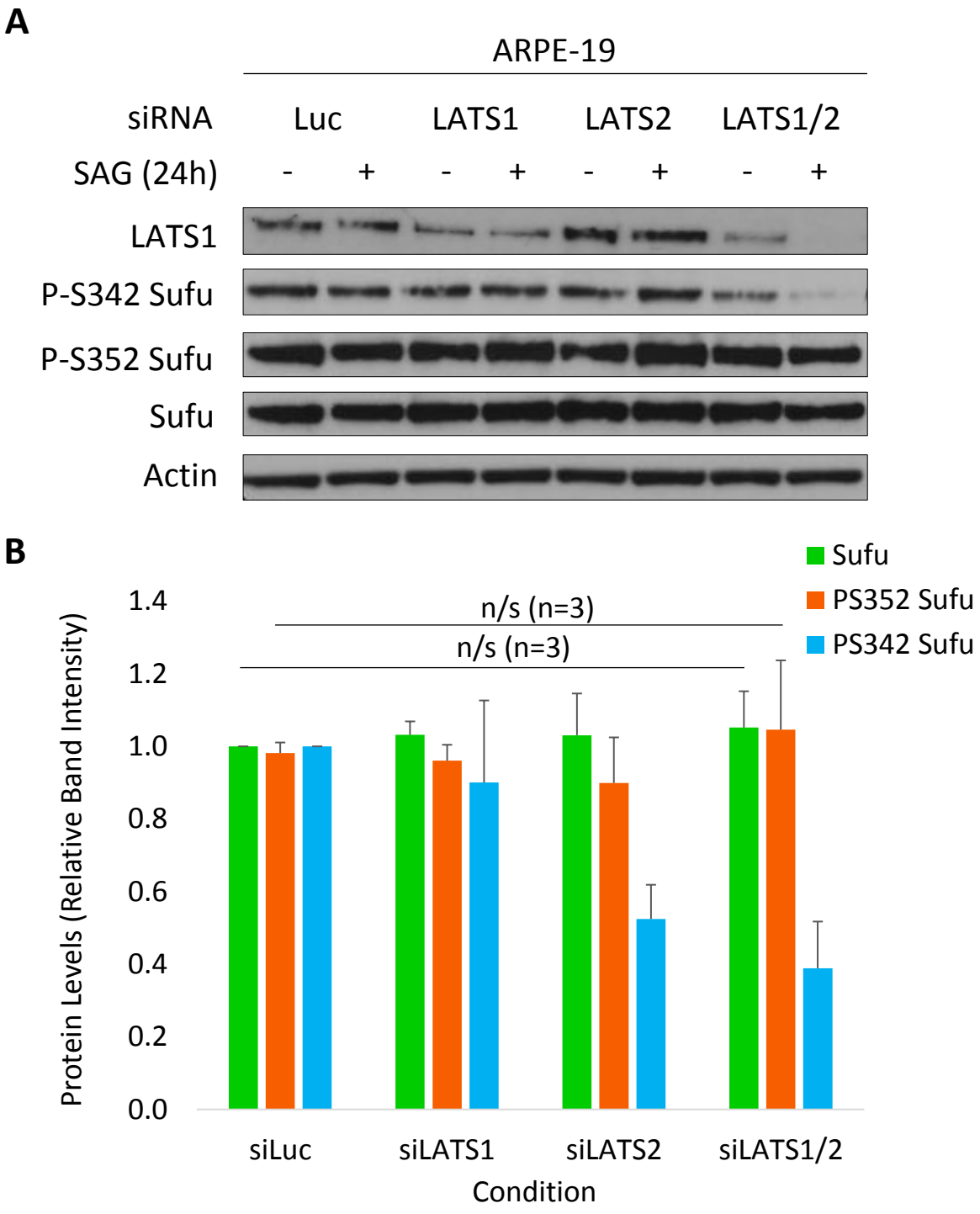

Figure 3.4 - LATS2 phosphorylation does not regulate Sufu stability or phosphorylation at S352

(A) Western blot analysis of LATS1, Sufu, S342 phosphorylated Sufu (P-S342 Sufu) and S352 phosphorylated Sufu (P-S352 Sufu) levels in lysates of ARPE-19 cells treated as in Figure 3.1.

(B) Quantification of relative Sufu, P-S352 Sufu and P-S342 Sufu levels by western blot analysis. Data shows mean and SD (error bars) of three independent experiments. Statistical significance was analysed using a two-tailed unpaired Student's t-test (n/s P>0.05).

3.2 Part II - Investigating the effect of LATS1/2 phosphorylation on SuFu ciliary localisation

3.2.1 Introduction

Rapid localisation of Sufu-Gli complexes to the distal tip of the primary cilium, in response to Hedgehog (Hh) pathway activation, is a key event in Hh signal transduction. Although basal levels of Sufu-Gli are constitutively present in the primary cilium of unstimulated cells, Shh-induced localisation of Sufu-Gli to the cilium tip is dependent on Smo activation (Tukachinsky *et al*., 2010). Chen *et al.* (2011) proposed that this is due to a dynamic balance between anterograde and retrograde intraflagellar transport (IFT) along the ciliary axoneme. Using their P-S342 Sufu phospho-specific antibody in immunofluorescence, they detected fluorescent signal at the tips of primary cilia, concluding that S342/S346 dual phosphorylated Sufu specifically localises to the cilium tip. They supported this by demonstrating that Sufu ciliary localisation is significantly reduced by S346A mutation and significantly increases with S342D/S346D mutation. Still, they do not investigate the effect of S342 phosphorylation separately, hindering any conclusion as to the contribution of S342 phosphorylation alone to Sufu ciliary localisation. Granted that LATS1/2 phosphorylate Sufu at this site, depletion of LATS1/2 may give insight into the influence of S342 phosphorylation on Sufu ciliary localisation.

3.2.2 LATS1/2 knockdown reduces Sufu ciliary localisation

To uncover the role of LATS1/2 phosphorylation in Sufu regulation, the effect of *LATS1/2* gene knockdown on Sufu ciliary localisation was examined by immunofluorescence (IF). Firstly, the anti-Sufu antibody was tested for use in immunofluorescence as it had not been verified for this application (Figure 3.5A). Untransfected, untreated ARPE-19 cells were serum starved for 24-48 hours to induce ciliogenesis. To visualise the primary cilia, acetylated α tubulin was used as a

marker of the ciliary axoneme, and Y tubulin was used to mark the centrosome. Immunostaining confirmed that Sufu localises to the primary cilium, and accumulates at the cilium tip. Weak and diffuse staining at the base of the cilium and along the axoneme illustrates the movement of Sufu up and down the axoneme by IFT. Here, the apparent accumulation of Sufu at the distal tip of the primary cilium corroborates findings that Sufu is constitutively present in the primary cilium of unstimulated cells. Fluorophore tagged secondary antibodies were also tested individually to ensure that they do not give any background fluorescent signal.

Immunofluorescence for detection of endogenous Sufu within the primary cilium was performed in ARPE-19 cells after single or combined siRNA-mediated gene knockdown of *LATS1* and *LATS2* (as in section 3.1.2). As Sufu ciliary localisation is induced by Shh, Smoothened agonist (SAG), a potent activator of Hedgehog signalling, was used to investigate whether pathway activation influenced any effect of LATS1/2 depletion on Sufu immunostaining. Imaging of fluorescently labelled cells by confocal fluorescence microscopy showed that endogenous Sufu can be detected in primary cilia after knockdown of LATS1 or LATS2, with all cells counted staining positive for Sufu (Figure 3.5B). In contrast, combined knockdown of LATS1 and LATS2 abolished Sufu ciliary immunofluorescence. As the removal of Sufu ciliary localisation only occurs after knockdown of both LATS1 and LATS2, this suggests that phosphorylation of Sufu at S342 by LATS1/2 is necessary for accumulation of Sufu in the primary cilium. Treatment with SAG did not appear to influence the effect of LATS1/2 knockdown on Sufu immunofluorescent staining (Appendix figure 2), which could imply that LATS1/2 phosphorylation is independent of Smo activation.

Quantification of mean Sufu immunofluorescent staining within three regions of the primary cilium - the basal body, the axoneme and the distal tip – revealed no significant changes in Sufu staining intensity after LATS1 or LATS2 knockdown, compared to the control (Appendix figure 3). Despite the dominant role of LATS2 in S342 phosphorylation, this may indicate that

LATS1 phosphorylation can rescue the effect of LATS2 knockdown, confirming the notion that there is redundancy in function of LATS1 and LATS2 at this site. Although not visible by eye, image analysis also detected basal levels of Sufu immunofluorescent staining in the LATS1/2 combined knockdown condition. This data is in agreement with the findings of Chen *et al*. (2011), who found that S346A mutant Sufu (lacking PKA phosphorylation to prime S342 phosphorylation by GSK3β) is still detectable at ciliary tips. Accordingly, both data sets are consistent with a role of S342 phosphorylation in promoting ciliary retention of Sufu, as opposed to being a requirement for entry into the primary cilium.

Chen *et al*. (2011) were able to detect immunofluorescent signal for endogenous S342 phosphorylated Sufu (P-S342 Sufu) at the tips of primary cilia using their P-S342 Sufu phospho-specific antibody in immunofluorescence. Thus, immunofluorescence using this antibody was performed in parallel with the anti-Sufu antibody. In my hands, however, this antibody failed to give any signal at the primary cilia in the majority of coverslips, and gave a lot of non-specific background staining, making any comparison of Sufu ciliary localisation between conditions too difficult to distinguish (Appendix Figure 4). This non-specific staining could not be removed by using a higher dilution of antibody (1:100 to 1:500) or by inclusion of an additional wash step in PHEM buffer prior to fixation. Therefore, any conclusions as to the effect of LATS1/2 depletion on ciliary localisation of the S342 phosphorylated form of Sufu could not be made.

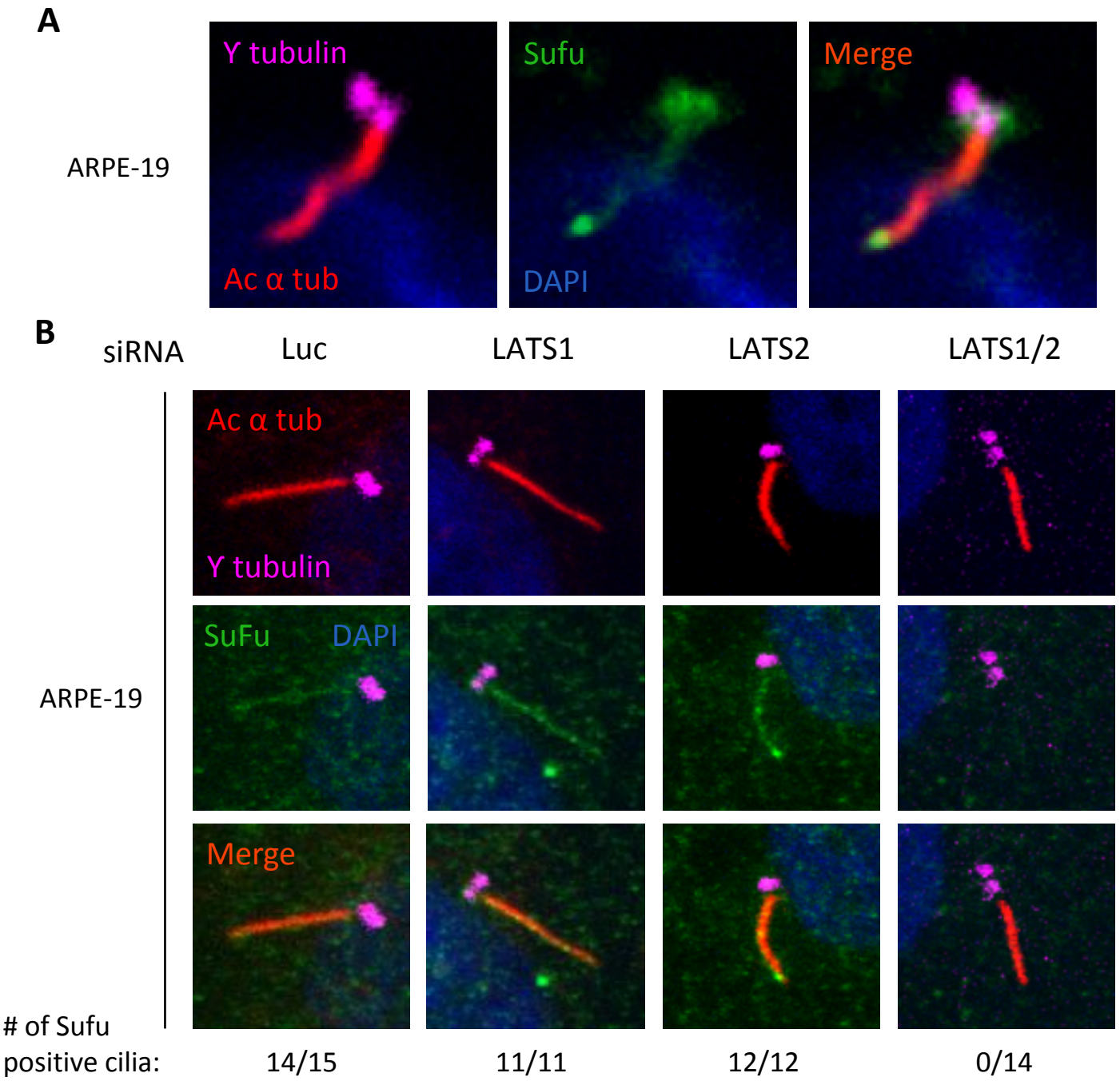

Figure 3.5 - LATS1/2 knockdown removes Sufu ciliary localisation

(A) Immunofluorescent staining of endogenous Sufu (green), ciliary axoneme marker acetylated α tubulin (Ac α tub, red), and centrosome marker Y tubulin (violet) in ARPE-19 cells. Cells were serum starved in 0.1% FBS DMEM for 24-48 hours.

(B) Immunofluorescent staining of endogenous Sufu after single or combined siRNA-mediated gene knockdown of *LATS1* and *LATS2* in ARPE-19 cells. Control cells were transfected with siRNA targeting Luciferase. Cells were serum starved in 0.1% FBS DMEM for 24-48h to induce ciliogenesis, and treated with Smoothened agonist SAG (200nM) for 24h to activate Hedgehog signalling. Numbers of cilia staining positive for Sufu in each condition are indicated.

3.2.3 S352 phosphorylated Sufu localises to the basal body of the primary cilium

Wang *et al.* (2016) identified NIMA-related expressed kinase 2A (Nek2A) as the kinase responsible for the stabilising phosphorylation of Sufu at Serine 352. They found that depletion of Nek2A in NIH3T3 cells by siRNA transfection increased recruitment of endogenous Sufu to primary cilia, indicating that S352 phosphorylation by Nek2A impairs translocation of Sufu into the cilium. Additionally, they observed that pathway stimulation with Shh failed to enhance recruitment of more Sufu to the cilia of Nek2A depleted cells. Considering the role of LATS1/2 phosphorylation on Sufu ciliary localisation, the influence of S342 phosphorylation on localisation of the S352 phosphorylated form of Sufu was investigated using immunofluorescence staining with the P-S352 phospho-specific antibody. As this antibody had not been used in IF previously, it was tested for this application prior to use in knockdown experiments (Appendix Figure 5). Immunofluorescence for detection of endogenous S352 phosphorylated Sufu (P-S352 Sufu) within the primary cilium was performed in ARPE-19 cells after single or combined siRNA-mediated gene knockdown of *LATS1* and *LATS2* (as in section 3.1.2). Treatment with Smoothened agonist (SAG) was used to examine whether Hedgehog pathway activation affects recruitment of S352 phosphorylated Sufu into the primary cilium. Astonishingly, P-S352 Sufu consistently localised to the basal body of primary cilia, co-localising with centrosome marker γ tubulin (Figure 3.6A). This apparent accumulation of S352 phosphorylated Sufu at the cilium base supports the findings of Wang *et al*. (2016) as it illustrates that S352 phosphorylation inhibits entry into the cilium. Treatment with SAG had no effect on P-S352 Sufu localisation in each condition (Figure 3.6B), in agreement with the lack of response to Shh stimulation observed in Nek2A depleted cells.

Following the same pattern seen for Sufu, PS352 Sufu can be detected at the basal body of primary cilia after single knockdown of LATS1 or LATS2, with all cells counted staining positive for Sufu, but combined knockdown of LATS1 and LATS2 removes Sufu ciliary immunofluorescence

(Figure 3.6A and B). This authenticates the role of S342 phosphorylation by LATS1/2 in promoting the accumulation of Sufu at the primary cilium. In line with this, quantification of mean immunofluorescent staining for S352 Sufu at the base of the cilia revealed small changes in staining intensity after LATS1 or LATS2 knockdown alone, but a substantial decrease with combined LATS1/2 knockdown, compared to control cells. This provides further evidence for the ability of LATS1 to rescue the effect of LATS2 knockdown, strengthening the theory of functional redundancy between LATS1 and LATS2.

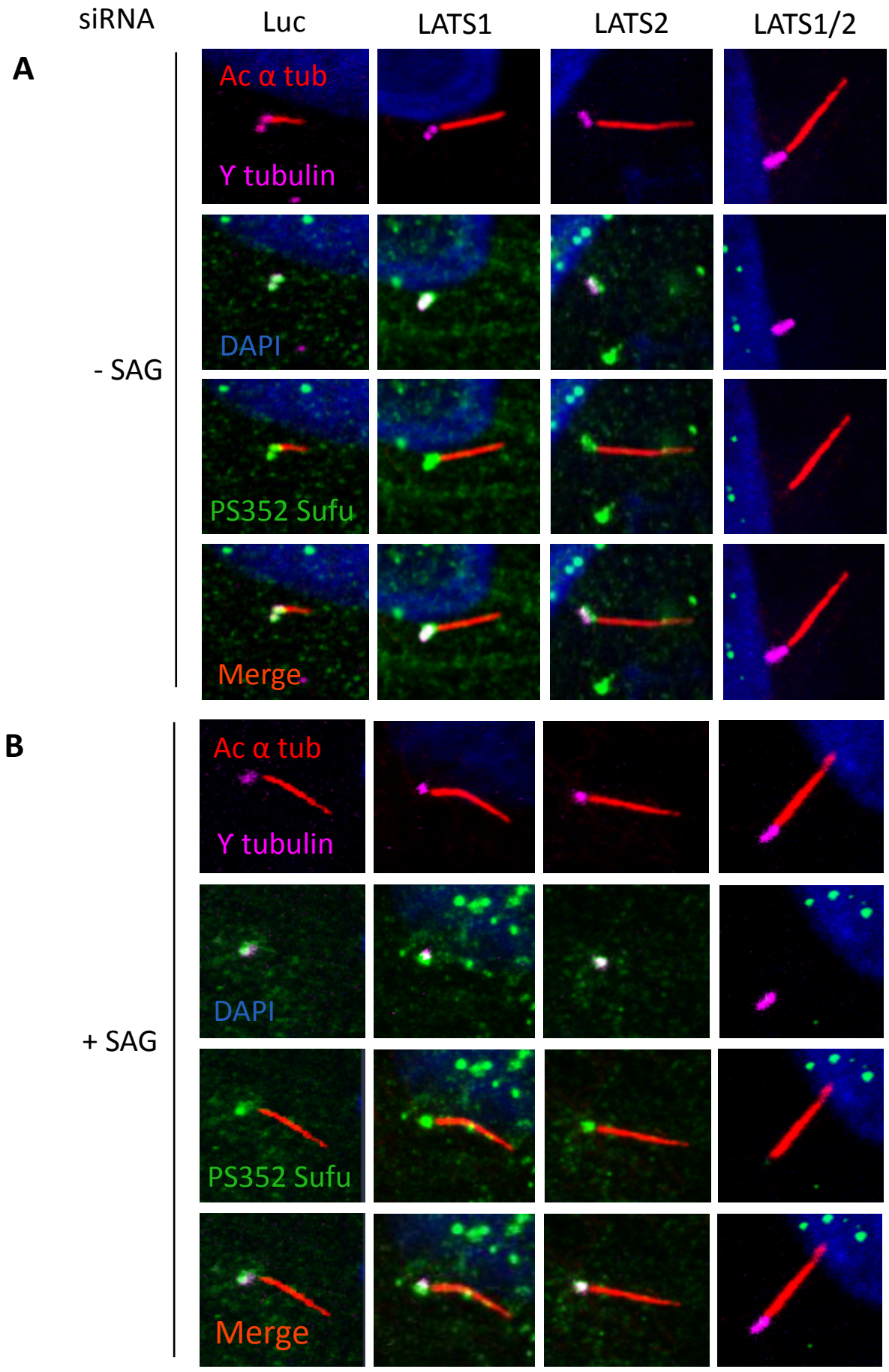
siRNA
Luc
LATS1
LATS2
LATS1/2
A
Ac α tub
Y tubulin
DAPI
PS352 Sufu
Merge
- SAG
B
Ac α tub
Y tubulin
DAPI
PS352 Sufu
Merge
+ SAG

C

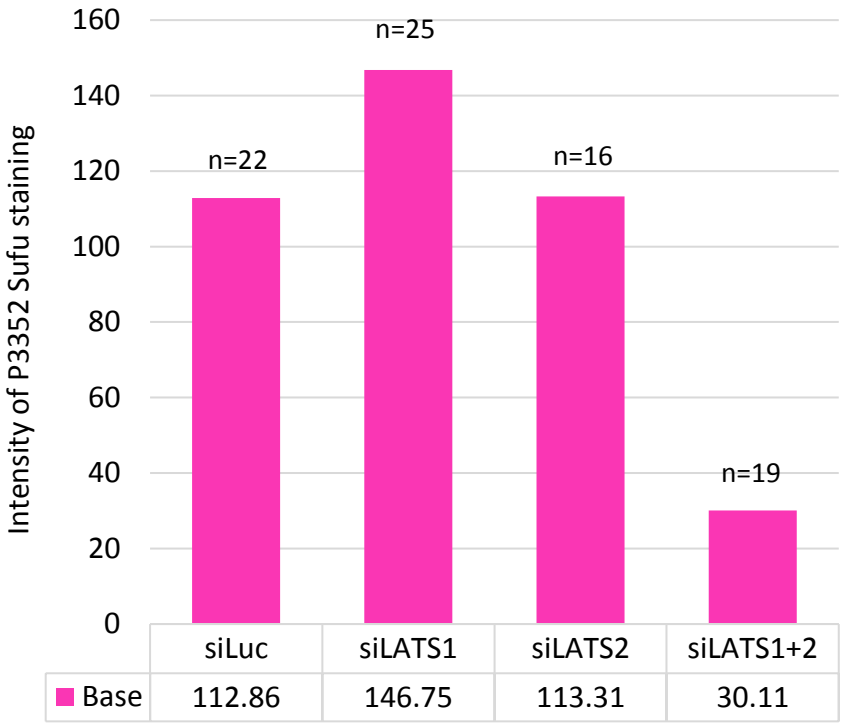

<u>Figure 3.6</u> – S352 phosphorylated Sufu localises to the basal body of the primary cilium

(A) Immunostaining for endogenous S352 phosphorylated Sufu (P-S352 Sufu; green), ciliary axoneme marker acetylated α tubulin (Ac α tub, red), and centrosome marker Y tubulin (violet) after single or double siRNA-mediated gene knockdown of *LATS1* and *LATS2* in ARPE-19 cells. Control cells were transfected with siRNA targeting Luciferase. Cells were serum starved in 0.1% FBS DMEM for 24-48h to induce ciliogenesis.

(B) As in (A), cells were treated with Smoothened agonist SAG (200nM) for 24h to activate Hedgehog signalling.

(C) Quantification of mean immunofluorescence intensity values of P-S352 Sufu at the base of primary cilia (number of cilia labelled above each band).

3.3 Part III – Establishing a role for LATS1/2 phosphorylation in the regulation of Sufu function

3.3.1 Introduction

Sufu is well known to negatively regulate Hedgehog signal transduction by repressing the activity of Gli transcription factors. This is achieved by direct binding of Sufu to Gli proteins in a complex which sequesters Gli in the cytoplasm or inhibits the transcriptional activity of DNA-bound Gli in the nucleus (Kogerman *et al*., 1999). Sufu binds to and stabilises full length Gli2/3, facilitating processing into transcriptional repressors and inhibiting conversion into transcriptional activators. Translocation of Sufu-Gli complexes to the tip of the primary cilium by intraflagellar transport (IFT) is essential for their dissociation and Gli activation in response to Hh pathway stimulation (Humke *et al*. 2010). Chen *et al.* (2011) found that the repressive activity of Sufu on Gli1-mediated transcription was significantly reduced in non-phosphorylatable S342A/S346A mutant Sufu, but slightly enhanced in S342D/S346D mutant Sufu, compared to the wild type. This is consistent with the stabilising role of PKA/GSK3β dual phosphorylation at these sites. Raducu *et al*. (2016) showed that Fbxl17 polyubiquitylation of Sufu, downstream of Ptch and Smo, allows Gli to dissociate and activate target gene transcription. As S342/S346 phosphorylation promotes ciliary retention, and dissociation of Sufu-Gli complexes, facilitated by Fbxl17, occurs in the cilium tip, a model emerges whereby Smo induced dephosphorylation of Sufu at S342, S346 and S352 at the cilium tip permits Fbxl17 binding, polyubiquitylation and degradation, accompanied by Gli dissociation and target gene transcription.

3.3.2 LATS1/2 phosphorylation maintains Sufu-mediated repression of Gli transcriptional activity

To determine whether S342 phosphorylation of Sufu by LATS1/2 is able to regulate its repressive activity on Gli target gene transcription, the use of wild type (WT), *Lats1/2*$^{-/-}$ and *Sufu*$^{-/-}$ mouse embryonic fibroblasts (MEF) was employed. In three independent experiments, each population of MEF was treated with Smo agonist (SAG) for 24 hours to activate the Hedgehog pathway. Following this, the mRNA expression of two well-known Gli target genes, *GLI1* and *PTCH1* was measured by qRT-PCR. In each type of MEF, the fold change in mRNA expression in SAG treated cells, relative to untreated cells, was calculated using two different primer pairs for each gene (Figure 3.7). Use of *Sufu*$^{-/-}$ MEFs as an experimental control confirmed that the primer pairs measure Hedgehog target genes as the GAPDH corrected ΔC_T values of each gene were at least 50 times higher in these cells than in WT cells. This demonstrates the repressive capacity of Sufu on Gli transcriptional activity. By comparing the fold change in mRNA expression of Gli target genes between *Lats1/2*$^{-/-}$ MEFs and WT MEFs, the effect of LATS1 and LATS2 loss on Gli transcriptional activity can be examined. The relative fold increase in mRNA expression for both *GLI1* and *PTCH1* was found to be significantly higher in *Lats1/2*$^{-/-}$ MEFs compared to WT MEFs, in response to Hedgehog pathway activation with SAG. This suggests that loss of LATS1/2 phosphorylation diminishes the repressive activity of Sufu on Gli target gene transcription. In agreement with the effect of S342D/S346D mutation reported by Chen *et al* (2011), LATS1/2 phosphorylation of Sufu at S342 appears to maintain its ability to repress Gli transcriptional activity.

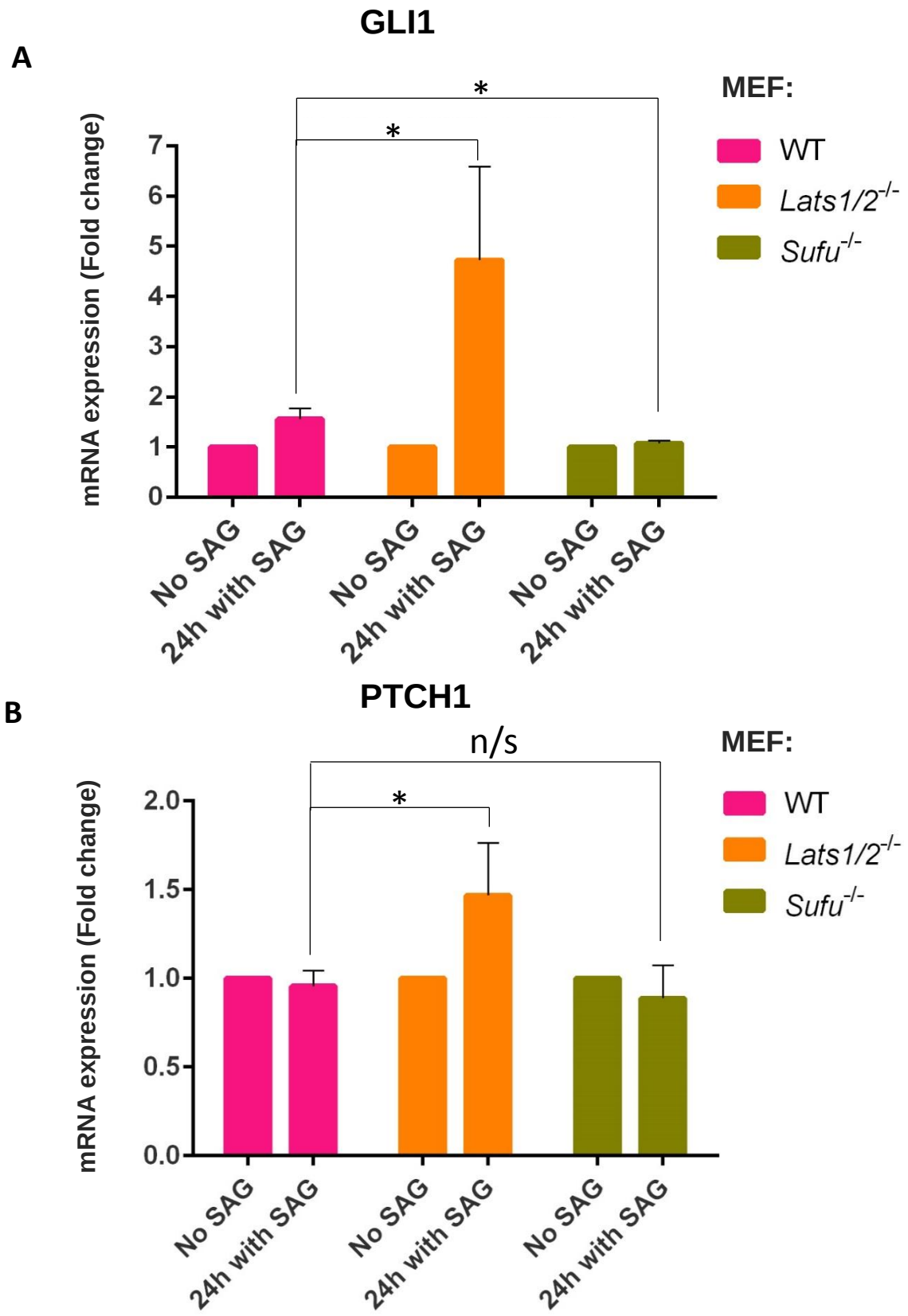

Figure 3.7 - LATS1/2 phosphorylation maintains Sufu-mediated repression of Gli transcriptional activity Relative mRNA expression of GLI1 (A), or PTCH1 (B), in wild type (WT), *LATS1/2*$^{-/-}$ and *Sufu*$^{-/-}$ MEFs after treatment with 200 nM SAG for 24 hours. Data shows mean and SD (error bars) of ΔC_T values for one primer pair in three independent experiments. Statistically significant changes were determined using a two-tailed unpaired Student's t-test (*P<0.05).

Chapter 4: Discussion

4.1 General Discussion

Both the Hippo and Hedgehog signalling pathways are highly complex signalling mechanisms which, when dysregulated, are implicated in the development of a wide range of different human cancers. In recent years, these two pathways have been shown to interact on multiple levels, and coordinate in the development of SHH subtype medulloblastoma and basal cell carcinoma (Fernandez-L *et al.*, 2008; Akladios *et al*., 2017). However, the extent of crosstalk between the Hippo pathway and Hedgehog signalling is relatively unknown. Thus, the overall aim of this project was to further characterise this relationship. Analysis of the amino acid sequence of human Sufu revealed that Serine 342 lies within a potential LATS consensus phosphorylation site. This lead to the hypothesis that LATS1/2 phosphorylate Sufu at S342 to regulate its activity.

The first aim of the project was to confirm that Sufu is phosphorylated by LATS1 or LATS2 at S342 *in vivo*. As a preliminary step, an effective and measurable reduction in LATS1 and LATS2 cellular levels must be achieved. In human retinal pigmented epithelium cells (ARPE-19), siRNA-mediated knockdown of LATS1 and LATS2 was confirmed. A 60-80% reduction in LATS1 protein levels was shown using densitometric analysis of LATS1 western blot bands. An antibody against LATS2 was also used in western blot, however this yielded bands that were not clear enough to distinguish protein levels, therefore qRT-PCR analysis was used to show that *LATS2* mRNA expression was reduced by 65-80%. This enabled the effect of LATS1/2 depletion on Sufu phosphorylation status to be tested.

Chen *et al.* (2011) reported that Glycogen Synthase Kinase 3 β (GSK3β) phosphorylates Sufu at S342, after a priming phosphorylation at S346 by Protein Kinase A (PKA). They demonstrated this by generating an antibody that specifically recognises S342 phosphorylated Sufu, and showing that inhibition of GSK3β, using SB216763, effectively removes S342

phosphorylation of endogenous Sufu within 4 hours. Here, 24-hour SB216763 treatment was used as a negative control for the measure of S342 phosphorylation status. A drastic reduction in S342 phosphorylation was shown in all conditions where the GSK3 inhibitor was present (Figure 3.2A), validating the findings of Chen *et al.* (2011). Knockdown of LATS2 caused a significant decrease in S342 phosphorylation, with densitometric analysis revealing that P-S342 Sufu levels were approximately 50% of those in seen in the control condition both in the absence and presence of the GSK3 inhibitor (Figure 3.2B). Therefore, it appears that LATS2 can phosphorylate Sufu *in vivo*. The finding that S342 phosphorylation is halved after LATS2 knockdown when GSK3 is inhibited reveals that GSK3β and LATS2 both contribute to phosphorylation of this site and act independently of one another. On the other hand, knockdown of LATS1 alone was unable to significantly reduce S342 phosphorylation. However, combined knockdown of LATS1 and LATS2 significantly lowered S342 phosphorylation, when compared to LATS2 knockdown alone, in presence of the GSK3 inhibitor. This indicates that there is some redundancy in function between LATS1 and LATS2 at this site.

Considering that the interactome and roles of LATS2 are much more extensive than that of LATS1, it is not surprising that LATS2 is likely to be dominant over LATS1 in its ability to phosphorylate Sufu (Furth and Aylon, 2017). LATS1/2 have been shown to have roles in mammalian tissue patterning (Lorthongpanich *et al*., 2013), where Hedgehog signalling executes its main function. The spatial distribution of LATS1 and LATS2 expression differs in the developing embryo, suggesting that they have separate roles during embryonic development. Like Sufu, *LATS2* (but not *LATS1*) deletion causes embryonic lethality in mice at E10.5-12.5, pointing to a critical role of LATS2 in early embryogenesis (McPherson *et al.*, 2004). LATS2 was later shown to be required for the maintenance of embryonic stem cell pluoripotency and in the response to differentiation signals. *LATS2*$^{-/-}$ embryonic bodies display abnormal germ layer organisation through aberrant developmental control (Aylon *et al.,* 2014). In light of this, it is highly plausible

that the importance of LATS2 in embryonic development may be related to its ability to regulate Hedgehog signalling via phosphorylation of Sufu.

The functional redundancy of LATS1 and LATS2 was demonstrated by Lorthongpanich *et al*. (2013) who found that siRNA mediated knockdown of LATS1 lead to up-regulation of LATS2 in a dose dependent manner, and vice versa. Here, this trend was also noted when comparing the *LATS2* mRNA expression of cells transfected with only *LATS2* targeting siRNA and cells transfected with siRNAs targeting both *LATS1* and *LATS2* (Appendix figure 6). This is suggestive of autoregulatory feedback loop between LATS1 and LATS2, which would explain why knockdown of both LATS1 and LATS2 is necessary to see a drastic reduction in S342 phosphorylated Sufu levels.

Immunoprecipitation was used with the aim of detecting an interaction between endogenous LATS1/2 and exogenously expressed HA-tagged Sufu. In HEK293T cells, LATS2 was weakly detected in HA-tagged Sufu immunoprecipitates, suggesting that LATS2 may interact with Sufu (Figure 3.3B). In contrast, LATS1 could not be detected. The band weak band of LATS2 and lack of LATS1 detected here could be due to the use of too low a concentration of primary antibodies in western blot of the immunoprecipitated protein samples. The weak signal could also be explained by the fact that protein kinase substrate phosphorylation involves a transient interaction between the kinase and substrate proteins, making such a brief interaction difficult to detect experimentally. Chen *et al.* (2011) proposed that Hedgehog signalling blocks the sequential phosphorylation of Sufu at S346 (by PKA) and S342 (by GSK3β). Therefore, in cells with high Hedgehog signalling activity, LATS1/2 may be unable to interact with and phosphorylate Sufu. In cell culture, full Hedgehog signalling only occurs under conditions of high cell density due to the dependence of Hedgehog signalling on cell-to-cell contact (Taipale *et al.*, 2000). Here, HEK293T cells were highly confluent before they were harvested due to the requirement of high cell confluence for efficient plasmid transfection. Taking this into account, the high level of Hedgehog

signalling activity in these cells may impede detection of an interaction between LATS1/2 and Sufu.

Having confirmed that LATS1/2 phosphorylates Sufu at S342, the next aim of the project was to elucidate the effect of this phosphorylation on Sufu activity. As the S342/S346 dual phosphorylation of Sufu by PKA and GSK3β stabilises Sufu by blocking Fbxl17 binding and preventing its ubiquitin-mediated proteosomal degradation (Chen *et al*., 2011; Raducu *et al*., 2016), it was logical to test the effect of LATS1/2 knockdown on Sufu stability. Densitometric analysis of endogenous Sufu levels, determined via western blot, show that LATS1/2 knockdown had no significant effect on Sufu protein levels (Figure 3.4B). From this data, it was concluded that S342 phosphorylation of Sufu by LATS1/2 does not regulate Sufu stability. This indicates that, unlike the S342/S346 dual phosphorylation, S342 phosphorylation alone is not sufficient to block Fbxl17 binding. The minimal region of Sufu sufficient for Fbxl17 binding is downstream of S342, spanning amino acids 350-425 (Raducu *et al*., 2016). Therefore, it can be hypothesised that phosphorylation of S342 is too far upstream to interfere with Fbxl17 binding, whereas S346 is close enough to the minimal binding region that phosphorylation of this residue inhibits interaction between Sufu and Fbxl17.

In addition to S346 phosphorylation by PKA, phosphorylation of Sufu at S352 by Nek2A was recently found to stabilise Sufu by blocking Fbxl17 recognition and binding (Raducu *et al*., 2016; Wang *et al.*, 2016). Subsequently, Nek2A was shown to be a transcriptional target of Gli, therefore Nek2A functions in a negative feedback loop via its negative regulation of Hedgehog signalling (Zhou *et al.*, 2017). Densitometric analysis of endogenous S352 phosphorylated Sufu levels, determined by western blot, revealed that LATS1/2 knockdown had no significant effect on the level of S352 phosphorylated Sufu (Figure 3.4B). This shows that LATS1/2 phosphorylation does not influence the ability of Nek2A to stabilise Sufu via S352 phosphorylation, which confirms

the finding that LATS1/2 phosphorylation has no effect on the stability of Sufu, both directly, and indirectly via Nek2A.

The negative role of Sufu on Gli transcriptional activity is regulated by events that occur in the primary cilium. In response to pathway activation, Sufu-Gli complexes rapidly translocate into the primary cilium and accumulate at the cilium tip, with phosphorylation of Sufu at S342 and S346 providing a ciliary retention signal (Tukachinsky, Lopez and Salic, 2010; Chen *et al*., 2011). Inactivation of Sufu, downstream of Smo, is dependent on primary cilia (Huangfu and Anderson, 2005). A model has been proposed where Sufu is dephosphorylated at S342, S346 and S352 within the cilium tip compartment, causing Sufu-Gli complexes to exit the primary cilium, and allowing Fbxl17 to bind to and polyubiquitylate Sufu, targeting it for proteosomal degradation (Chen *et al*., 2011; Raducu *et al*., 2016). This facilitates dissociation of Sufu-Gli complexes, leading to Gli transcription factor activation, nuclear translocation, and upregulation of Hedgehog target genes (Raducu *et al*., 2016). Here, knockdown of LATS1 or LATS2 alone had no significant effect on Sufu ciliary localisation, whereas combined knockdown of both LATS1 and LATS2 dramatically reduced the immunofluorescent staining of Sufu in the primary cilium (Figure 3.5B). Although LATS2 appears to be the dominant kinase at S342, LATS1 phosphorylation seems to rescue the effect of LATS2 knockdown, maintaining Sufu ciliary localisation. This points to a role of LATS1/2 in the regulation of Sufu ciliary localisation, whereby S342 phosphorylation promotes the accumulation of Sufu at the cilium tip. Data shown here supports that of Chen *et al*. (2011), who had pinned this phosphorylation site as a ciliary retention signal. Loss of Sufu ciliary immunofluorescent signal with LATS1/2 knockdown supports the hypothesis that loss of S342 phosphorylation causes Sufu to translocate out of the primary cilium. Outside of the cilium, only Sufu that had also been dephosphorylated at S346 and S352 would be recognised and polyubiquitylated by Fbxl17, leading to proteosomal degradation.

Serine 342 lies within the highly mobile 'intrinsically disordered region' of Sufu, which reorganises to stabilise its interaction with Gli transcription factors (Cherry *et al.* 2013; Zhang *et al.*, 2013). Post-translational modification of this region is thought to be required for inhibition of Sufu downstream of Smo (Cherry *et al.* 2013). Therefore, it is possible that S342 phosphorylation of Sufu by LATS1/2 strengthens its binding affinity for Gli transcription factors and enhances their co-translocation to the cilium tip in response to Smo activation. In response to Hh pathway activation, dephosphorylation of S342 at the cilium tip may reduce the binding affinity between Sufu and Gli, aiding their dissociation.

Sufu ciliary localisation was also shown to be regulated by Nek2A phosphorylation at S352. The data of Wang *et al.* (2016) suggests that phosphorylation of Sufu at S352 by Nek2A impairs translocation of Sufu into the cilium. Here, immunofluorescent staining of endogenous S352 phosphorylated Sufu (P-S352 Sufu) was consistently at the basal body, co-localising with the centrosome marker γ tubulin (Figure 3.6A and B). This corroborates the findings of Wang *et al.* (2016) as it suggests that Nek2A phosphorylation prevents Sufu from passing through the transition zone of the cilium (immediately distal to the basal body), leading to the accumulation of P-S352 Sufu at the basal body. As for total Sufu, knockdown of LATS1 or LATS2 alone did not affect the localisation of P-S352 Sufu, whereas the combined knockdown of LATS1 and LATS2 removed the immunofluorescent signal of P-S352 Sufu at the basal body of primary cilia. This supports the observed effect of LATS1/2 double knockdown on the localisation of total Sufu, and strengthens the argument that LATS1/2 phosphorylation of Sufu at S342 promotes ciliary entry and retention of Sufu within the primary cilium. The requirement of both LATS1 and LATS2 knockdown for a visual reduction in P-S352 Sufu at the basal body provides further evidence for the ability of LATS1 to rescue the effect of LATS2 knockdown, strengthening the theory of functional redundancy between LATS1 and LATS2.

The data generated in this project indicate that LATS1/2 regulate the activity of Sufu by phosphorylation of S342. This phosphorylation appears to promote its translocation into the cilium in complex with Gli (possibly by strengthening its binding affinity for Gli) and form a ciliary retention signal. This would suggest that LATS1/2 maintains the function of Sufu as a negative regulator of Hedgehog signalling. The final aim of this project was to investigate the effect of LATS1/2 phosphorylation on Sufu function by studying its ability to repress Gli-transcriptional activity. To do this, the mRNA expression of two well-known Gli transcriptional targets, *GLI1* and *PTCH1,* were compared between wild type and *LATS1/2*$^{-/-}$ MEFs, after treatment with Smoothened agonist (SAG), a potent activator of Hedgehog signalling. In line with the observed role of LATS1/2 in maintaining Sufu function, it was hypothesised that LATS1/2 phosphorylation enhances the ability of Sufu to repress Gli target gene transcription. As expected, the relative fold increase in *GLI1* and *PTCH1* mRNA expression was significantly higher in *LATS1/2*$^{-/-}$ MEFs compared to wild type MEFs, in response to Hedgehog pathway activation with SAG (Figure 3.7). This indicates that loss of LATS1/2 phosphorylation diminishes the repressive activity of Sufu on Gli target gene transcription, confirming the hypothesis that LATS1/2 phosphorylation maintains the repressive activity of Sufu on Gli-mediated gene transcription.

Recent work had suggested that S342/S346 dual phosphorylation of Sufu by PKA and GSK3β stabilises Sufu by blocking Fbxl17 binding and preventing its ubiquitin-mediated proteosomal degradation (Chen *et al*., 2011; Raducu *et al*., 2016). Data in this project rules out the role of S342 phosphorylation alone in regulating Sufu stability, therefore it shows that S346 phosphorylation by PKA may be sufficient to stabilise Sufu. Cyclic AMP (cAMP) dependent Protein Kinase A (PKA) is regarded as the master negative regulator of the Hedgehog signalling pathway (Pak and Segal, 2016). In the absence of Hh ligand, PKA is activated at the base of the cilium via G protein-coupled receptor 161 (Gpr161), which promotes Adenylyl Cyclase-mediated cAMP production through Gαs (Mukhopadhyay *et al*., 2013). This provides a pool of active PKA which acts at the basal body of the primary cilium (Tuson *et al.,* 2011). PKA phosphorylation of full

length Sufu-bound Gli2 and Gli3 is essential for their proteosomal processing into transcriptional repressors, and Gli2 was shown to be the main target of PKA in neural tube patterning during embryonic development (Wang, Fallon and Beachy, 2000; Tuson *et al.*, 2011). More recently, it was found that PKA directly phosphorylates LATS2 and activates its kinase activity, resulting in an increase in YAP1 phosphorylation. Similarly to effect of PKA phosphorylation on neural development via negative regulation of Hedgehog signalling, PKA induced inactivation of YAP via LATS2 phosphorylation was found to regulate the proliferation of neural stem cells and neural progenitors (Kim *et al.*, 2013). Therefore, PKA mediated phosphorylation and activation of LATS2 at the basal body may negatively regulate Hedgehog signalling by driving LATS2 phosphorylation of Sufu. This would mean that activation of LATS2 by PKA phosphorylation acts to regulate neural cell proliferation via two mechanisms: inactivation of YAP, and maintenance of Sufu function.

Phosphorylation of YAP/TAZ by LATS1/2 creates a binding site for the small phosphoserine/phosphothreonine binding protein 14-3-3, which causes their cytoplasmic retention (Zhao *et al*., 2007). 14-3-3 proteins bind to phosphorylated serine or threonine residues within two consensus binding sequences: RSXpSXP or RXXXpSXP (Bridges and Moorhead, 2005). 14-3-3ε was identified as a binding partner of all three Gli transcription factors through their homologous sites. The 14-3-3 binding site in Gli1, Serine 640, was found with the aid of Scan-site, an online library-based searching algorithm which identifies motifs likely to bind to protein domains. PKA was identified as the kinase responsible for creating the 14-3-3 binding sites on Gli transcription factors, which was shown to repress Gli transcriptional activity. However, further analysis showed that 14-3-3 binding of Gli is not the only mechanism by which PKA downregulates Gli target gene transcription (Asoaka *et al*., 2010). Using Scan-site, S342 of Sufu was found to be a potential 14-3-3 binding site. Therefore, given that LATS1/2 can promote 14-3-3 binding to YAP/TAZ, LATS1/2 phosphorylation of Sufu may also promote 14-3-3 binding. 14-3-3 binding to Gli does not affect the binding affinity between Sufu and Gli, however 14-3-3 binding to Sufu could provide the mechanism by which LATS1/2 phosphorylation strengthens the Sufu-Gli

interaction. Alternatively, LATS1/2 induced binding of 14-3-3 to Sufu could recruit 14-3-3 to the site of Gli, and thereby enhance the PKA-dependent repression of Gli target gene transcription.

The findings of this project give evidence of crosstalk between the Hippo pathway and Hedgehog signalling through LATS1/2 phosphorylation of Sufu. This post-translational modification maintains the negative role of Sufu on Gli transcription factors, the effectors of Hedgehog signal transduction. Therefore, the Hippo pathway acts to negatively regulate Hedgehog signalling through regulation of Sufu, which has important implications in the control of cell proliferation. LATS1/2 phosphorylation of Sufu may be key in the prevention of unscheduled Hedgehog pathway activation in the absence of ligand, thereby preventing Hedgehog pathway dependent tumorigenesis. Aberrant regulation of Sufu activity has a role in the development of SHH-subtype medulloblastoma (Raducu *et al.* 2016). Considering the role of LATS2 in the control of neural stem cell and neural progenitor proliferation, phosphorylation of Sufu may be another mechanism employed by LATS2 to restrict neural tissue overgrowth. Thus, discovery of a novel role for LATS2 in restricting Hedgehog signalling via Sufu highlights the importance of LATS2 as a tumour suppressor, and may identify LATS2 as a potential target in the treatment of SHH-subtype medulloblastoma.

4.2 Future Work

In order to confirm that the kinase activity of LATS1/2 is responsible for phosphorylation of Sufu at S342, LATS1/2 constructs with mutations that increase their kinase activity or render them 'kinase-dead' could be employed. Levels of S342 phosphorylated Sufu could be compared between cells transfected with one of these mutants and cells transfected with wild type LATS1 or LATS2. If Sufu is directly and specifically phosphorylated by LATS1 or LATS2, endogenous S342 phosphorylated Sufu levels would increase in cells transfected with an overactive LATS1/2 kinase mutant, and would decrease in cells transfected with a kinase-dead LATS1/2 mutant. Additionally, to show that LATS1/2 specifically phosphorylate Sufu at S342, an *in vitro* kinase assay could be

performed, comparing LATS1/2 phosphorylation of exogenously expressed wild type and non-phosphorylatable S342A mutant Sufu in *Sufu*$^{-/-}$ MEFs.

Optimisation of the immunoprecipitation protocol may be able improve detection of an interaction between Sufu and LATS1/2. Additionally, the interaction between Sufu and LATS1/2 could have been prolonged by co-transfection of HA-tagged Sufu with kinase-dead LATS1/2 mutants. If these kinase dead mutants bind to Sufu, they would be unable to catalyse the transfer of a phosphate group to the S342 residue, and therefore, they would presumably remain bound to Sufu for longer before they detach.

Here, endogenous Sufu protein levels were measured by densitometric analysis of western blot bands on X-ray film, and this was used an indicator of Sufu stability. However, this not the most accurate way to measure protein levels due to the many sources of variation in SDS-PAGE, western blotting, and band density quantification (e.g. variation in the amount of protein loaded in each sample lane, uneven electrotransfer, uneven application of ECL chemiluminescent substrate, rapid saturation of X-ray film and subjective selection of band areas in Image J). Accuracy in detection of protein band signal could have been improved by using charge-coupled device (CCD) imaging systems, such as the LI-COR Odyssey system. Additionally, many factors can influence the stability of a protein, including protein binding and post-translational modifications. Raducu *et al.* (2016) used immunoprecipitation of HA-tagged Sufu and S342/S346 mutants to show that dual phosphorylation of S342 and S346 stabilises Sufu by reducing binding of Fbxl17. To test the ability of S342 phosphorylation to stabilise Sufu, the same immunoprecipitation procedure could be employed to compare Fbxl17 binding between HA-tagged Sufu and HA-tagged S342A mutant Sufu. Use of an *in vivo* ubiquitylation assay could also be performed to detect polyubiquitylation of endogenous Sufu after LATS1/2 knockdown and treatment with proteosomal inhibitor MG-132 to prevent ubiquitin-mediated proteolysis.

A range of different LATS2 antibodies, verified for western blot, immunoprecipitation and immunofluorescence applications, could have been tested in the hope of identifying an antibody that yields clear enough bands for protein level detection using western blot. This would allow for indication of successful LATS2 knockdown without the use of qRT-PCR. Better resolving LATS2 western blot bands may also improve detection of LATS2 in HA-tagged Sufu immunoprecipitates. Use of a LATS2 antibody in immunofluorescence may have been useful for analysis of the localisation of LATS2 to confirm that LATS2 localises at the centrosome, and to look for colocalization of LATS2 and Sufu. If other antibodies are not available, an alternative option would be to transfect cells with plasmids containing tagged LATS2 and use antibody for the tag.

Chen *et al*. (2011) detected specific immunofluorescent signal for endogenous S342 phosphorylated Sufu (P-S342 Sufu) at the tips of primary cilia using the P-S342 Sufu specific antibody. Here, this antibody tended to give a lot of non-specific background staining, and specific staining at the cilium tips was undetectable in most coverslips incubated with this antibody, making any comparison of P-S342 Sufu ciliary localisation between conditions too difficult to distinguish (Appendix Figure 4). To try and improve this staining, the immunoprecipitation procedure was modified by the inclusion of an additional wash step in PHEM buffer prior to fixation, changing the fixation protocol (use of methanol or PFA both alone and sequentially), and use of a higher dilution of antibody (1:100 to 1:500). With more time, the immunofluorescence procedure could have been optimised further by experimenting with the protocol for fixation, blocking, washing steps, permeabilisation and antibody incubations.

Although both phospho-specific Sufu antibodies had been tested for specific recognition of S342 or S352 phosphorylated Sufu by western blotting (Chen *et al*., 2011; Raducu *et al.* 2016; Appendix figure 1), phospho-specificity had not been confirmed in immunofluorescence. This could be performed by comparing immunostaining between exogenously expressed wild type

Sufu and S342A or S352A mutant Sufu in *SUFU*$^{-/-}$ MEFs, where the phospho-specificity would be indicated by loss of immunostaining in the mutants.

Both the data presented here, and the data of Chen *et al.* (2011) show that GSK3β is the dominant kinase acting at S342 of Sufu, as treatment with the GSK3 inhibitor, SB216763, effectively removes S342 phosphorylation. The effect of GSK3 inhibitor treatment on Sufu ciliary localisation could have been visualised by immunofluorescence, and compared with the immunofluorescent Sufu staining seen after LATS1/2 knockdown. This would determine whether S342 phosphorylation by GSK3β has the same effect on Sufu ciliary localisation as LATS1/2 phosphorylation. Here, it would be expected that ciliary localisation of Sufu would be removed with GSK3 inhibition. This would confirm the findings of Chen *et al.* (2011), and in the LATS1/2 knockdown experiments used here, that S342 phosphorylation promotes ciliary retention of Sufu.

Changes in *GLI1* and *PTCH1* mRNA expression were compared between wild type and *LATS1/2*$^{-/-}$ MEFs, after treatment with Smoothened agonist (SAG). The effect of SAG treatment on *GLI1* and *PTCH1* mRNA expression could also be examined in ARPE-19 cells, comparing cells transfected with LATS1/2 siRNA with control cells transfected with siRNA targeting Luciferase. This would test whether a reduction in LATS1 or LATS2 phosphorylation diminishes the Sufu-mediated repression of Gli target gene transcription in response to Hh pathway activation, to help confirm the finding that S342 phosphorylation by LATS1/2 maintains its ability to repress Gli transcriptional activity. Prior to qRT-PCR analysis of *GLI1* and *PTCH1* mRNA expression in wild type and *LATS1/2*$^{-/-}$ MEFs, cells were treated with SAG for 24 hours to activate Hedgehog signalling. Given more time, changes in *GLI1* and *PTCH1* mRNA expression could have been measured after different lengths of exposure to SAG in order to track changes in gene expression over time.

Here, LATS1/2 phosphorylation of Sufu has been proposed to have a role in the prevention of medulloblastoma development. DAOY human medulloblastoma cells are responsive to Smo activation using SAG, and Fbxl17 knockdown impaired *GLI1* gene expression in

DAOY cells treated with SAG (Raducu *et al*. 2016). In a future experiment, the effect of LATS1/2 knockdown on Hedgehog pathway activity could be examined in this cell line by looking at changes in *GLI1* and *PTCH1* mRNA expression after treatment with SAG or SHH.

With more time, the effect of LATS1/2 on the interaction between Sufu and Gli could be tested. This could be performed by immunoprecipitation of exogenously expressed HA-tagged Sufu, comparing the amount of Sufu-bound Gli detected between cells with and without siRNA-mediated knockdown of LATS1 and LATS2. If LATS1/2 was found to strengthen the Sufu-Gli interaction, immunoprecipitation could also be used to detect an interaction between Sufu and 14-3-3 by looking for the presence of 14-3-3 in the HA-tagged protein immunoprecipitates. If an interaction was detected, this would support the hypothesis that LATS1/2 phosphorylation of Sufu at S342 strengthens the Sufu-Gli interaction by promoting 14-3-3 binding.

Chapter 5: Appendix Figures

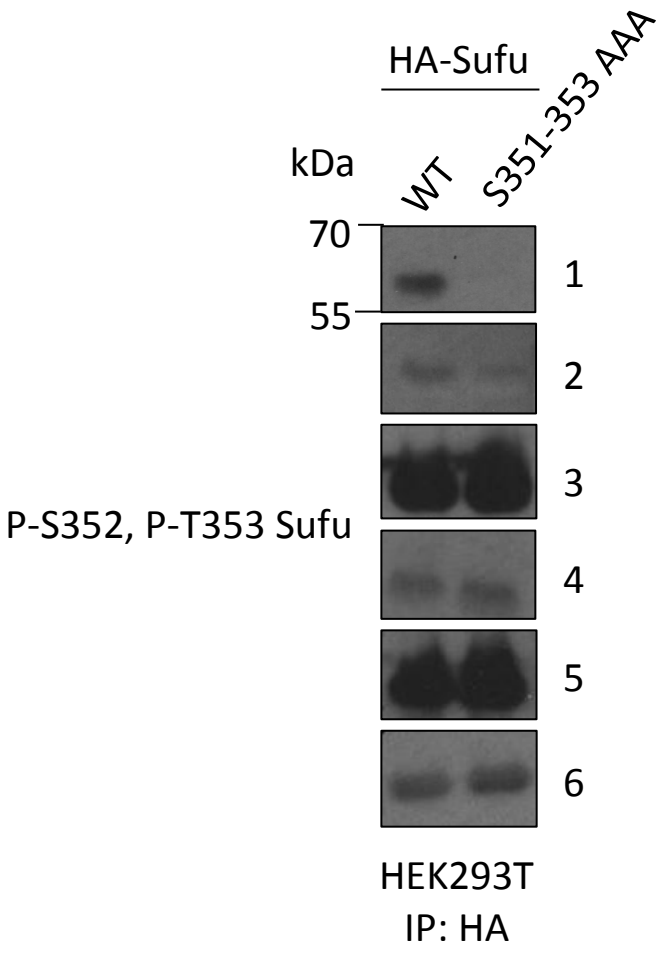

Appendix Figure 1 – Testing of P-S352, P-S353 Sufu antibodies for phospho-specificity

HEK293T cells were transfected with plasmids containing HA-tagged full length (WT) or 351-353 AAA (S352A) mutant Sufu, and HA-tagged proteins were isolated by immunoprecipitation. Western blot analysis of six different Sufu (P-S352, P-S353) antibodies was used to test for specific recognition of Sufu phosphorylated at S352. Only antibody 1 (top bands) appears to be phospho-specific, and was therefore used in subsequent experiments.

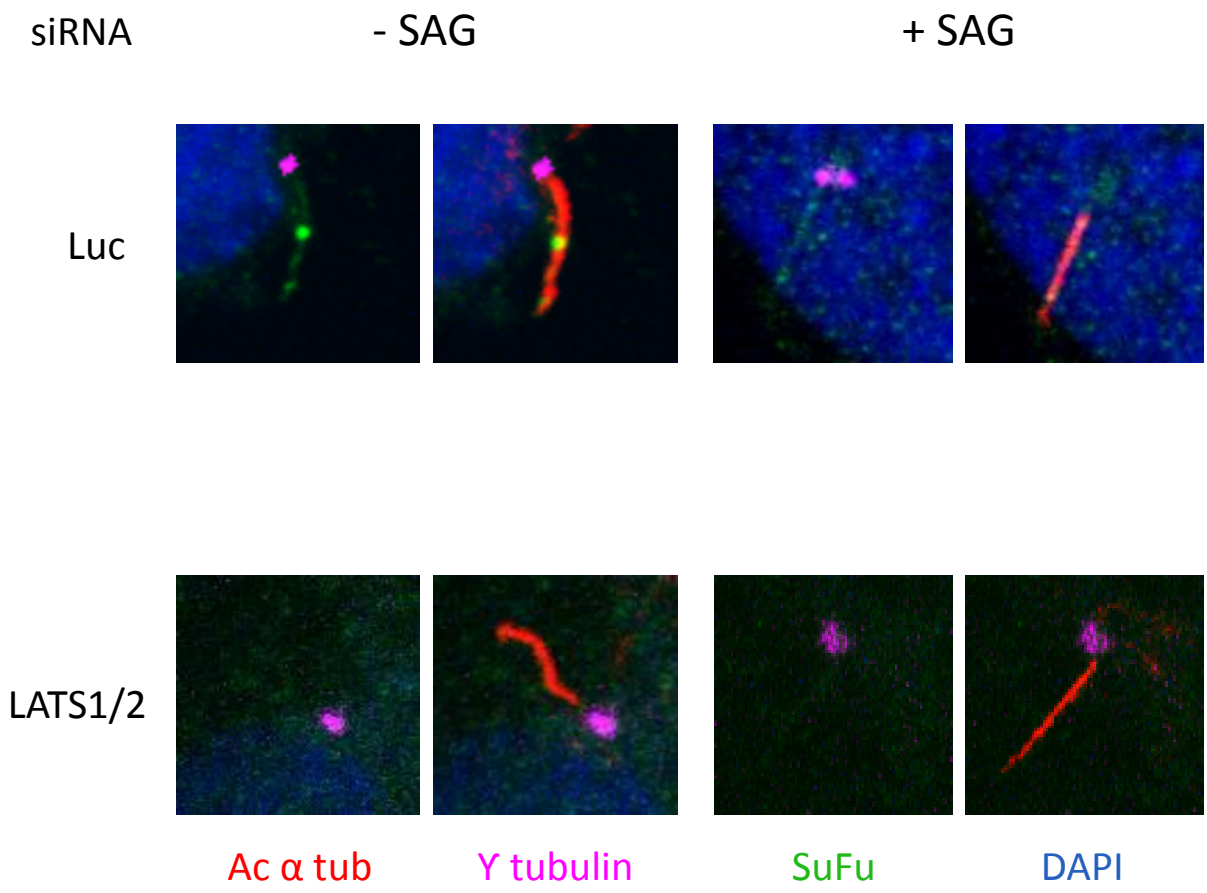

<u>Appendix Figure 2</u> – Hedgehog pathway activation does not appear to influence the effect of LATS1/2 knockdown on Sufu ciliary localisation

Immunofluorescent staining of endogenous Sufu after siRNA-mediated gene knockdown of *LATS1* and *LATS2* in ARPE-19 cells, with or without 24h treatment with 200 nM Smoothened agonist (SAG), a potent activator of Hedgehog signalling. Control cells were transfected with siRNA targeting Luciferase. Cells were serum starved in 0.1% FBS DMEM for 24-48h to induce ciliogenesis.

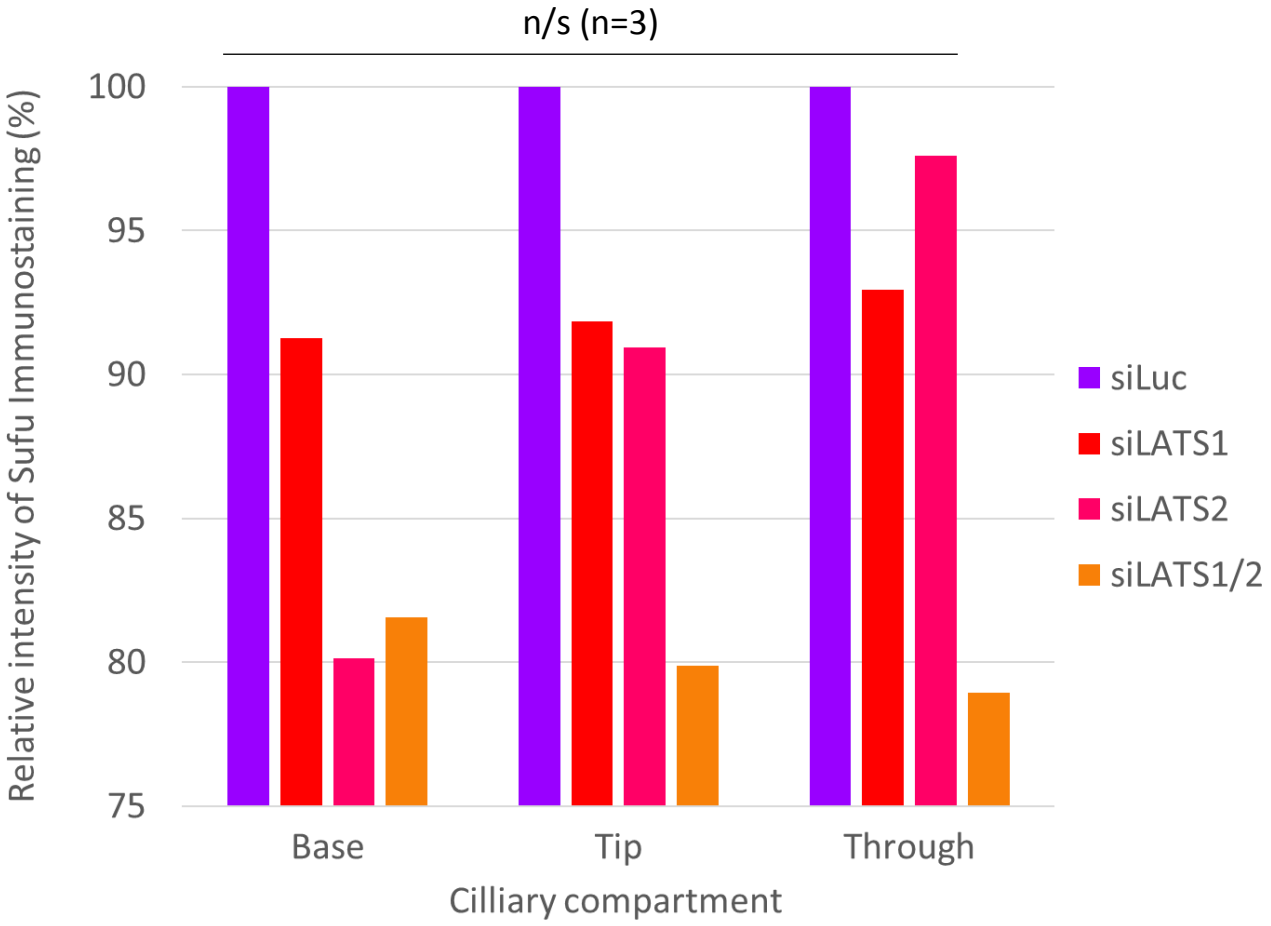

Appendix Figure 3 – The effect of LATS1/2 knockdown on endogenous Sufu staining intensity.

Quantification of mean Sufu Immunofluorescent staining within the basal body (Base), at the distal tip (Tip) and through the axoneme (Through) of primary cilia after siRNA-mediated gene knockdown of *LATS1* and *LATS2* in ARPE-19 cells. Control cells were transfected with siRNA targeting Luciferase. Mean intensity values are representative of a minimum of three independent experiments. Statistical significance was analysed using a two-tailed unpaired Student's t-test (n/s P>0.05).

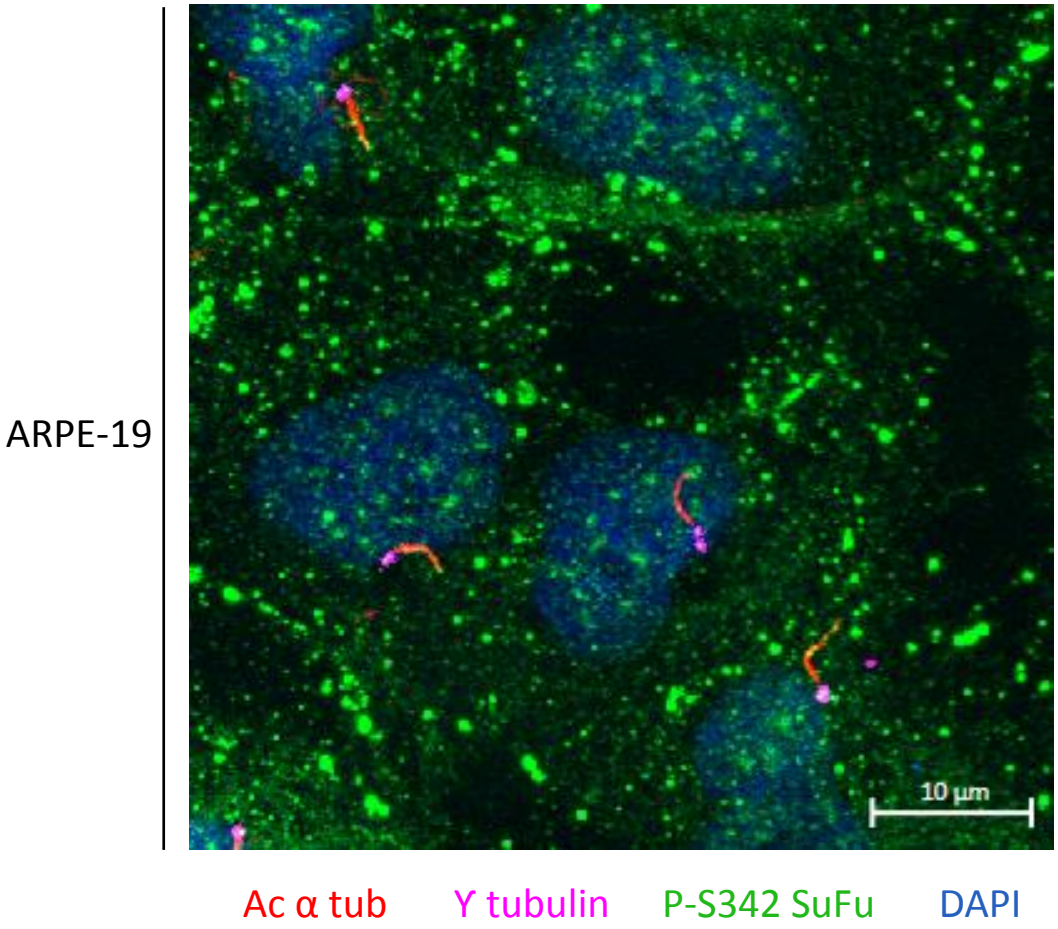

<u>Appendix Figure 4</u> – Background staining issues with PS342 Sufu antibody

Immunofluorescence staining of endogenous S342 phosphorylated Sufu (P-S342 Sufu) in ARPE-19 cells transfected with siRNA targeting Luciferase. Cells were serum starved in 0.1% FBS DMEM for 24-48h to induce ciliogenesis, and treated with Smoothened agonist SAG (200nM) for 24h to activate Hedgehog signalling. In my hands, the PS342 phospho-specific antibody gave a lot of background staining, making any changes in ciliary localisation too difficult to distinguish.

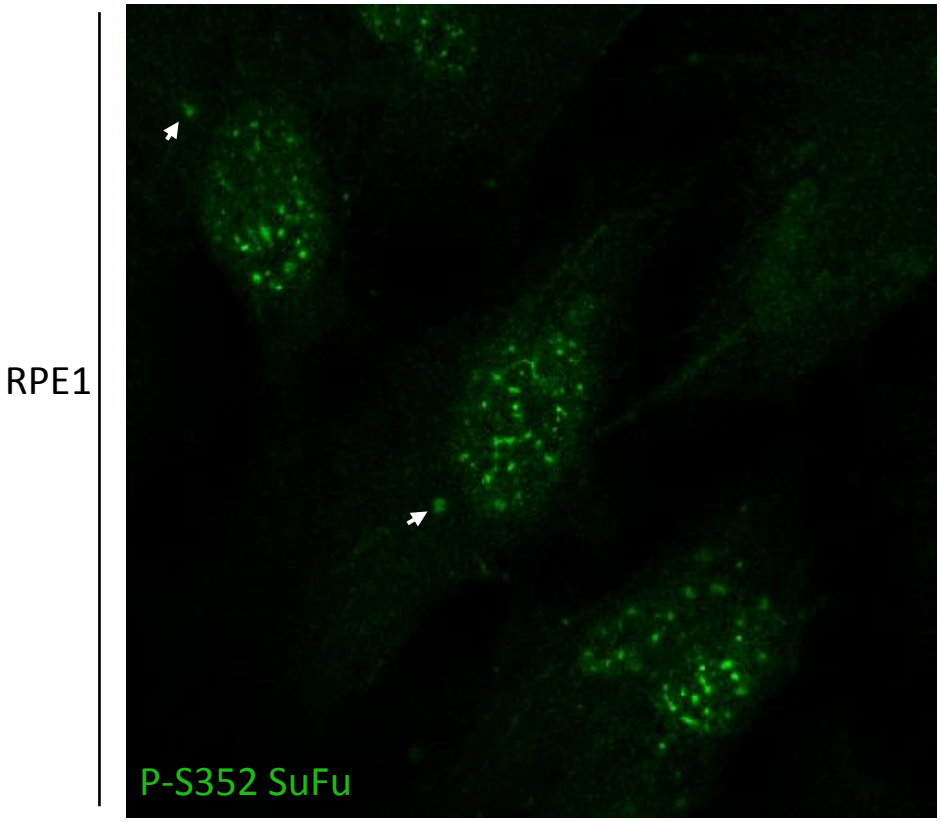

<u>Appendix Figure 5</u> – Testing of phospho-specific PS352, P-T353 Sufu antibody in immunofluorescence

Immunofluorescence staining of endogenous S352 phosphorylated Sufu in RPE1 cells, serum starved in 0.1% FBS DMEM for 24-48h to induce ciliogenesis. Arrows indicate signal at the basal body of two primary cilia. Nuclear foci may indicate that the majority of P-S352 Sufu resides in the nucleus.

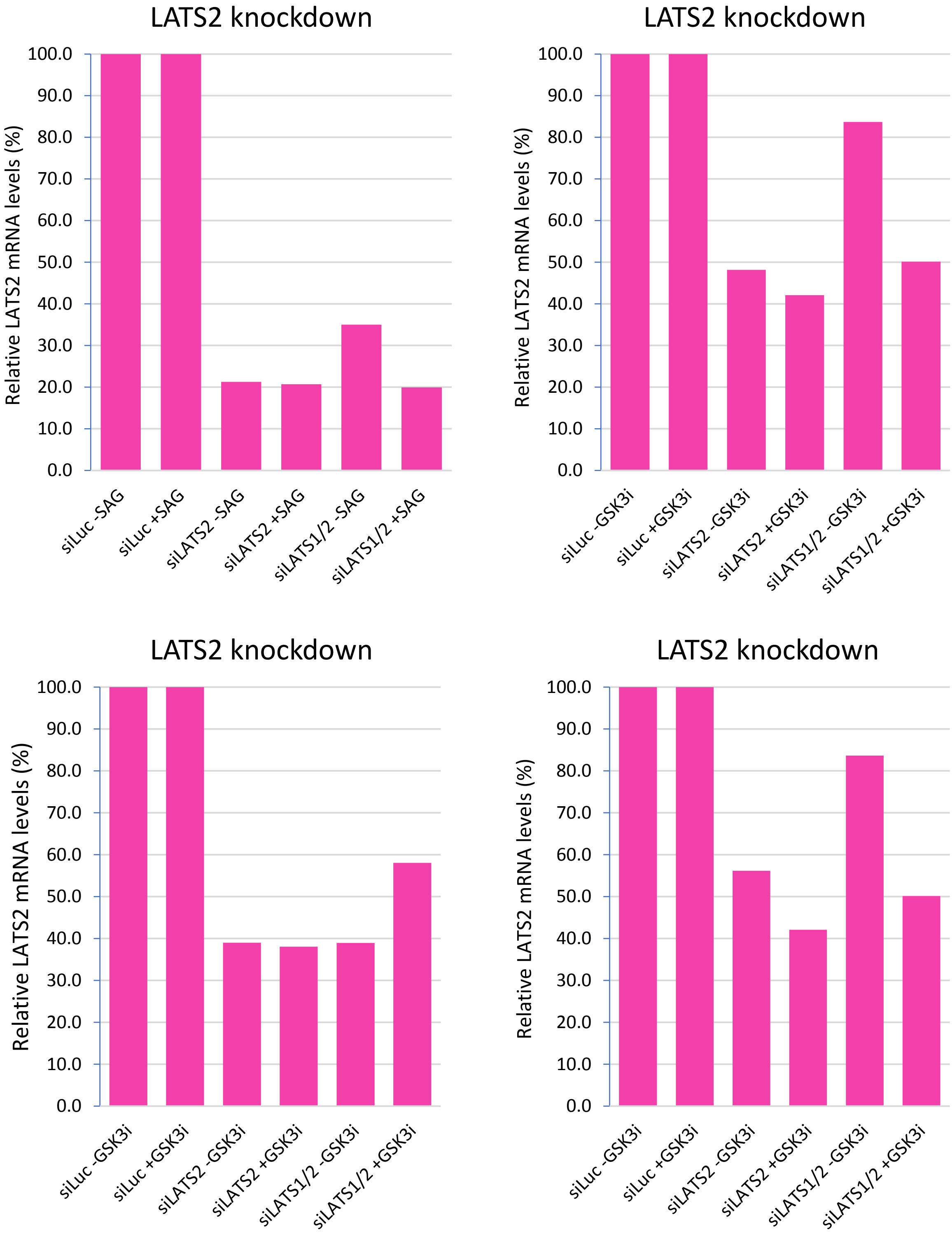

<u>Appendix Figure 6</u> – LATS2 mRNA expression tends to increase in response to LATS1 depletion.
Quantification of LATS2 mRNA levels after single or combined siRNA-mediated gene knockdown of *LATS1* and *LATS2* in ARPE-19 cells, with or without 24 hr treatment with 200 nM SAG or 10 mM GSK3 inhibitor SB216763 (GSK3i). Values are relative to control cells transfected with siRNA targeting Luciferase (siLuc).

Chapter 6: References

Abe, Y., Ohsugi, M., Haraguchi, K., Fujimoto, J. and Yamamoto, T. (2006) LATS2-Ajuba complex regulates γ-tubulin recruitment to centrosomes and spindle organization during mitosis. *FEBS Letters*, 580(3), pp. 782–788.

Ahn, S. and Joyner, A. L. (2005) In vivo analysis of quiescent adult neural stem cells responding to Sonic Hedgehog. *Nature*, 437(7060), pp. 894–897.

Akladios, B., Mendoza Reinoso, V., Cain, J. E., Wang, T., Lambie, D. L., Watkins, D. N. and Beverdam, A. (2017) Positive regulatory interactions between YAP and Hedgehog signalling in skin homeostasis and BCC development in mouse skin in vivo. *PLOS ONE*, 12(8), p. e0183178.

Asaoka, Y., Kanai, F., Ichimura, T., Tateishi, K., Tanaka, Y., Ohta, M., Seto, M., Tada, M., Ijichi, H., Ikenoue, T., Kawabe, T., Isobe, T., Yaffe, M. B. and Omata, M. (2010) Identification of a suppressive mechanism for Hedgehog signaling through a novel interaction of gli with 14-3-3. *Journal of Biological Chemistry*, 285(6), pp. 4185–4194.

Aylon, Y., Sarver, A., Tovy, A., Ainbinder, E. and Oren, M. (2014) Lats2 is critical for the pluripotency and proper differentiation of stem cells. *Cell death and differentiation*. Nature Publishing Group, 21(4), pp. 624–33.

Basten, S. G. and Giles, R. H. (2013) Functional aspects of primary cilia in signaling, cell cycle and tumorigenesis. *Cilia,* 2(6).

Beachy, P. a, Karhadkar, S. S. and Berman, D. M. (2004) Tissue repair and stem cell renewal in carcinogenesis. *Nature*, 432(7015), pp. 324–331.

Boggiano, J. C., Vanderzalm, P. J. and Fehon, R.G. (2011) Tao-1 phosphorylates Hippo/MST kinases to regulate the Hippo-Salvador-Warts tumor suppressor pathway. *Developmental Cell,* 21, pp. 888–895.

Bridges, D. and Moorhead, G. B. G. (2005) 14-3-3 Proteins: a Number of Functions for a Numbered Protein. *Science's STKE: signal transduction knowledge environment*, 2005(296), p. re10.

Burke, R., Nellen, D., Bellotto, M., Hafen, E., Senti, K.-A., Dickson, B. J. and Basler, K. (1999) Dispatched, a Novel Sterol-Sensing Domain Protein Dedicated to the Release of Cholesterol-Modified Hedgehog from Signaling Cells. *Cell*, 99(7), pp. 803–815.

Cai, C., Thorne, J. and Grabel, L. (2008) Hedgehog Serves as a Mitogen and Survival Factor During Embryonic Stem Cell Neurogenesis. *Stem Cells*, 26(5), pp. 1097–1108.

Chan, E. H. Y., Nousiainen, M., Chalamalasetty, R. B., Schäfer, A., Nigg, E. A. and Silljé, H. H. W. (2005) The Ste20-like kinase Mst2 activates the human large tumor suppressor kinase Lats1. *Oncogene*, 24(12), pp. 2076–2086.

Chen, M., Wilson, C. W., Li, Y., Ruel, L., Thérond, P. P., King, K., Law, L., Lu, C., Gacayan, R., Zhang, X., Hui, C. and Chuang, P. (2009) Cilium-independent regulation of Gli protein function by Sufu in Hedgehog signaling is evolutionarily conserved. *Genes & Development*, pp. 1910–1928.

Chen, Y., Sasai, N., Ma, G., Yue, T., Jia, J., Briscoe, J. and Jiang, J. (2011) Sonic Hedgehog Dependent Phosphorylation by CK1 a and GRK2 Is Required for Ciliary Accumulation and Activation of Smoothened. *PLoS Biology*, 9(6), p. e1001083.

Chen, Y., Yue, S., Xie, L., Pu, X., Jin, T. and Cheng, S. Y. (2011) Dual Phosphorylation of Suppressor of Fused (Sufu) by PKA and GSK3β Regulates Its Stability and Localization in the Primary Cilium. *The Journal of Biological Chemistry*, 286(15), pp. 13502–13511.

Cherry, A. L., Finta, C., Karlström, M., Jin, Q., Schwend, T., Astorga-Wells, J., Zubarev, R. A., Del Campo, M., Criswell, A. R., De Sanctis, D., Jovine, L. and Toftgård, R. (2013) Structural basis of SUFU-GLI interaction in human Hedgehog signalling regulation. *Acta Crystallographica Section D: Biological Crystallography,* 69(12), pp. 2563–2579.

Cole, D. G., Diener, D. R., Himelblau, A. L., Beech, P. L., Fuster, J. C. and Rosenbaum, J. L. (1998) Chlamydomonas kinesin-II-dependent intraflagellar transport (IFT): IFT particles contain proteins required for ciliary assembly in Caenorhabditis elegans sensory neurons. *The Journal of Cell Biology*, 141(4), pp. 993–1008.

Cooper, A. F., Yu, K. P., Brueckner, M., Brailey, L. L., Johnson, L., McGrath, J. M. and Bale, A. E. (2005) Cardiac and CNS defects in a mouse with targeted disruption of suppressor of fused. *Development*, 132, pp. 4407–4417.

Dahmane, N. and Ruiz, A. (1999) Sonic Hedgehog regulates the growth and patterning of the cerebellum. *Development*, 126, pp. 3089–3100.

Dahmane, N., Lee, J., Robins, P., Heller, P. and Ruiz i Altaba, A. (1997) Activation of the transcription factor Gli1 and the Sonic Hedgehog signalling pathway in skin tumours., *Nature*, 389 (October), pp. 876–881.

Dai, P., Akimaru, H., Tanaka, Y., Maekawa, T., Nakafuku, M. and Ishii, S. (1999) Sonic Hedgehog-induced activation of the Gli1 promoter is mediated by GLI3. *The Journal of Biological Chemistry.* American Society for Biochemistry and Molecular Biology, 274(12), pp. 8143–52.

Deng, J., Zhang, W., Liu, S., An, H., Tan, L. and Ma, L. (2017) LATS1 suppresses proliferation and invasion of cervical cancer. *Molecular medicine reports*. Spandidos Publications, 15(4), pp. 1654–1660.

Dorn, K. V, Hughes, C. E. and Rohatgi, R. (2012) A Smoothened-Evc2 Complex Transduces the Hedgehog Signal at Primary Cilia. *Developmental Cell*, 23, pp. 823–835.

Dunaeva, M., Michelson, P., Kogerman, P. and Toftgard, R. (2003) Characterization of the physical interaction of Gli proteins with SUFU proteins, Journal of Biological Chemistry, 278(7), pp. 5116–5122.

Echelard, Y., Epstein, D. J., St-Jacques, B., Shen, L., Mohler, J., McMahon, J. A. and McMahon, A. P. (1993) Sonic Hedgehog, a member of a family of putative signaling molecules, is implicated in the regulation of CNS polarity, *Cell*, 75 (7), pp. 1417-1430.

Ehmer, U. and Sage, J. (2015) Control of proliferation and cancer growth by the Hippo signaling pathway. *Molecular cancer research*: MCR, pp. 127–141.

Evans, D. G., Farndon, P. A., Burnell, L. D., Gattamaneni, H. R. and Birch, J. M. (1991) The incidence of Gorlin syndrome in 173 consecutive cases of medulloblastoma., *British journal of cancer*, 64 (5), pp. 959–61.

Farzan, S. F., Singh, S., Schilling, N. S. and Robbins, D. J. (2008) The adventures of sonic Hedgehog in development and repair. III. Hedgehog processing and biological activity. *American journal of physiology, Gastrointestinal and liver physiology*, 294 (4), pp. G844-9.

Fernandez-L, A., Northcott, P. A., Dalton, J., Fraga, C., Ellison, D., Angers, S., Taylor, M. D. and Kenney, A. M. (2009) YAP1 is amplified and up-regulated in Hedgehog-associated medulloblastomas and mediates Sonic Hedgehog-driven neural precursor proliferation. *Genes and Development*, 23(23), pp. 2729–2741.

Fujii, H., Zhou, W. and Gabrielson, E. (1996) Detection of frequent allelic loss of 6q23-q25.2 in microdissected human breast cancer tissues. *Genes, chromosomes & cancer*. Wiley-Liss Inc., 16(1), pp. 35–9.

Furth, N. and Aylon, Y. (2017) The LATS1 and LATS2 tumor suppressors: beyond the Hippo pathway. *Cell Death and Differentiation*, 24(9), pp. 1488–1501.

Garcia-Gonzalo, F. R. and Reiter, J. F. (2012) Scoring a backstage pass: mechanisms of ciliogenesis and ciliary access. *The Journal of cell biology.* Rockefeller University Press, 197(6), pp. 697–709.

Glantschnig H., Rodan G. A. and Reszka A. A. (2002) Mapping of MST1 kinase sites of phosphorylation. Activation and autophosphorylation. *The Journal of biological chemistry*, 277, pp. 42987–42996.

Goetz, S. C. and Anderson, K. V (2010) The primary cilium: a signalling centre during vertebrate development. *Nature reviews Genetics*. Nature Publishing Group, 11(5), pp. 331–44.

Guerrero, I. and Chiang, C. (2007) A conserved mechanism of Hedgehog gradient formation by lipid modifications. Trends in Cell Biology, 17(1), pp. 1–5.

Guo, C., Wang, X., & Liang, L. (2015). LATS2-mediated YAP1 phosphorylation is involved in HCC tumorigenesis. *Int J Clin Exp Pathol*, *8* (2), 1690–1697.

Hahn, H., Wicking, C., Zaphiropoulos, P. G., Gailani, M. R., Shanley, S., Chidambaram, A., Vorechovsky, I., Holmberg, E., Unden, A. B., Gillies, S., Negus, K., Smyth, I., Pressman, C., Leffell, D. J., Gerrard, B., Goldstein, A. M., Dean, M., Toftgård, R., Chenevix-Trench, G., Wainwright, B. and Bale, A. E. (1996) Mutations of the human homolog of drosophila patched in the nevoid basal cell carcinoma syndrome, *Cell*, 85 (6), pp. 841–851.

Harvey, K. F., Pfleger, C. M. and Hariharan, I. K. (2003) 'The Drosophila Mst ortholog, Hippo, restricts growth and cell proliferation and promotes apoptosis', Cell, 114(4), pp. 457–467.

Harvey, K. F., Zhang, X. and Thomas, D. M. (2013) The Hippo pathway and human cancer. *Nature Reviews Cancer*, 13(4), pp. 246–257.

Haycraft, C. J., Banizs, B., Aydin-Son, Y., Zhang, Q., Michaud, E. J. and Yoder, B. K. (2005) Gli2 and Gli3 Localize to Cilia and Require the Intraflagellar Transport Protein Polaris for Processing and Function, *PLoS Genetics*, 1(4), p. e53.

Hergovich, A., Cornils, H. and Hemmings, B. A. (2008) Mammalian NDR protein kinases: From regulation to a role in centrosome duplication. *Biochimica et Biophysica Acta* - Proteins and Proteomics, 1784(1), pp. 3–15.

Hergovich, A., Schmitz, D. and Hemmings, B. A. (2006) The human tumour suppressor LATS1 is activated by human MOB1 at the membrane. *Biochemical and Biophysical Research Communications*, 345(1), pp. 50–58.

Hsu, T.-H., Yang, C.-Y., Yeh, T.-H., Huang, Y.-C., Wang, T.-W. and Yu, J.-Y. (2017) The Hippo pathway acts downstream of the Hedgehog signaling to regulate follicle stem cell maintenance in the Drosophila ovary. *Nature Scientific Reports*, 7(4480), pp. 1–13.

Huang, J., Wu, S., Barrera, J., Matthews, K. and Pan, D. (2005) The Hippo signaling pathway coordinately regulates cell proliferation and apoptosis by inactivating Yorkie, the Drosophila homolog of YAP, *Cell*, 122(3), pp. 421–434.

Huangfu, D. and Anderson, K. V (2005) Cilia and Hedgehog responsiveness in the mouse. *Proceedings of the National Academy of Sciences of the United States of America*, 102(32), pp. 11325–11330.

Huangfu, D., Liu, A., Rakeman, A. S., Murcia, N. S., Niswander, L. and Anderson, K. V. (2003) Hedgehog signalling in the mouse requires intraflagellar transport proteins, *Nature*, 426(6962), pp. 83–87.

Hui, C. and Angers, S. (2011) Gli Proteins in Development and Disease. *Annual Review of Cell and Developmental Biology*, 27(1), pp. 513–537.

Humke, E. W., Dorn, K. V., Milenkovic, L., Scott, M. P. and Rohatgi, R. (2010) The output of Hedgehog signaling is controlled by the dynamic association between Suppressor of Fused and the Gli proteins. *Genes & Development*, 24(7), pp. 670–682.

Incardona, J. P., Lee, J. H., Robertson, C. P., Enga, K., Kapur, R. P. and Roelink, H. (2000) Receptor-mediated endocytosis of soluble and membrane-tethered Sonic Hedgehog by Patched-1. *Proceedings of the National Academy of Sciences of the United States of America.* National Academy of Sciences, 97(22), pp. 12044–9.

Ingham, P. W. and McMahon, A. P. (2001) Hedgehog signaling in animal development: paradigms and principles, *Genes and Development*, 15 (23), pp. 3059–3087.

Jia, J., Kolterud, Å., Zeng, H., Hoover, A., Teglund, S., Toftgård, R. and Liu, A. (2009) Suppressor of Fused inhibits mammalian Hedgehog signaling in the absence of cilia. *Developmental Biology*. Elsevier Inc., 330(2), pp. 452–460.

Johnson, R. L., Rothman, A. L., Xie, J., Goodrich, L. V, Bare, J. W., Bonifas, J. M., Quinn, A. G., Myers, R. M., Cox, D. R., Epstein, E. H. and Scott, M. P. (1996) Human homolog of patched, a candidate gene for the basal cell nevus syndrome., *Science*, 272 (5268), pp. 1668–71.

Justice, R. W., Zilian, O., Woods, D. F., Noll, M. and Bryant, P. J. (1995) The Drosophila tumor suppressor gene warts encodes a homolog of human myotonic dystrophy kinase and is required for the control of cell shape and proliferation. *Genes & development*, 9(5), pp. 534–46.

Karhadkar, S. S., Steven Bova, G., Abdallah, N., Dhara, S., Gardner, D., Maitra, A., Isaacs, J. T., Berman, D. M. and Beachy, P. A. (2004) Hedgehog signalling in prostate regeneration, neoplasia and metastasis, *Nature*, 431(7009), pp. 707–712.

Kim, M., Kim, M., Lee, M.-S., Kim, C.-H. and Lim, D.-S. (2014) The MST1/2-SAV1 complex of the Hippo pathway promotes ciliogenesis. *Nature Communications*, Nature Publishing Group 5: 5370

Kogerman, P., Grimm, T., Kogerman, L., Krause, D., Undén, A.B., Sandstedt, B., Toftgård, R., Zaphiropoulos, P.G. (1999). Mammalian suppressor-of-fused modulates nuclear-cytoplasmic shuttling of Gli-1. *Nature Cell Biology*, 1(5), 312–319.

Koontz, L. M., Liu-Chittenden, Y., Yin, F., Zheng, Y., Yu, J., Huang, B., Chen, Q., Wu, S. and Pan, D. (2013) The Hippo Effector Yorkie Controls Normal Tissue Growth by Antagonizing Scalloped-Mediated Default Repression. *Developmental Cell*. Elsevier, 25(4), pp. 388–401.

Kozminski, K. G., Johnson, K. A., Forscher, P. and Rosenbaum, J. L. (1993) A motility in the eukaryotic flagellum unrelated to flagellar beating. *Proceedings of the National Academy of Sciences*, 90(12), pp. 5519–5523.

Lai, Z. C., Wei, X., Shimizu, T., Ramos, E., Rohrbaugh, M., Nikolaidis, N., Ho, L. L. and Li, Y. (2005) Control of cell proliferation and apoptosis by mob as tumor suppressor, mats. *Cell*, 120(5), pp. 675–685.

Lee, Y., Kawagoe, R., Sasai, K., Li, Y., Russell, H. R., Curran, T. and McKinnon, P. J. (2007) Loss of suppressor-of-fused function promotes tumorigenesis. *Oncogene*, 26(44), pp. 6442–7.

Li, Y., Pei, J., Xia, H., Ke, H., Wang, H. and Tao, W. (2003) Lats2, a putative tumor suppressor, inhibits G1/S transition. *Oncogene*, 22(28), pp. 4398–4405.

Li, Y., Zhang, H., Litingtung, Y. and Chiang, C. (2006) Cholesterol modification restricts the spread of Shh gradient in the limb bud. *Proceedings of the National Academy of Sciences of the United States of America*. National Academy of Sciences, 103(17), pp. 6548–53.

Lin, C., Yao, E., Wang, K., Nozawa, Y., Shimizu, H., Johnson, J. R., Chen, J. N., Krogan, N. J. and Chuang, P. T. (2014) Regulation of Sufu activity by p66b and Mycbp provides new insight into vertebrate Hedgehog signaling. *Genes and Development*, 28(22), pp. 2547–2563.

Liu, C.-Y., Zha, Z.-Y., Zhou, X., Zhang, H., Huang, W., Zhao, D., Li, T., Chan, S. W., Lim, C. J., Hong, W., Zhao, S., Xiong, Y., Lei, Q.-Y. and Guan, K.-L. (2010) The Hippo Tumor Pathway Promotes TAZ Degradation by Phosphorylating a Phosphodegron and Recruiting the SCF β-TrCP E3 Ligase. *Journal of Biological Chemistry*, 285(48), pp. 37159–37169.

Lorthongpanich, C., Messerschmidt, D. M., Chan, S. W., Hong, W., Knowles, B. B. and Solter, D. (2013) Temporal reduction of LATS kinases in the early preimplantation embryo prevents ICM lineage differentiation. *Genes & development*. Cold Spring Harbor Laboratory Press, 27(13), pp. 1441–6.

Manoranjan, B., Venugopal, C., McFarlane, N., Doble, B. W., Dunn, S. E., Scheinemann, K. and Singh, S. K. (2012) Medulloblastoma stem cells: where development and cancer cross pathways. *Pediatric Research*, 71(4), pp. 516–522.

Marigo, V., Davey, R. A., Zuo, Y., Cunningham, J. M. and Tabin, C. J. (1996) Biochemical evidence that Patched is the Hedgehog receptor, *Nature*, 384(6605), pp. 176–179.

McPherson, J. P., Tamblyn, L., Elia, A., Migon, E., Shehabeldin, A., Matysiak-Zablocki, E., Lemmers, B., Salmena, L., Hakem, A., Fish, J., Kassam, F., Squire, J., Bruneau, B. G., Hande, M. P. and

Hakem, R. (2004) Lats2/Kpm is required for embryonic development, proliferation control and genomic integrity. *The EMBO Journal*, 23(18), pp. 3677–3688.

Meng, Z., Moroishi, T. and Guan, K. (2016) Mechanisms of Hippo pathway regulation. *Genes and Development*, 30(1), pp. 1–17.

Meng, Z., Moroishi, T., Mottier-Pavie, V., Plouffe, S. W., Hansen, C. G., Hong, A. W., Park, H. W., Mo, J.-S., Lu, W., Lu, S., Flores, F., Yu, F.-X., Halder, G. and Guan, K.-L. (2015) MAP4K family kinases act in parallel to MST1/2 to activate LATS1/2 in the Hippo pathway. *Nature Communications*, 6, p. 8357.

Mo, J., Meng, Z., Kim, Y. C., Park, H. W., Hansen, C. G. and Kim, S. (2015). Cellular energy stress induces AMPK-mediated regulation of YAP and the Hippo pathway. *Nature Cell Biology,* 17(4), 500-510.

Mukhopadhyay, S., Wen, X., Ratti, N., Loktev, A., Rangell, L., Scales, S. and Jackson, P. (2013) The Ciliary G-Protein-Coupled Receptor Gpr161 Negatively Regulates the Sonic Hedgehog Pathway via cAMP Signaling, *Cell*, 152(1–2), pp. 210–223.

Nishiyama, Y., Hirota, T., Morisaki, T., Hara, T., Marumoto, T., Iida, S. I., Makino, K., Yamamoto, H., Hiraoka, T., Kitamura, N. and Saya, H. (1999) A human homolog of Drosophila warts tumor suppressor, h-warts, localized to mitotic apparatus and specifically phosphorylated during mitosis. *FEBS Letters*, 459(2), pp. 159–165.

Oren, M. and Aylon, Y. (eds.) (2013) The Hippo Signalling Pathway and Cancer. New York: Springer

Paces-Fessy, M., Boucher, D., Petit, E., Paute-Briand, S. and Blanchet-Tournier, M.-F. (2004) The negative regulator of Gli, Suppressor of fused (Sufu), interacts with SAP18, Galectin3 and other nuclear proteins. *The Biochemical Journal*, 378(Pt 2), pp. 353–62.

Pan, Y., Brian Bai, C., Joyner, A. L. and Wang, B. (2006) Sonic Hedgehog Signaling Regulates Gli2 Transcriptional Activity by Suppressing Its Processing and Degradation. *Molecular and Cellular Biology*, 26(9), pp. 3365–3377.

Park, G.-S., Oh, H., Kim, M., Kim, T., Johnson, R. L., Irvine, K. D., Lim, D.-S., Park, G.-S., Oh, H., Kim, M., Kim, T., Johnson, R. L., Irvine, K. D. and Lim, D.-S. (2016) An evolutionarily conserved negative feedback mechanism in the Hippo pathway reflects functional difference between LATS1 and LATS2. *Oncotarget*, 7(17), pp. 24063–24075.

Park, H. L., Bai, C., Platt, K. A., Matise, M. P., Beeghly, A., Hui, C. C., Nakashima, M. and Joyner, A. L. (2000) Mouse Gli1 mutants are viable but have defects in SHH signaling in combination with a Gli2 mutation. *Development*, 127(8), pp. 1593–605.

Pepinsky, R. B., Zeng, C., Wen, D., Rayhorn, P., Baker, D. P., Williams, K. P., Bixler, S. A., Ambrose, C. M., Garber, E. A., Miatkowski, K., Taylor, F. R., Wang, E. A. and Galdes, A. (1998) Identification of a palmitic acid-modified form of human Sonic Hedgehog., *The Journal of biological chemistry*, 273 (22), pp. 14037–45.

Plotnikova, O. V., Pugacheva, E. N. and Golemis, E. A. (2009) Primary Cilia and the Cell Cycle, *Methods in Cell Biology*. Academic Press, 94, pp. 137–160.

Poon, C. L., Lin J. I., Zhang, X., Harvey, K. F. (2011) The sterile 20-like kinase Tao-1 controls tissue growth by regulating the Salvador–Warts–Hippo pathway. *Developmental Cell*, 21, pp. 896–906.

Porter, J. A., Young, K. E. and Beachy, P. A. (1996) Cholesterol Modification of Hedgehog Signaling Proteins in Animal Development, *Science*, 274 (5285), pp. 255–259.

Praskova, M., Khoklatchev, A., Ortiz-Vega, S. and Avruch, J. (2004) Regulation of the MST1 kinase by autophosphorylation, by the growth inhibitory proteins, RASSF1 and NORE1, and by Ras. *Biochemical Journal*, 381, pp. 453–462.

Praskova, M., Xia, F. and Avruch, J. (2008) MOBKL1A/MOBKL1B Phosphorylation by MST1 and MST2 Inhibits Cell Proliferation. *Current Biology*, 18(5), pp. 311–321.

Raducu, M., Fung, E., Serres, S., Infante, P., Barberis, A., Fischer, R., Bristow, C., Thézénas, M., Finta, C., Christianson, J.C., Buffa, F.M., Kessler, B.M., Sibson, N.R., Marcotullio, L.D., Toftgård, R. & D'Angiolella, V. (2016). SCF (Fbxl17) ubiquitylation of Sufu regulates

Hedgehog signaling and medulloblastoma development. *The EMBO Journal*, 35(13), 1400–1416.

Raffel, C., Jenkins, R. B., Frederick, L., Hebrink, D., Alderete, B., Fults, D. W. and James, C. D. (1997) Sporadic medulloblastomas contain PTCH mutations. *Cancer research*. American Association for Cancer Research, 57(5), pp. 842–5.

Rohatgi, R., Milenkovic, L. and Scott, M. P. (2007) Patched1 Regulates Hedgehog Signaling at the Primary Cilium, *Science*, 317(5836), pp. 372–376.

Rosenbaum, J. L. and Child, F. M. (1967) Flagellar regeneration in protozoan flagellates. *The Journal of Cell Biology*, 34(1), pp. 345–64.

Rosenbaum, J. L. and Witman, G. B. (2002) Intraflagellar transport. *Nature Reviews Molecular Cell Biology*, 3(11), pp. 813–825.

Sasaki, H., Nishizaki, Y., Hui, C., Nakafuku, M. and Kondoh, H. (1999) Regulation of Gli2 and Gli3 activities by an amino-terminal repression domain: implication of Gli2 and Gli3 as primary mediators of Shh signaling. Development, 126(17), pp. 3915–24.

Satir, P. and Christensen, S. T. (2007) Overview of structure and function of mammalian cilia. *Annual review of physiology*, 69, pp. 377–400.

Smith, M. J., Beetz, C., Williams, S. G., Bhaskar, S. S., O'Sullivan, J., Anderson, B., Daly, S. B., Urquhart, J. E., Bholah, Z., Oudit, D., Cheesman, E., Kelsey, A., McCabe, M. G., Newman, W. G. and Evans, D. G. R. (2015) Germline mutations in SUFU cause Gorlin syndrome-associated childhood medulloblastoma and redefine the risk associated with PTCH1 mutations. *Journal of Clinical Oncology*, 32(36), pp. 4155–4161.

Sorokin, S. (1962) Centrioles and the formation of rudimentary cilia by fibroblasts and smooth muscle cells. *The Journal of Cell Biology*, 15(2), 363–377.

St John, M. A., Tao, W., Fei, X., Fukumoto, R., Carcangiu, M. L., Brownstein, D. G., Parlow, A. F., McGrath, J. and Xu, T. (1999) Mice deficient of Lats1 develop soft-tissue sarcomas, ovarian tumours and pituitary dysfunction. *Nature genetics*, 21(2), pp. 182–6.

Steinhardt, A. A., Gayyed, M. F., Klein, A. P., Dong, J., Maitra, A., Pan, D., Montgomery, E. A. and Anders, R. A. (2008) Expression of Yes-associated protein in common solid tumors. *Human Pathology*. Elsevier Inc., 39 (11), pp. 1582–1589.

Strazisar M, Mlakar V, Glavac D. (2009) LATS2 tumour specific mutations and down-regulation of the gene in non-small cell carcinoma. *Lung Cancer*; 64: 257–262.

Taipale, J., Chen, J. K., Cooper, M. K., Wang, B., Mann, R. K., Milenkovic, L., Scott, M. P. and Beachy, P. A. (2000) Effects of oncogenic mutations in Smoothened and Patched can be reversed by cyclopamine. *Nature*, 406(6799), pp. 1005–1009.

Tao, W., Zhang, S., Turenchalk, G. S., Stewart, R. A., St John, M. A., Chen, W. and Xu, T. (1999) Human homologue of the Drosophila melanogaster lats tumour suppressor modulates CDC2 activity. *Nature genetics*, 21(2), pp. 177–81.

Tapon, N., Harvey, K. F., Bell, W., Wahrer, D. C. R., Taryn, a, Haber, D. a and Iswar, K. (2002) Salvador Promotes Both Cell Cycle Exit and Apoptosis in Drosophila and Is Mutated in Human Cancer Cell Lines. *Cell,* 110, pp. 467–478.

Taylor, M. D., Liu, L., Raffel, C., Hui, C., Mainprize, T. G., Zhang, X., Agatep, R., Chiappa, S., Gao, L., Lowrance, A., Hao, A., Goldstein, A. M., Stavrou, T., Scherer, S. W., Dura, W. T., Wainwright, B., Squire, J. a, Rutka, J. T. and Hogg, D. (2002) Mutations in SUFU predispose to medulloblastoma. *Nature* Genetics, 31(3), pp. 306–310.

Teglund, S. and Toftgård, R. (2010). Hedgehog beyond medulloblastoma and basal cell carcinoma. *Biochimica et Biophysica Acta (BBA) - Reviews on Cancer*, 1805 (2), 181–208.

Tempé, D., Casas, M., Karaz, S., Blanchet-Tournier, M.-F. and Concordet, J.-P. (2006) Multisite protein kinase A and glycogen synthase kinase 3beta phosphorylation leads to Gli3 ubiquitination by SCFbetaTrCP. *Molecular and cellular biology*. American Society for Microbiology, 26(11), pp. 4316–26.

Tukachinsky, H., Lopez, L. V. and Salic, A. (2010) A mechanism for vertebrate Hedgehog signaling: Recruitment to cilia and dissociation of SuFu-Gli protein complexes. *Journal of Cell Biology*, 191(2), pp. 415–428.

Urman, N. M., Mirza, A., Atwood, S. X., Whitson, R. J., Sarin, K. Y., Tang, J. Y. and Oro, A. E. (2016) Tumor-derived suppressor of fused mutations reveal Hedgehog pathway interactions. *PLoS ONE*, 11(12), pp. 1–10.

Wang, B. and Li, Y. (2006) Evidence for the direct involvement of βTrCP in Gli3 protein processing. *Proceedings of the National Academy of Sciences of the United States of America*. National Academy of Sciences, 103(1), pp. 33–8.

Wang, B., Fallon, J. F. and Beachy, P. A. (2000) Hedgehog-Regulated Processing of Gli3 Produces an Anterior/Posterior Repressor Gradient in the Developing Vertebrate Limb. *Cell*, 100, pp. 423–434.

Wang, Y., Li, Y., Hu, G., Huang, X., Rao, H., Xiong, X., Luo, Z., Lu, Q. and Luo, S. (2016) Nek2A phosphorylates and stabilizes SuFu: A new strategy of Gli2/Hedgehog signaling regulatory. *Cellular Signalling*. Elsevier Inc., 28(9), pp. 1304–1313.

Xia, H., Qi, H., Li, Y., Pei, J., Barton, J., Blackstad, M., Xu, T. and Tao, W. (2002) LATS1 tumor suppressor regulates G2/M transition and apoptosis. *Oncogene*, 21(8), pp. 1233–41.

Xu, T., Wang, W., Zhang, S., Stewart, R. A. and Yu, W. (1995) Identifying tumor suppressors in genetic mosaics: the Drosophila lats gene encodes a putative protein kinase. *Development*, 121(4), pp. 1053–63.

Yabuta, N., Fujii, T., Copeland, N. G., Gilbert, D. J., Jenkins, N. A., Nishiguchi, H., Endo, Y., Toji, S., Tanaka, H., Nishimune, Y. and Nojima, H. (2000) Structure, Expression, and Chromosome Mapping of LATS2, a Mammalian Homologue of the Drosophila Tumor Suppressor Gene lats/warts. *Genomics*, 63(2), pp. 263–270.

Yabuta, N., Mukai, S., Okada, N., Aylon, Y. and Nojima, H. (2011) The tumor suppressor Lats2 is pivotal in Aurora A and Aurora B signaling during mitosis. *Cell Cycle*, 10(16), pp. 2724–2736.

Yang, C., Chen, W., Chen, Y. and Jiang, J. (2012) Smoothened transduces Hedgehog signal by forming a complex with Evc/Evc2. *Cell Research*. Nature Publishing Group, 22(11), pp. 1593–1604.

Yang, X., Li, D. M., Chen, W. and Xu, T. (2001) Human homologue of Drosophila lats, LATS1, negatively regulate growth by inducing G(2)/M arrest or apoptosis. *Oncogene*, 20(45), pp. 6516–6523.

Yao, F., Liu, H., Li, Z., Zhong, C. and Fang, W. (2015) Down-regulation of LATS2 in non-small cell lung cancer promoted the growth and motility of cancer cells. *Tumor Biology*, 36(3), pp. 2049–2057.

Yin, F., Yu, J., Zheng, Y., Chen, Q., Zhang, N. and Pan, D. (2013) Spatial organization of Hippo signaling at the plasma membrane mediated by the tumor suppressor merlin/NF2. *Cell*. Elsevier, 154(6), pp. 1342–1355.

Yoon, J. W., Kita, Y., Frank, D. J., Majewski, R. R., Konicek, B. A., Nobrega, M. A., Jacob, H., Walterhouse, D. and Iannaccone, P. (2002) Gene expression profiling leads to identification of GLI1-binding elements in target genes and a role for multiple downstream pathways in GLI1-induced cell transformation. *The Journal of biological chemistry*. American Society for Biochemistry and Molecular Biology, 277(7), pp. 5548–55.

Zhang, Y., Fu, L., Qi, X., Zhang, Z., Xia, Y., Jia, J., Jiang, J., Zhao, Y. and Wu, G. (2013) Structural insight into the mutual recognition and regulation between Suppressor of Fused and Gli/Ci. *Nature Communications.* Nature Publishing Group, 4, pp. 1–12.

Zhang, Z., Shen, L., Law, K., Zhang, Z., Liu, X., Hua, H., Li, S., Huang, H., Yue, S., Hui, C. and Cheng, S. Y. (2017) Suppressor of Fused Chaperones Gli Proteins to Generate Transcriptional Responses to Sonic Hedgehog Signaling. *Molecular and Cellular Biology*, 37(3), pp. e00421-16.

Zhao, B., Li, L., Tumaneng, K., Wang, C.-Y. and Guan, K.-L. (2010) A coordinated phosphorylation by Lats and CK1 regulates YAP stability through SCF(β-TRCP). *Genes & Development*, 24(1), pp. 72–85.

Zhao, B., Wei, X., Li, W., Udan, R. S., Yang, Q., Kim, J., Xie, J., Ikenoue, T., Yu, J., Li, L., Zheng, P., Ye, K., Ye, K., Chinnaiyan, A., Halder, G., Lai, Z., and Guan, K.-L. (2007) Inactivation of YAP oncoprotein by the Hippo pathway is involved in cell contact inhibition and tissue growth control, *Genes & Development*, 21 (21), pp. 2747–2761.

Zhao, B., Ye, X., Yu, J., Li, L., Li, W., Li, S., Yu, J. and Lin, J. D. (2008) TEAD mediates YAP-dependent gene induction and growth control TEAD mediates YAP-dependent gene induction and growth control. *Genes & Development*, 22, pp. 1962–1971.

Zhou, F., Huang, D., Li, Y., Hu, G., Rao, H., Lu, Q., Luo, S. and Wang, Y. (2017) Nek2A/SuFu feedback loop regulates Gli-mediated Hedgehog signaling pathway. *International Journal of Oncology*, 50(2), pp. 373–380.

Zurawel, R. H., Allen, C., Wechsler-Reya, R., Scott, M. P. and Raffel, C. (2000) Evidence that haploinsufficiency of Ptch leads to medulloblastoma in mice. *Genes Chromosomes and Cancer*, 28 (1), pp. 77–81.